



Searching for the origin of Cosmic Rays

Dmitri Semikoz

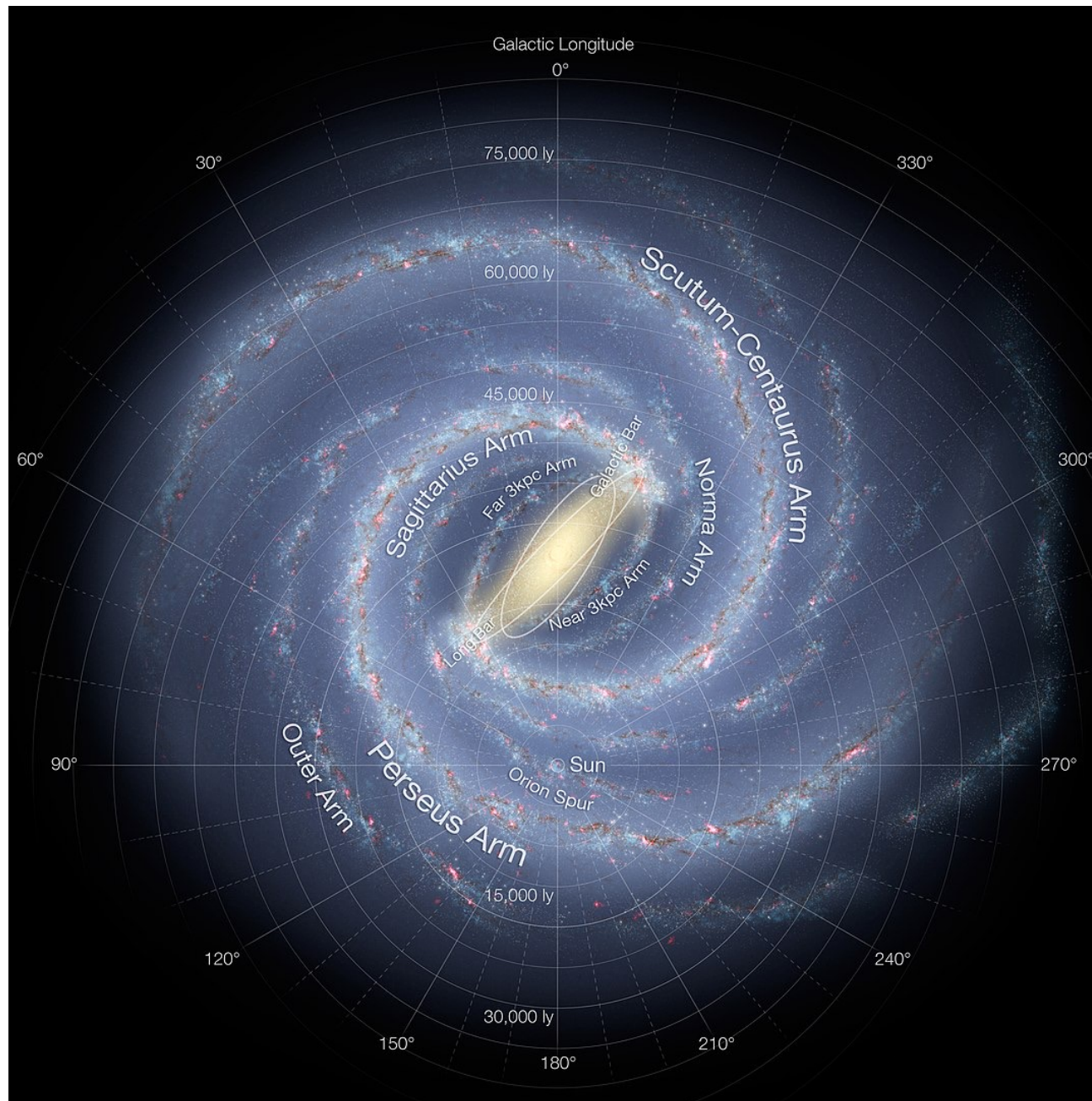
APC, Paris

Plan

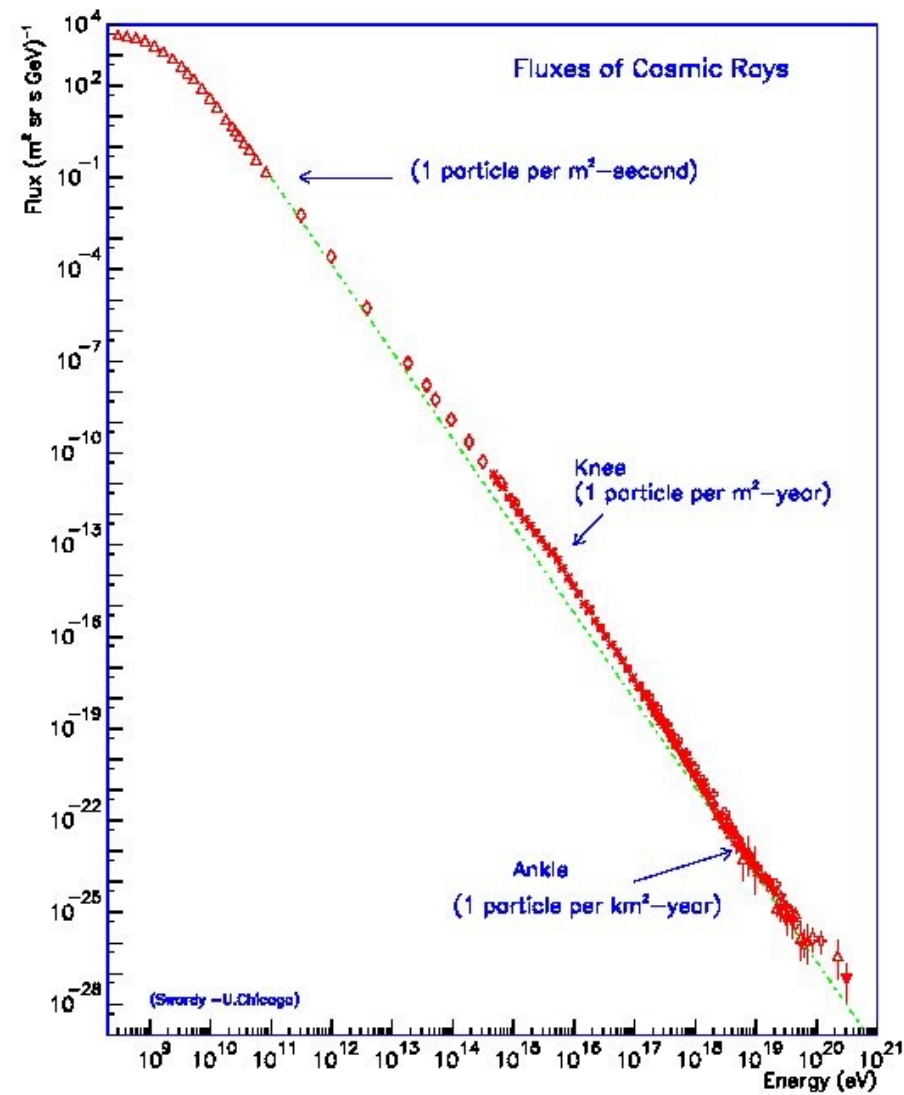
- Cosmic ray measurements at Earth
- Galactic Magnetic Field and cosmic ray propagation
- Search of extra-galactic sources with UHECR
- Gamma-ray and neutrino signatures of Galactic sources
- Conclusions

Cosmic ray measurements at Earth

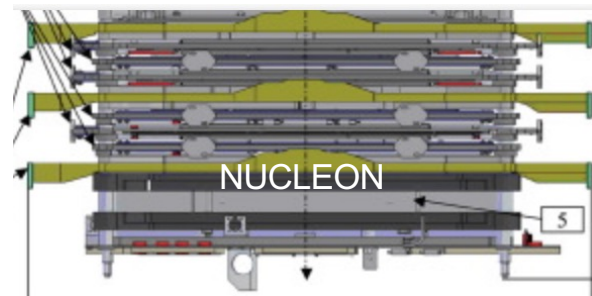
TAUP 2025, Searching for sources of cosmic rays Dmitri Semikoz



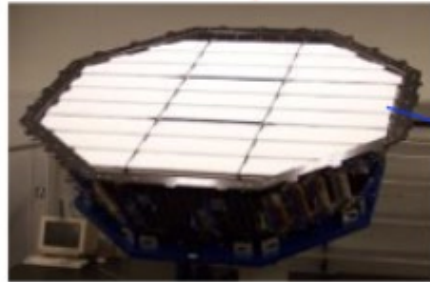
TAUP 2025, Searching for sources of cosmic rays Dmitri Semikoz



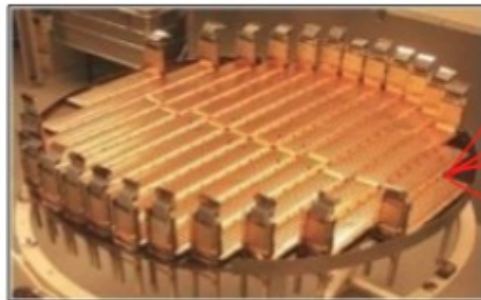
Direct Cosmic Ray measurements



Transition Radiation Detector
Electron/proton, Z



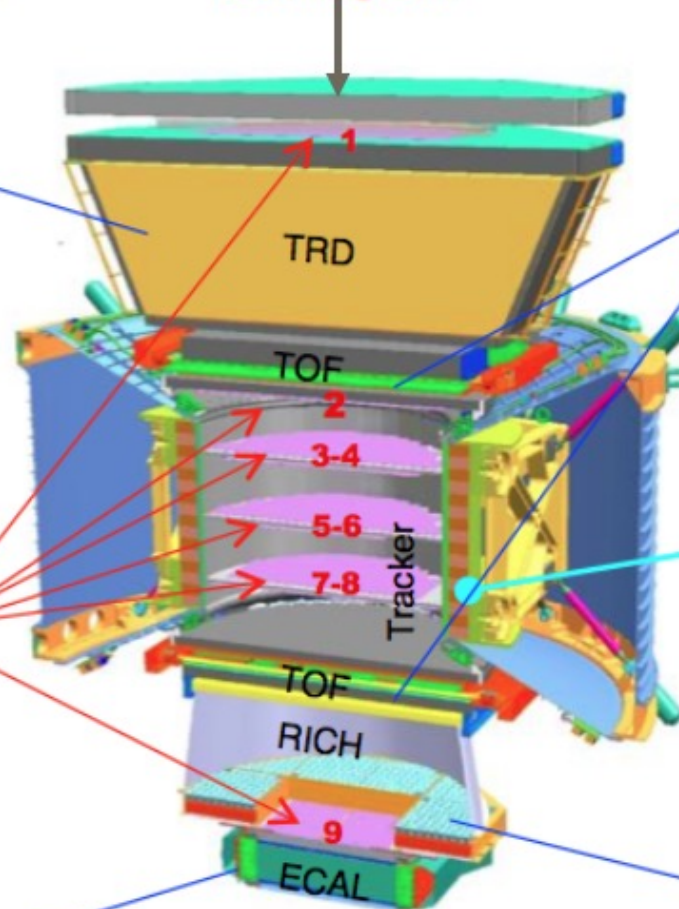
Silicon Tracker
Z, P



Electromagnetic Calorimeter
E of electrons



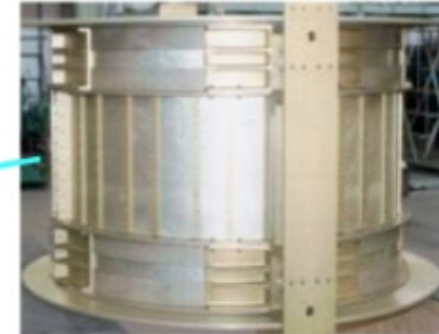
Incoming CRs



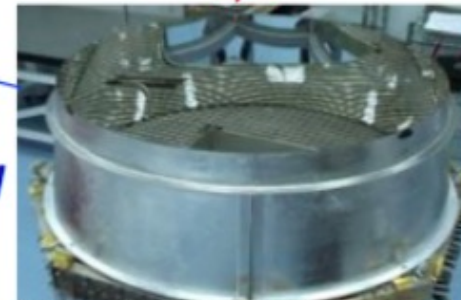
Time of Flight
Z, E



Magnet
 $\pm Z$

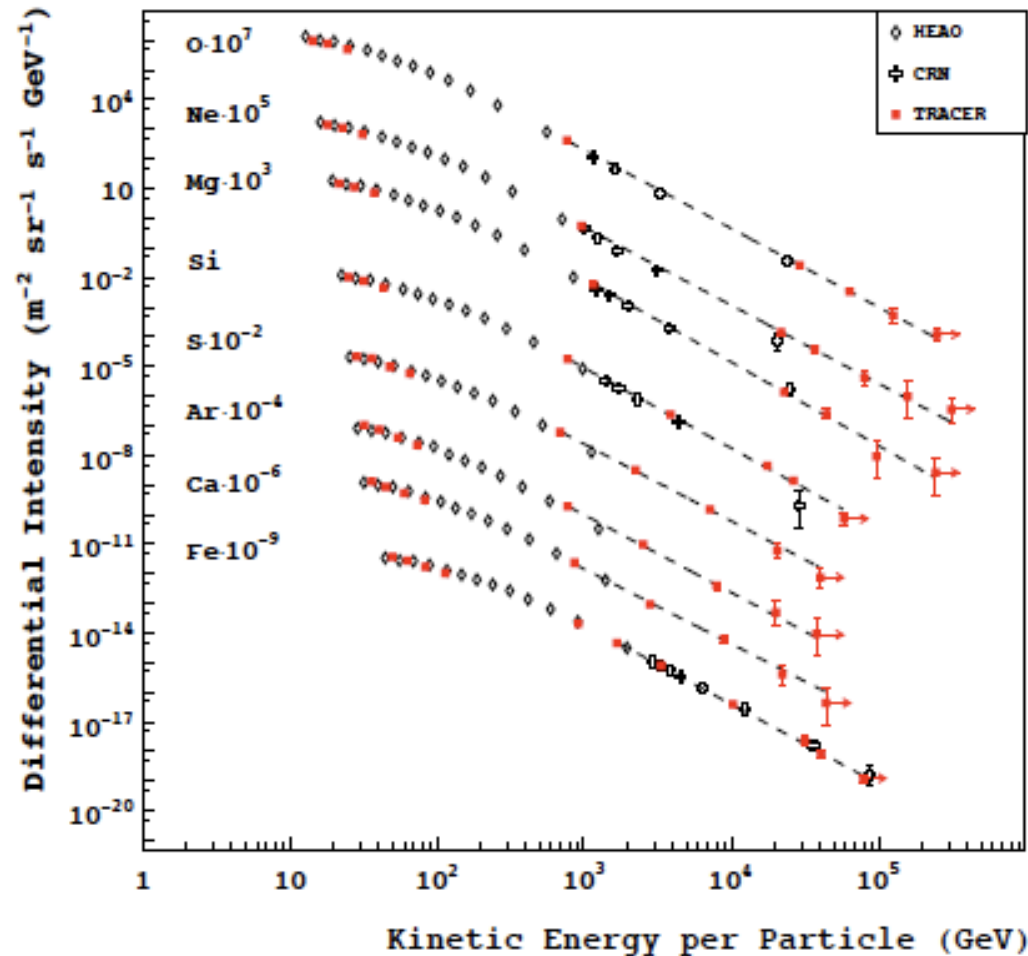


Ring Imaging Cherenkov
Z, E

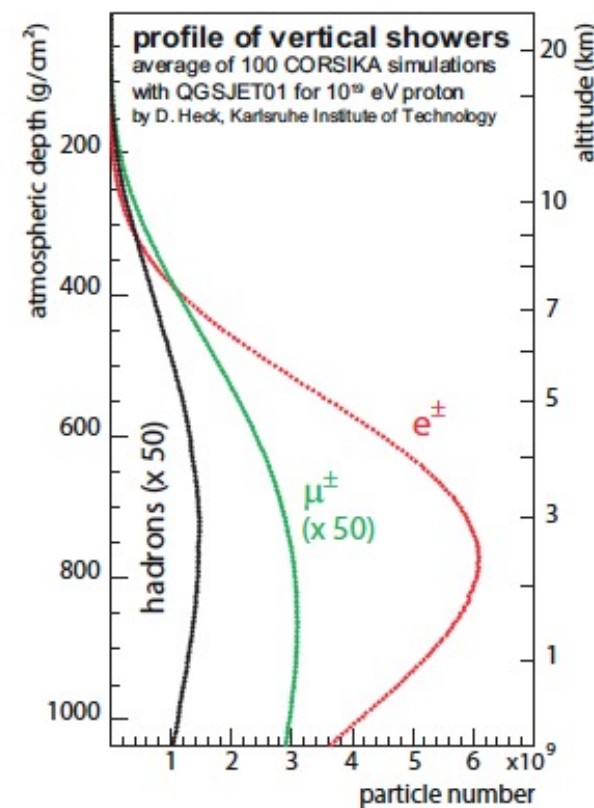
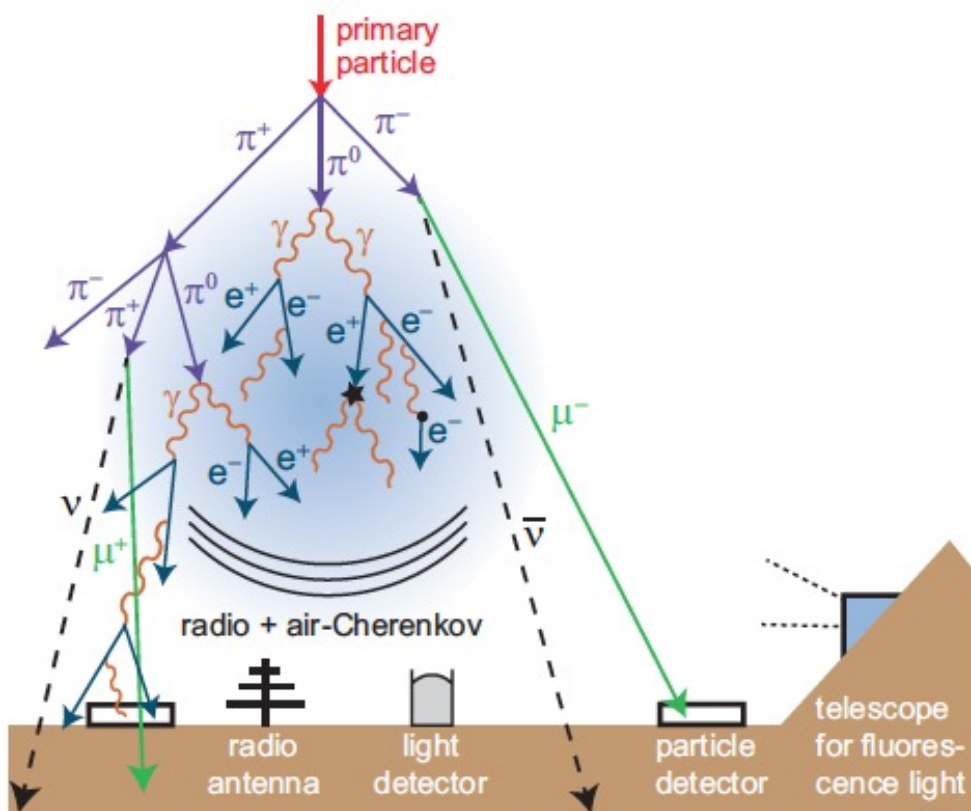


The Charge and Energy are measured independently by several detectors

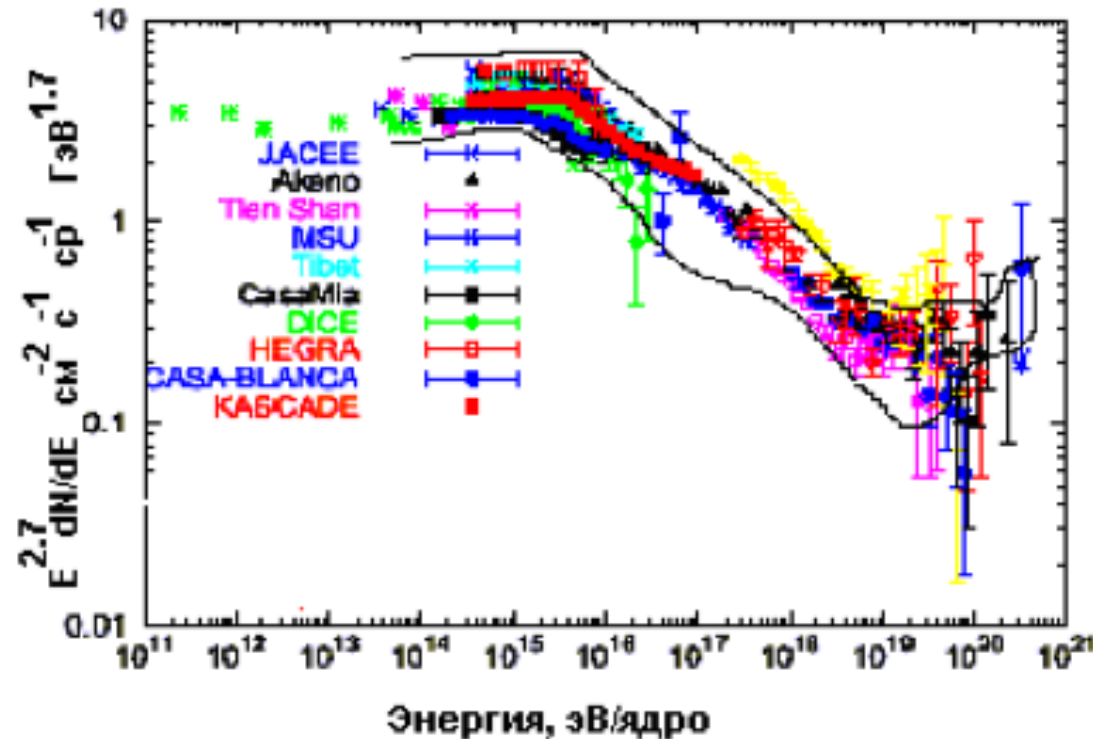
Spectra of individual nuclei



Detection techniques



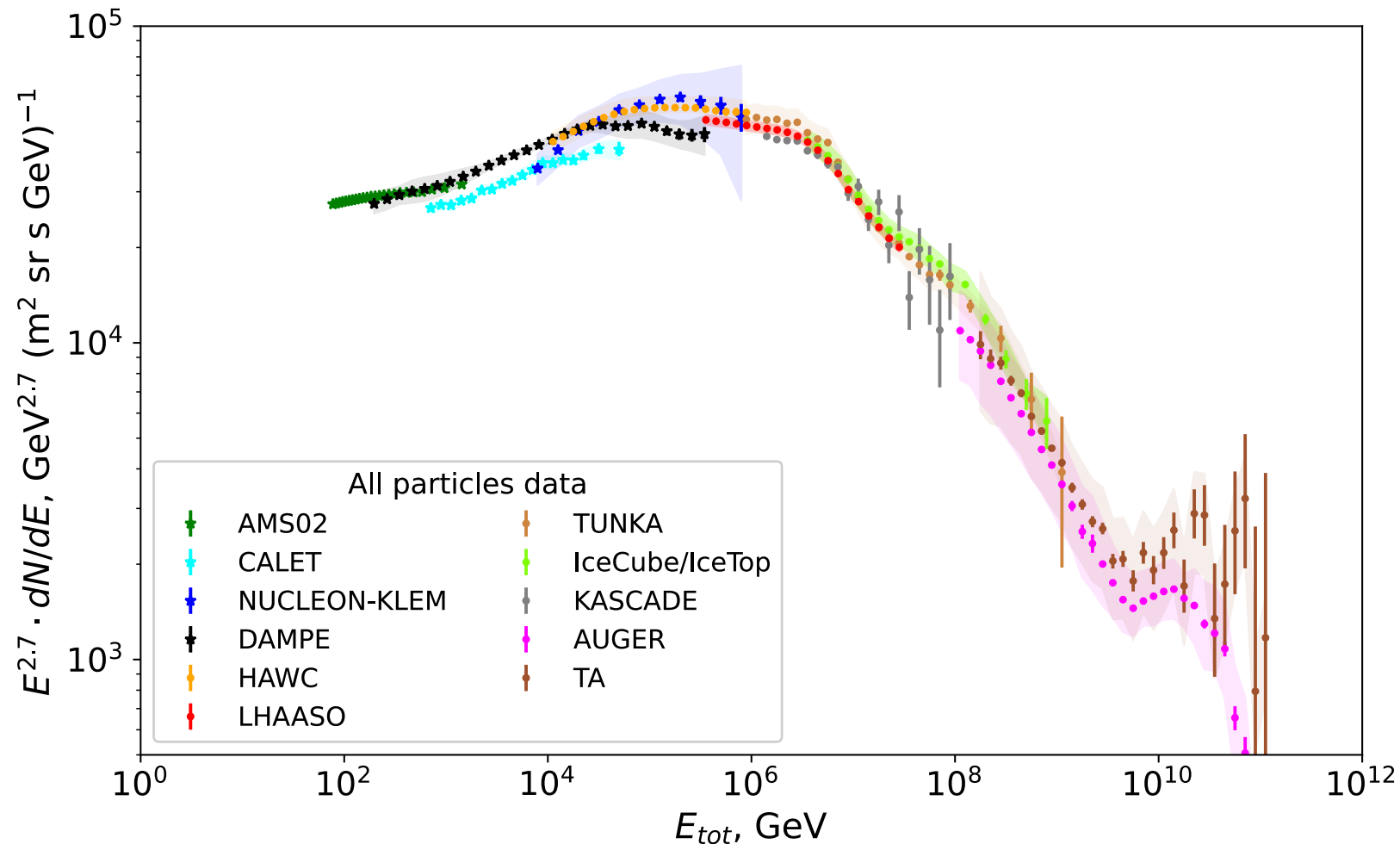
Knee in CR spectrum



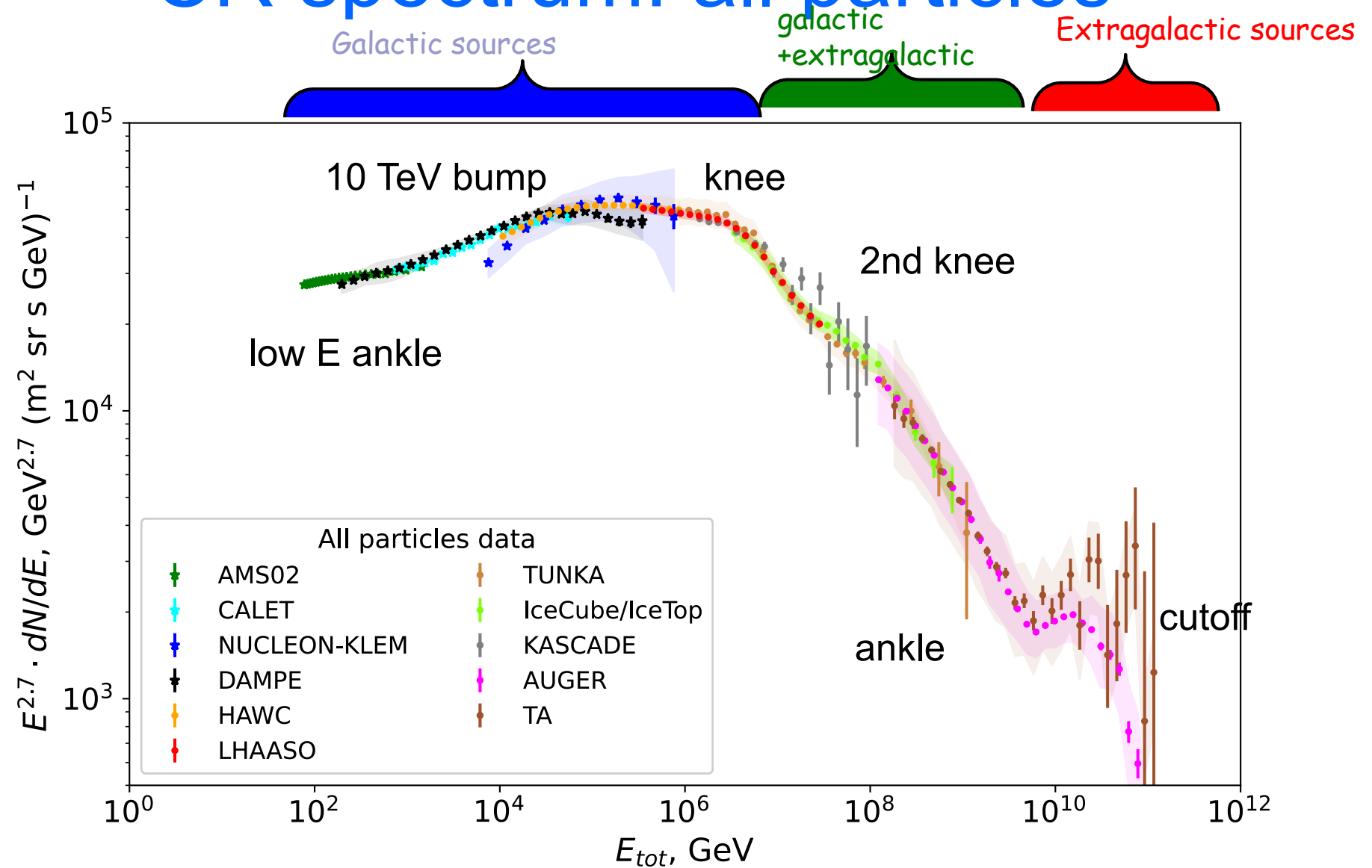
Knee was discovered by Kulikov and Khristiansen in data of MSU Experiment in 1958

All particle spectrum change power law from 2.7 to 3.1 at $E=4$ PeV

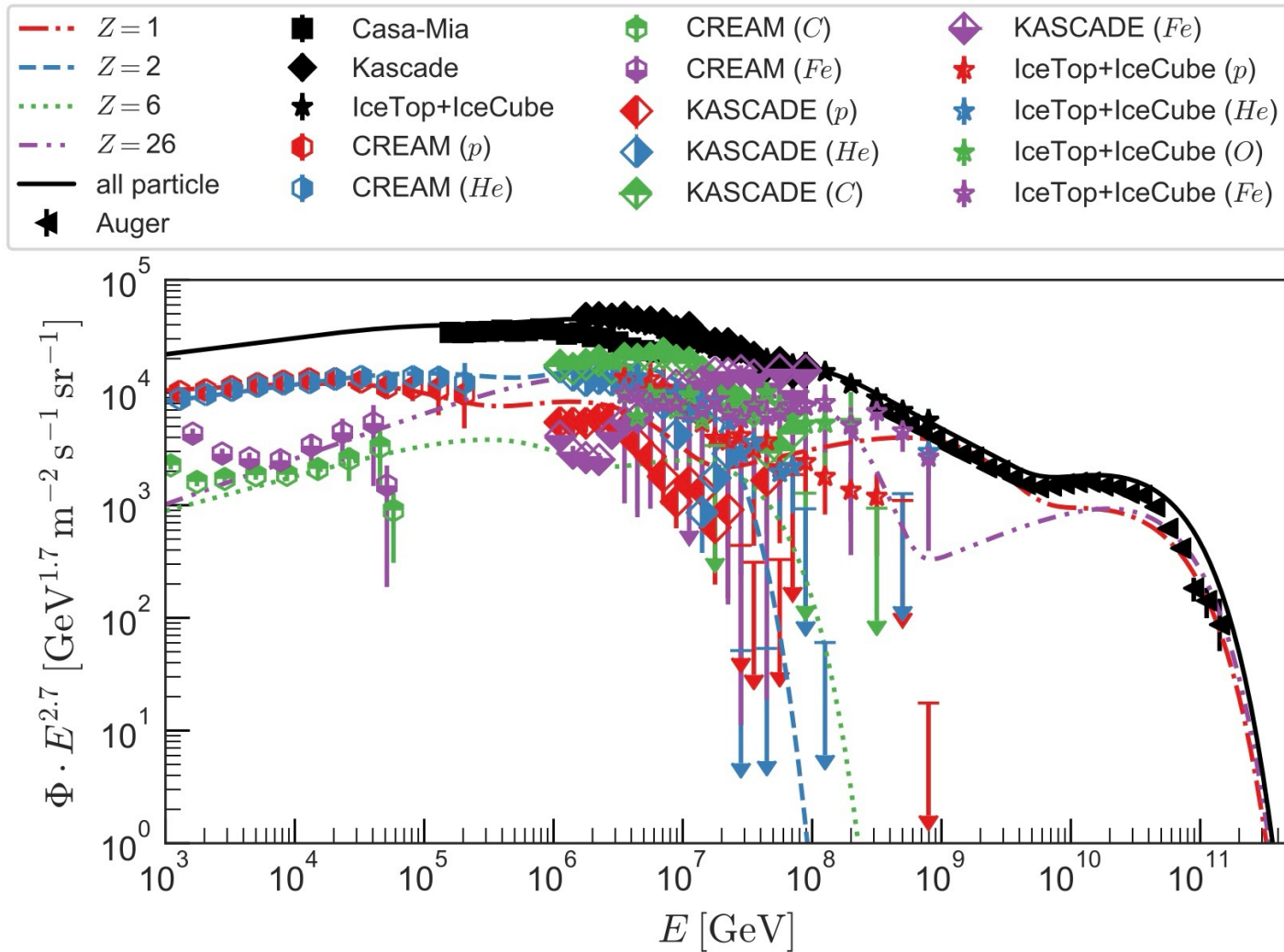
CR spectrum: all particles



CR spectrum: all particles

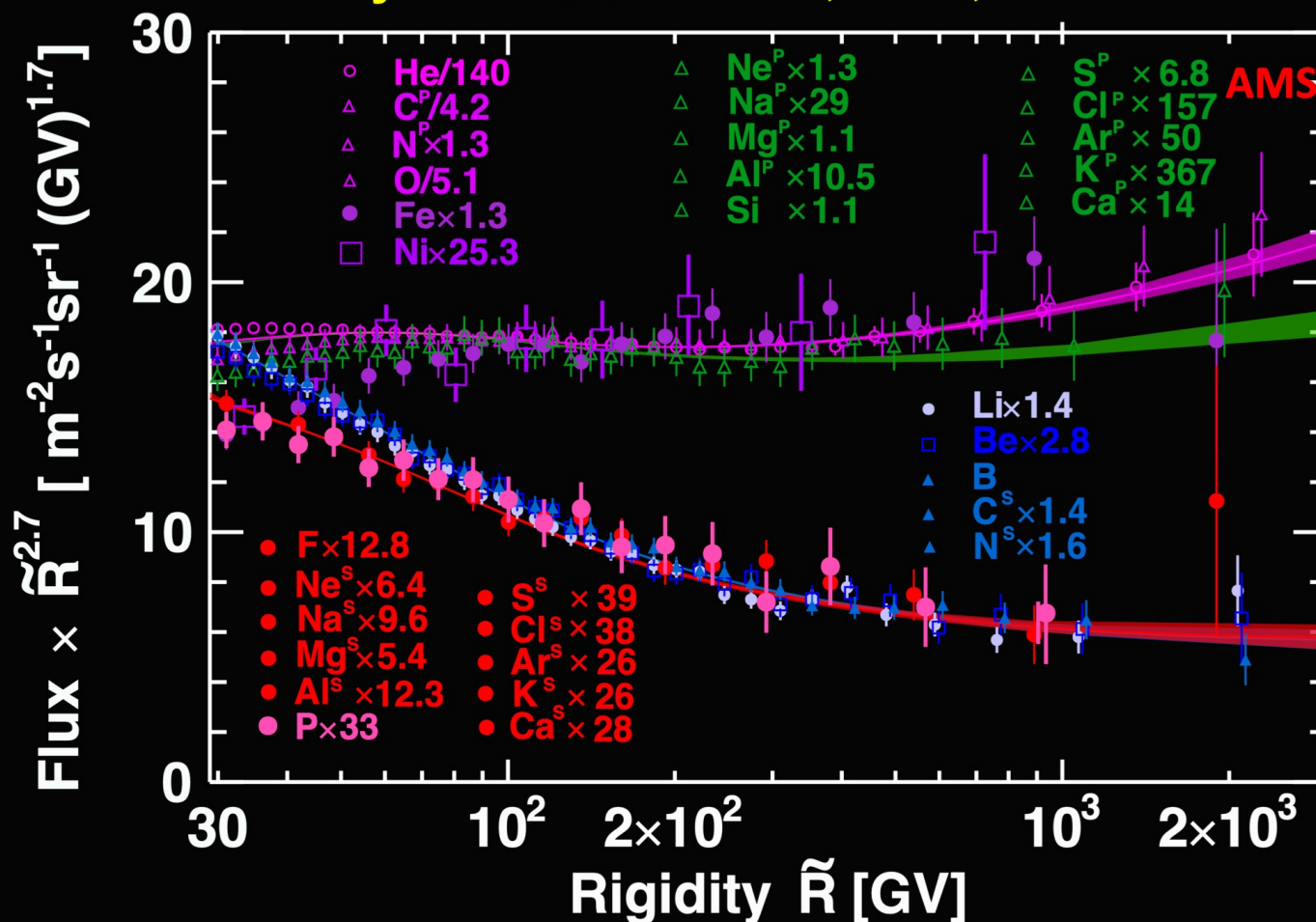


CR-composition

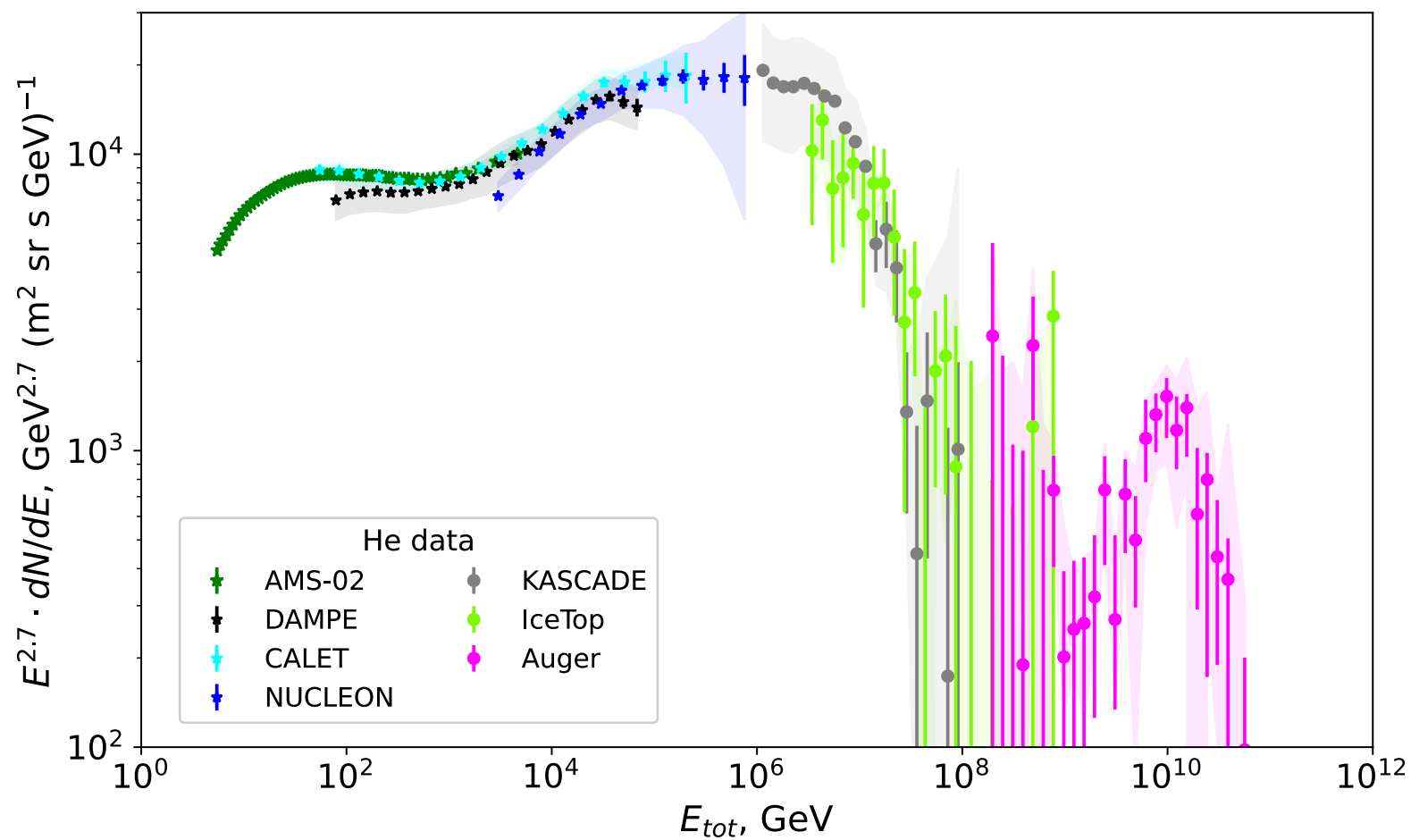


AMS-02 spectra

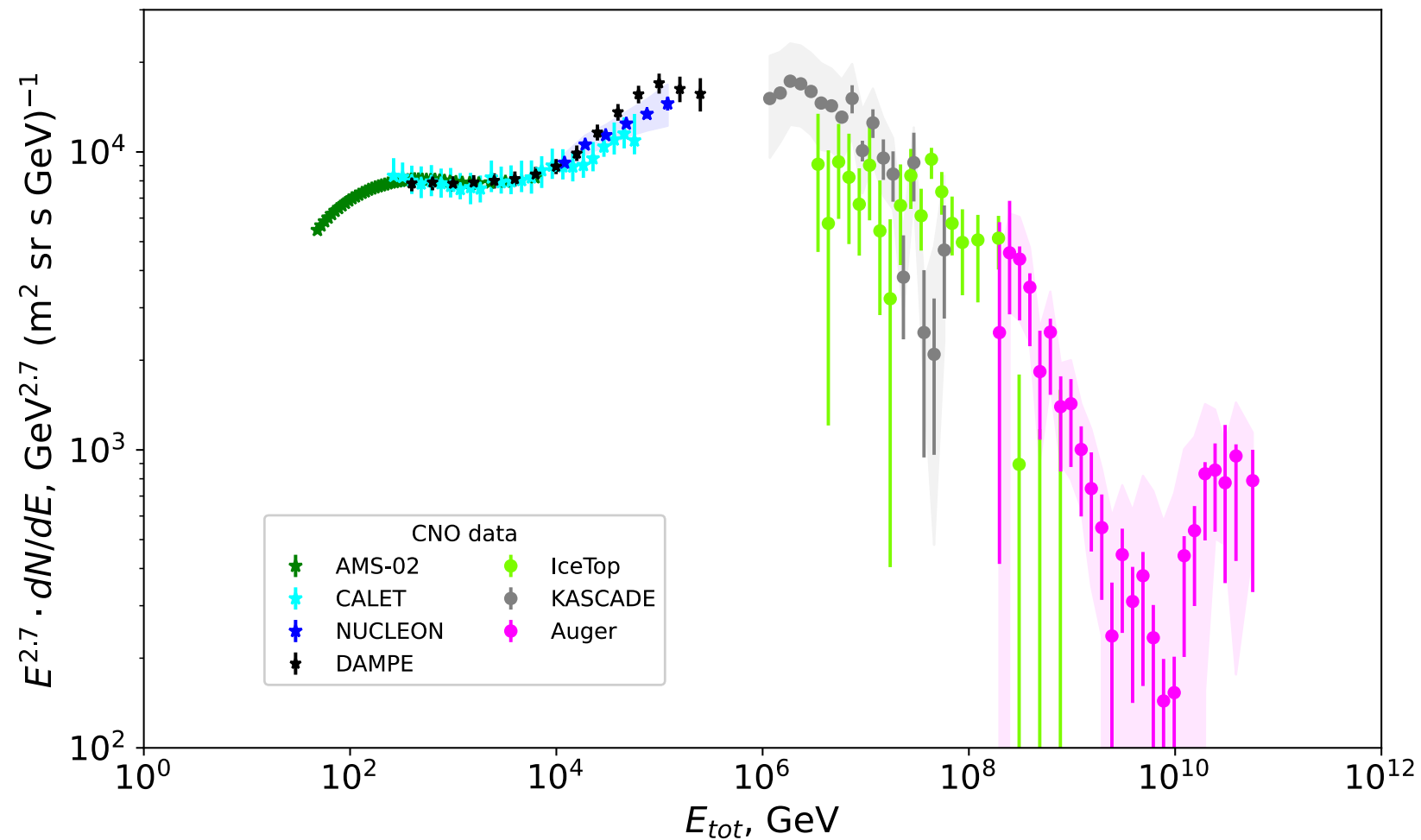
Primary and Secondary Decomposition for All Cosmic Ray Fluxes of $2 \leq Z \leq 20$, $Z=26$, $Z=28$



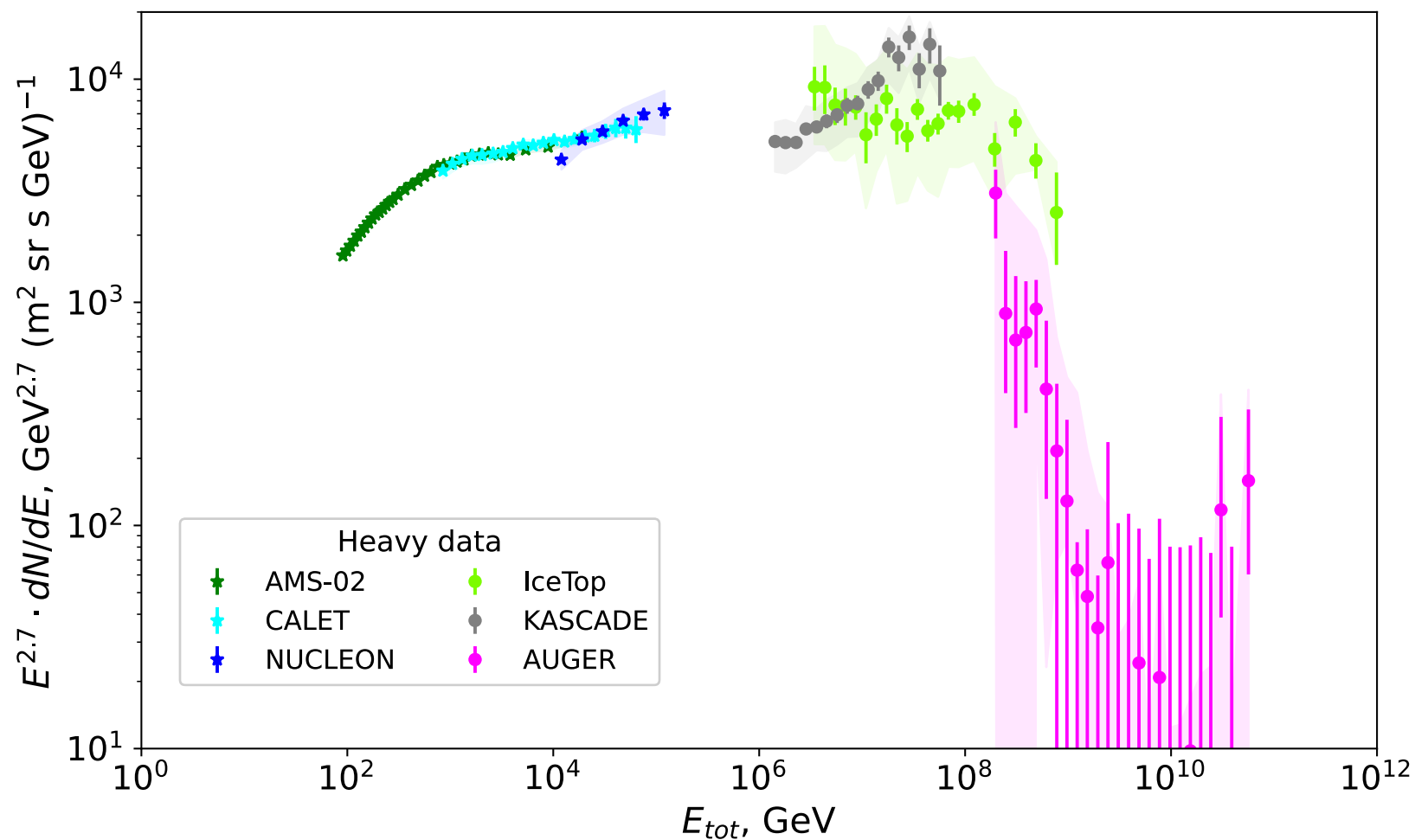
He spectrum



CNO spectrum



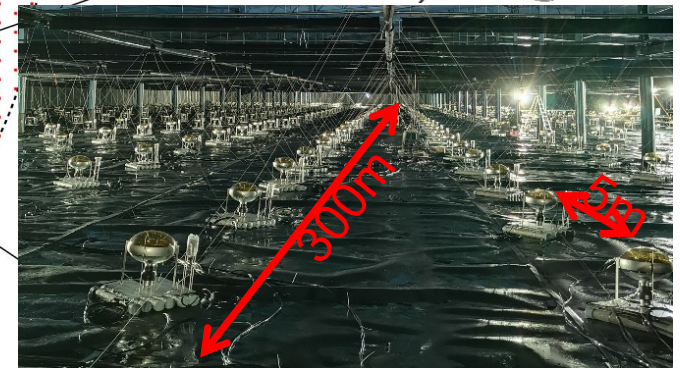
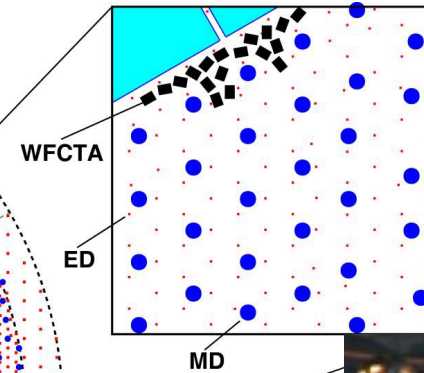
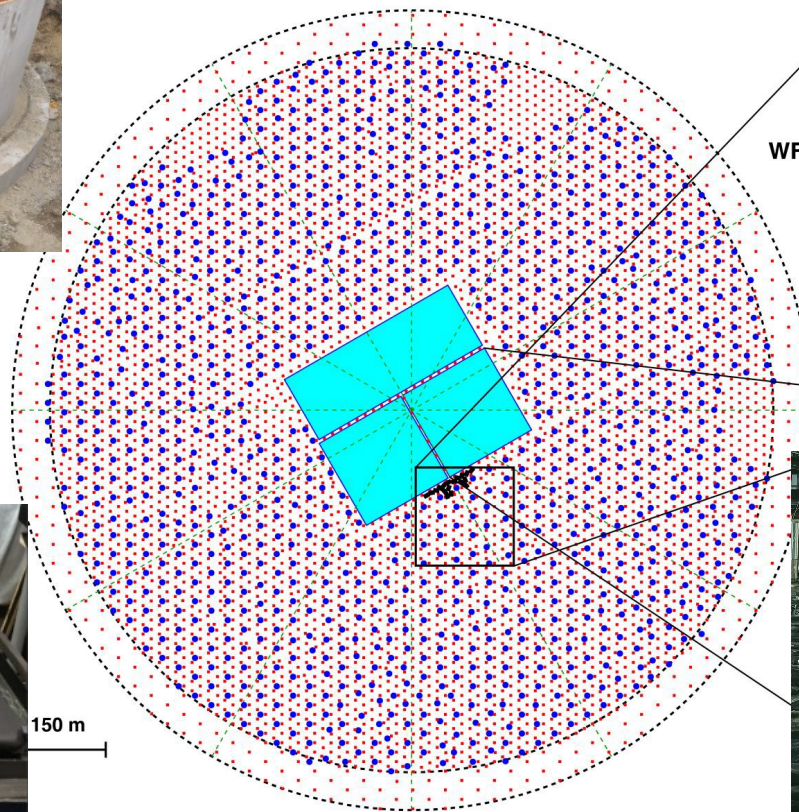
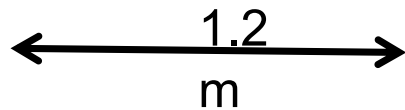
Fe spectrum





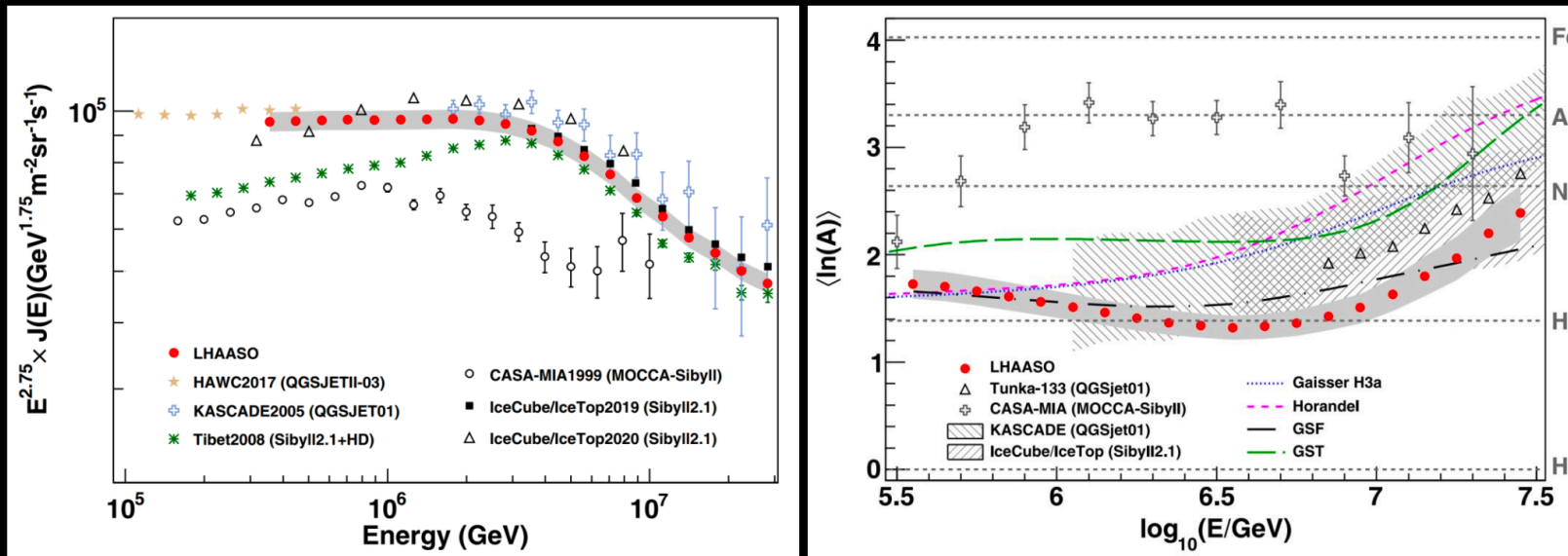
25, Searching for sources of cosmic rays Dmitri Semikoz

LHAASO: 3 types of detectors from 100 TeV



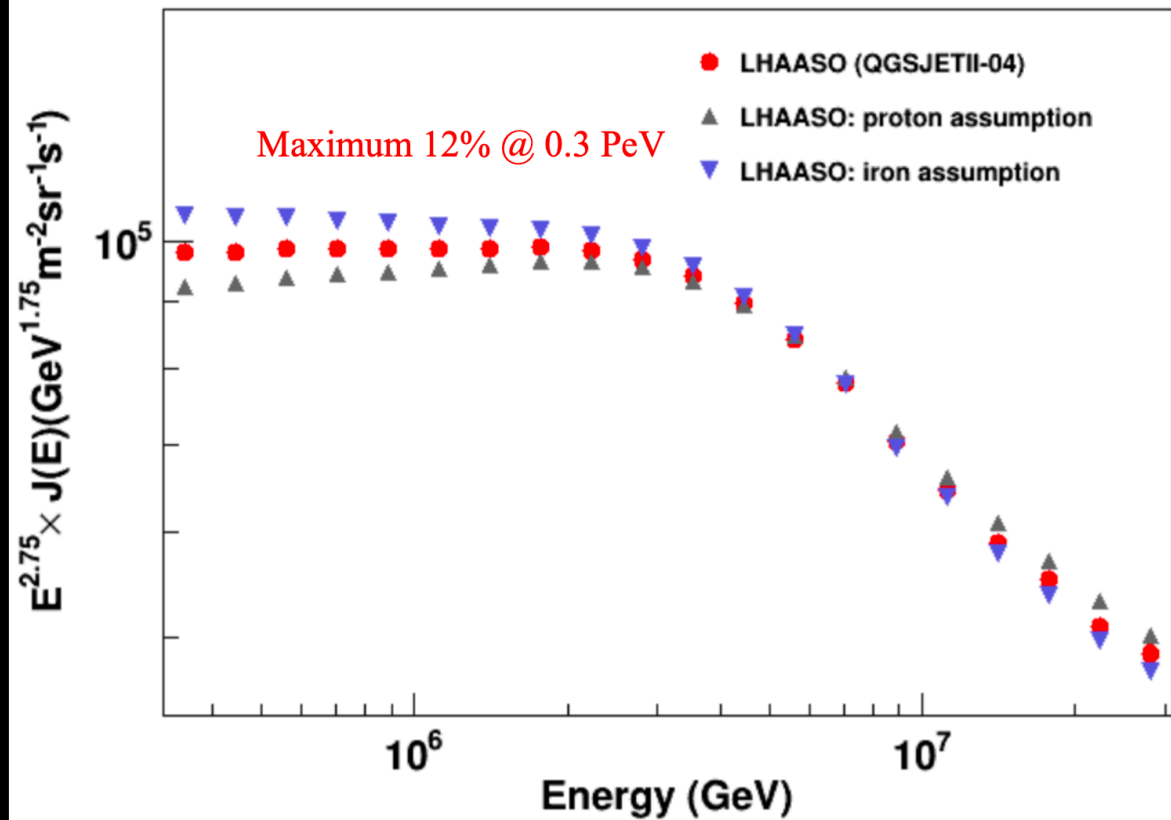
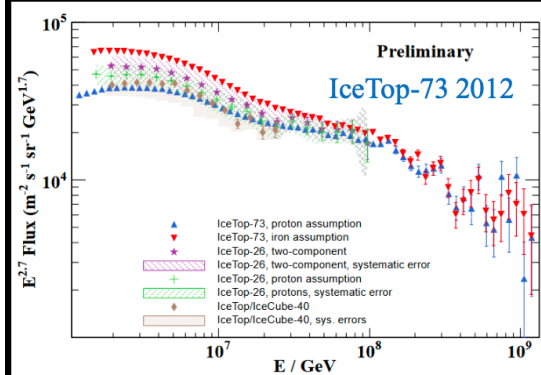
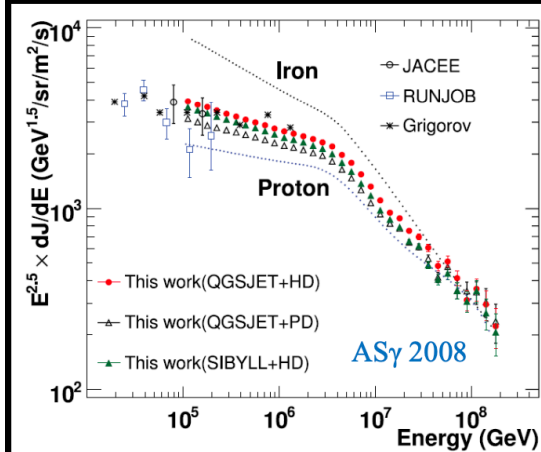
Construction finished on July 2021,
Gamma-ray results from 2019, CR results from 2024

All-particle energy spectrum & $\langle \ln A \rangle$

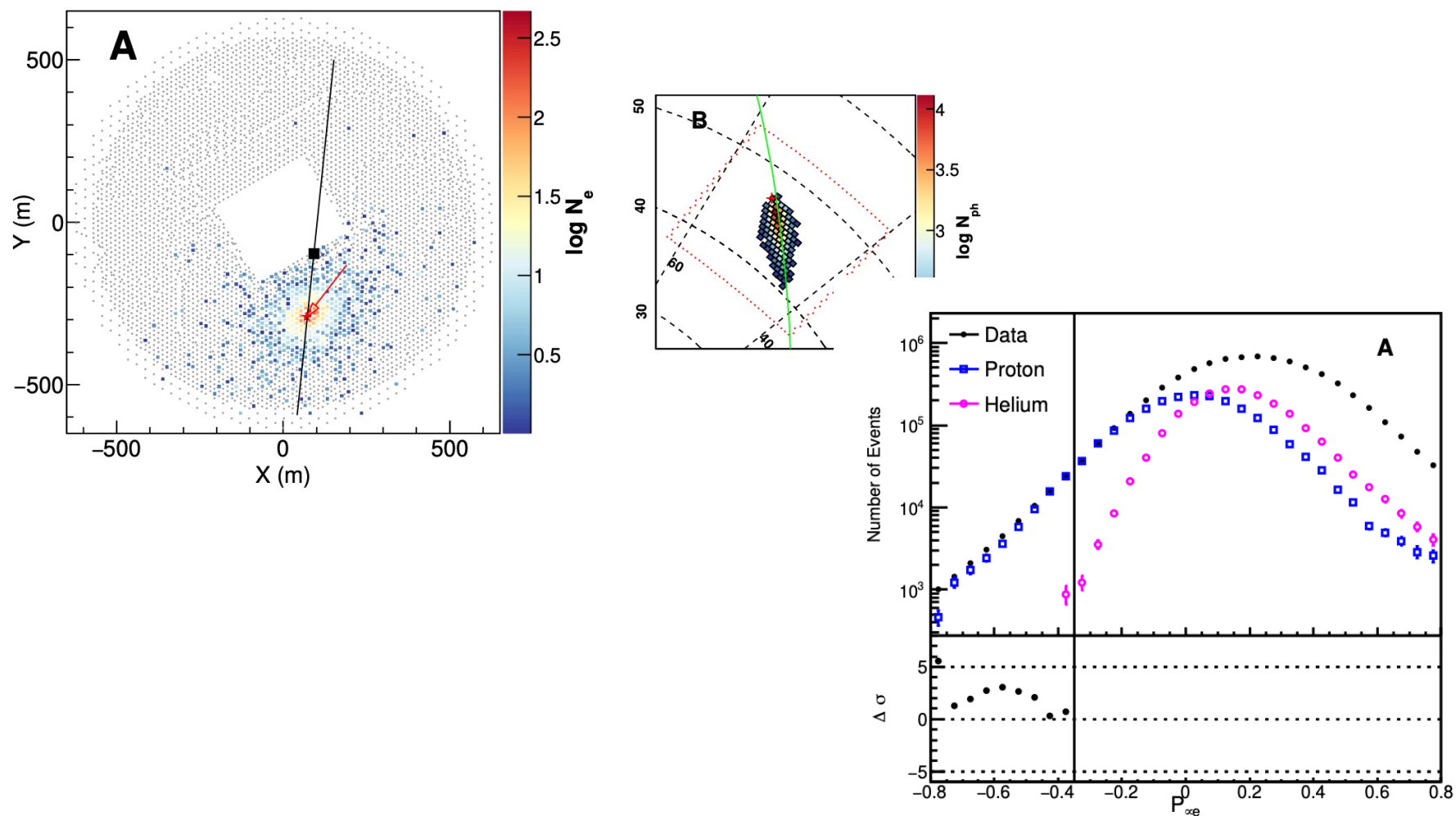


	Flux $J(E)$	$\langle \ln(A) \rangle$
Air preeure	$\pm 3\%$	$\pm 4\%$
Composition models	$\pm 1.5\%$	$\pm 3\%$
Interaction models	$\pm 2.5\%$	$\pm 6\%$

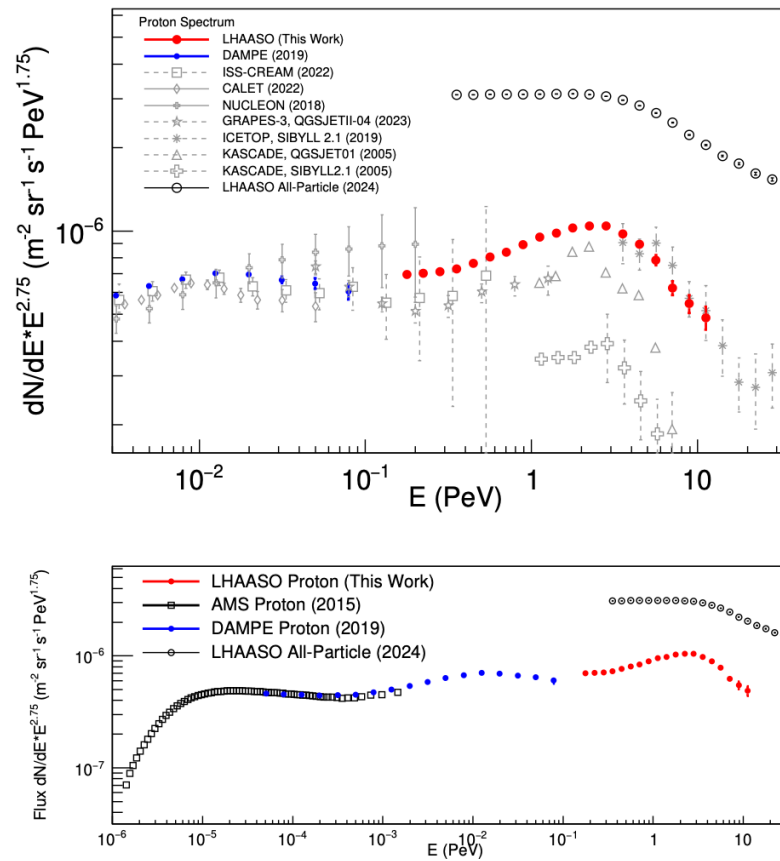
From 350%(150%) to 12%



LHAASO Proton measurement

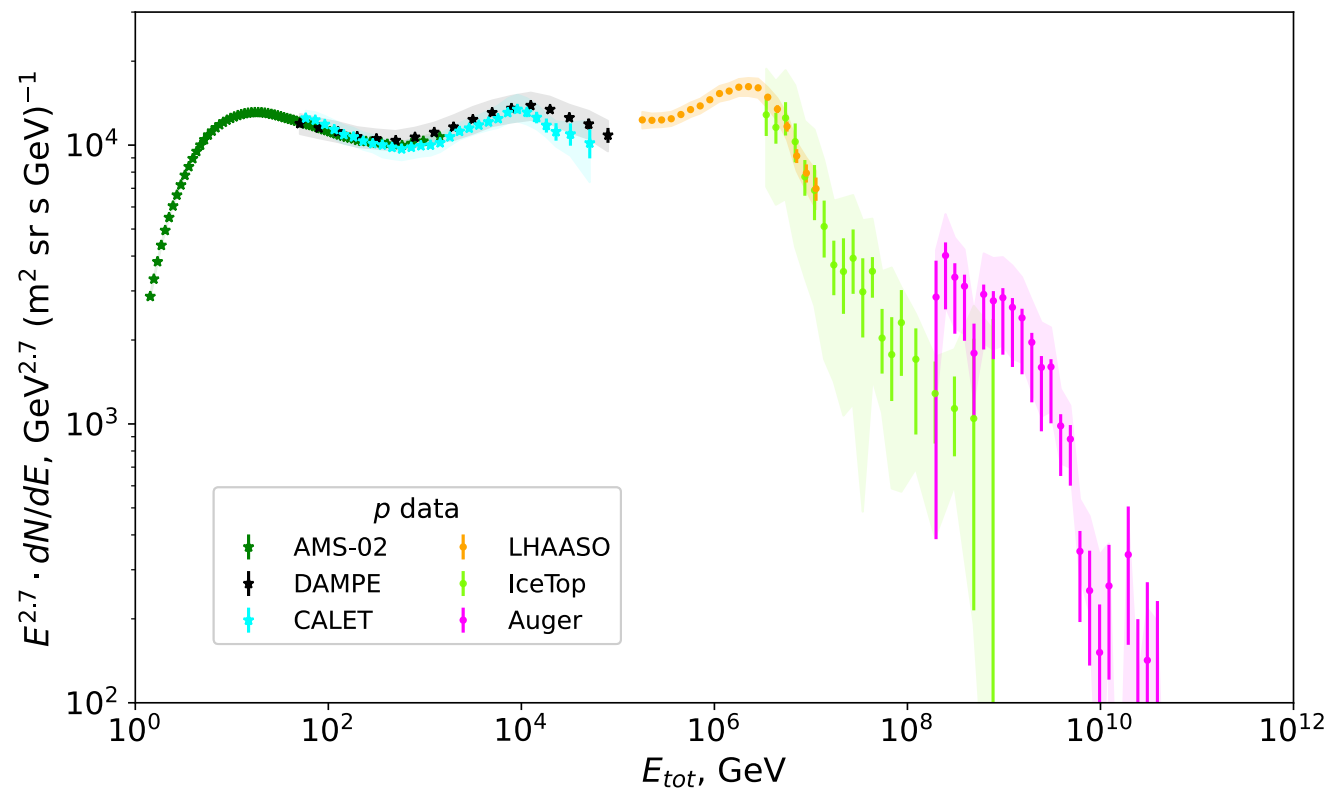


Proton spectrum

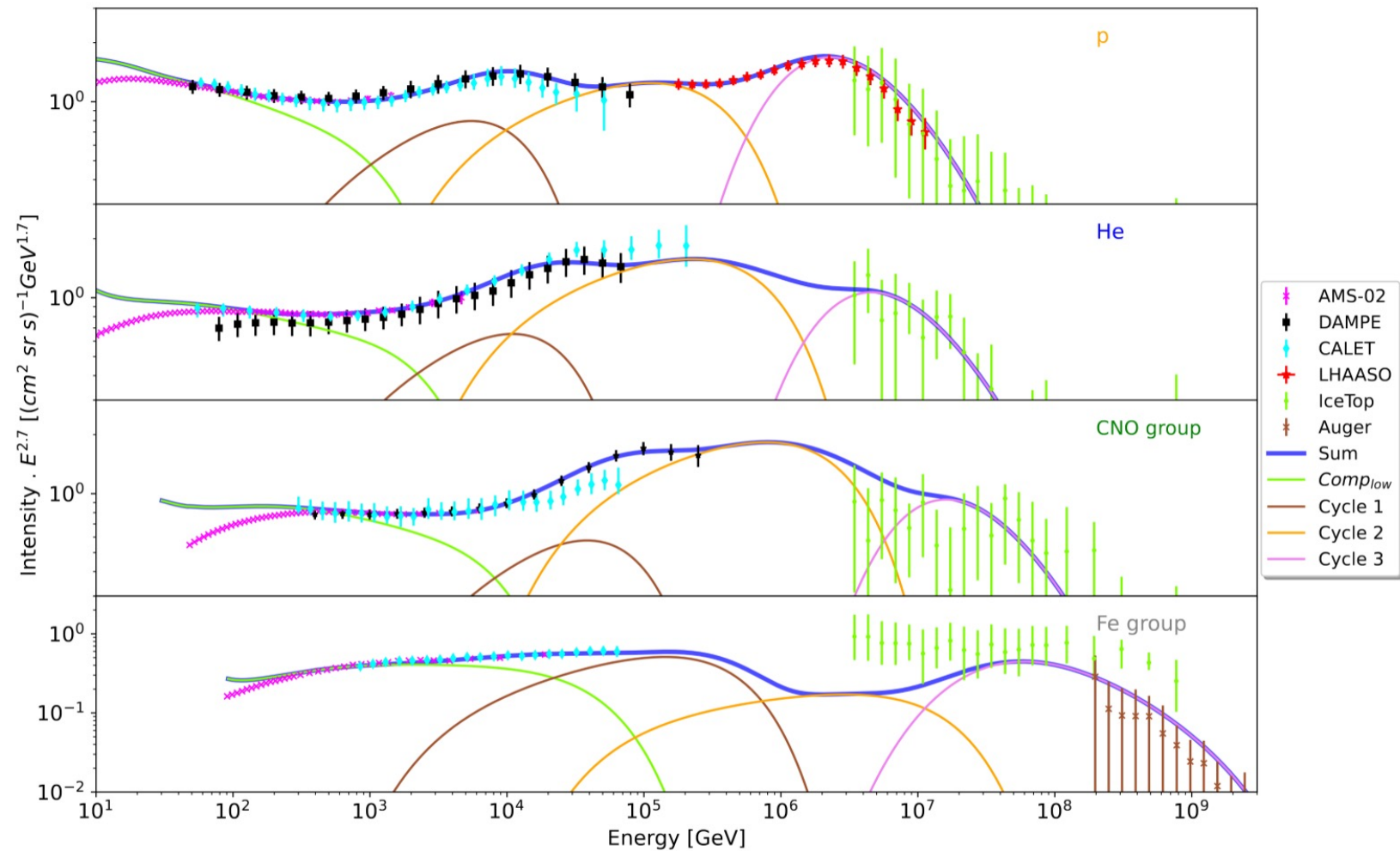


LHAASO collaboration, 2505.14447

Proton spectrum



TAUP 2025, Searching for sources of cosmic rays Dmitri Semikoz



C. Prevotat et al, [2407.11911](#), [2507.10823](#)

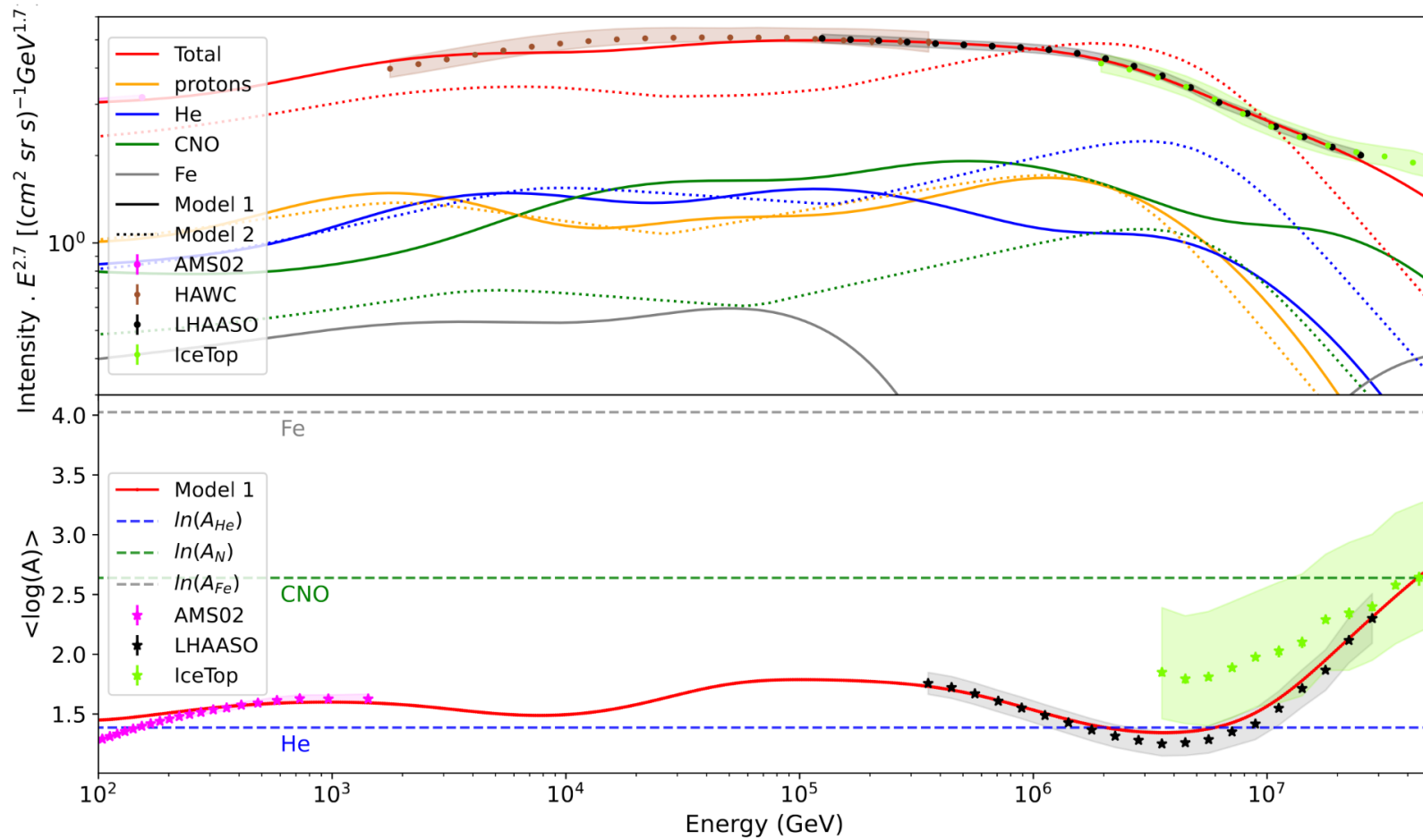
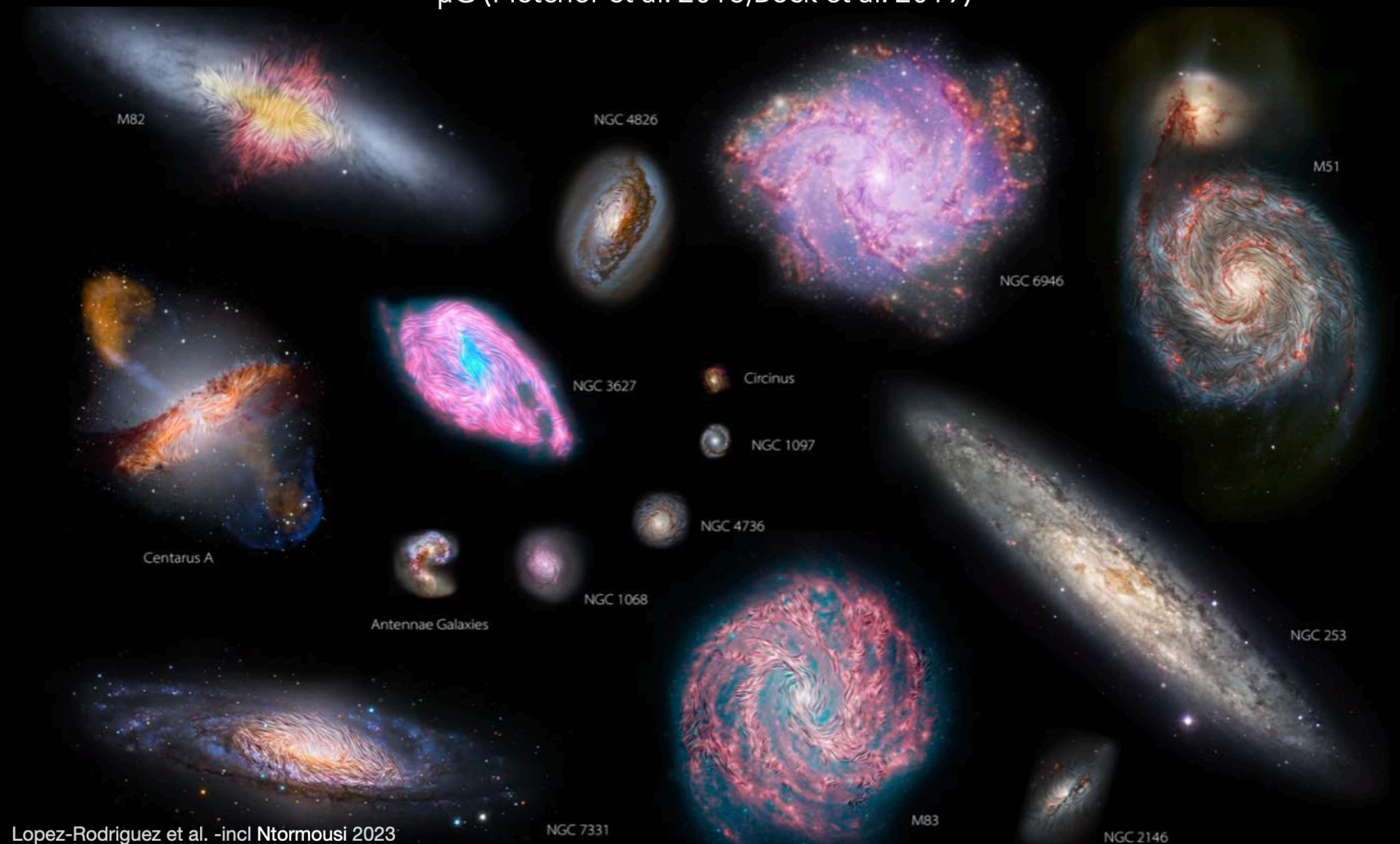


FIG. 2: Result of the fit for the all-particles spectrum, and mean logarithmic mass of the CR spectrum.

Cosmic ray propagation in Milky Way and Galactic Magnetic Field

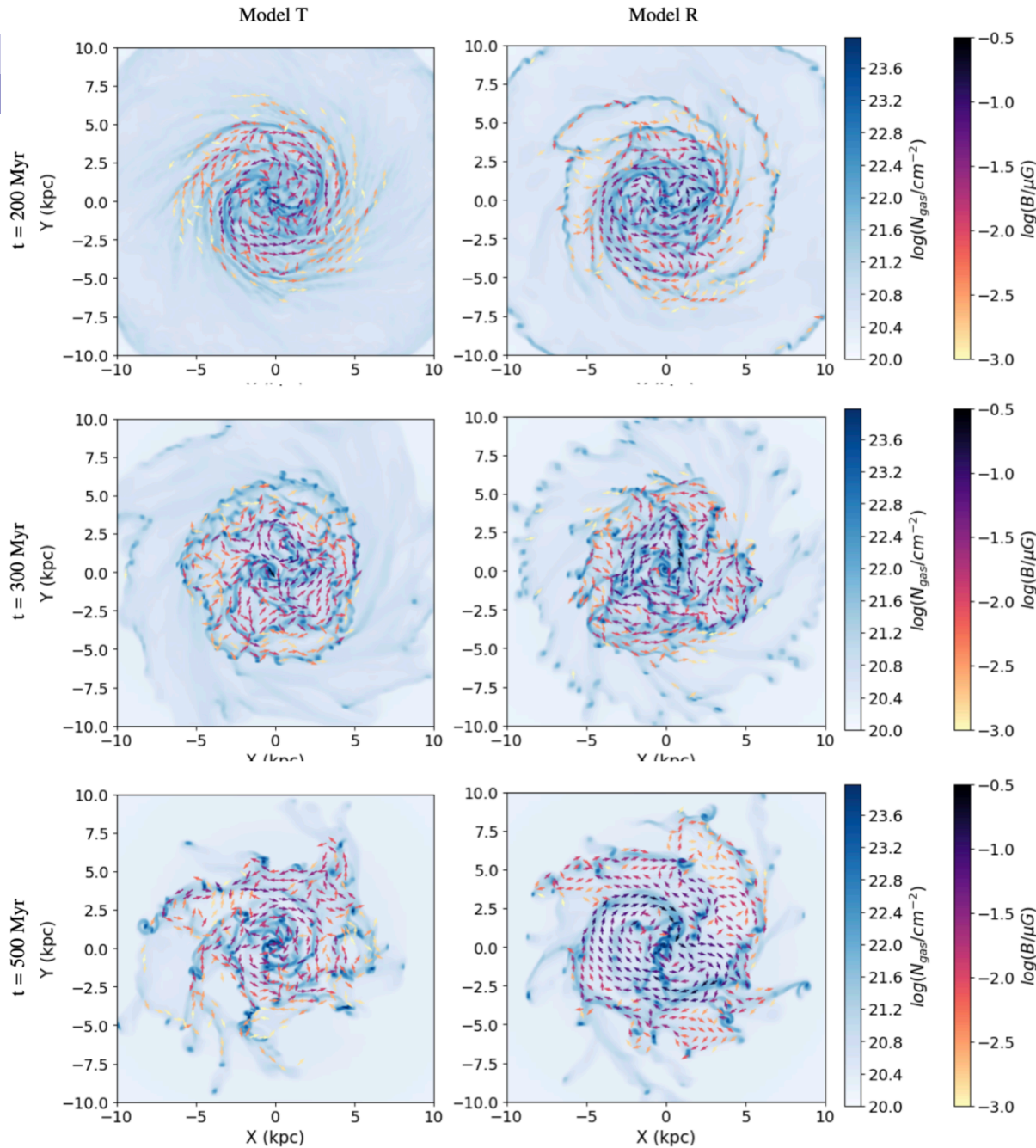
TAUP 2025, Searching for sources of cosmic rays Dmitri Semikoz

Present-day spirals host large-scale coherent magnetic fields with a typical strength of a few μG (Fletcher et al. 2016, Beck et al. 2019)



Lopez-Rodriguez et al. -incl Ntormousi 2023

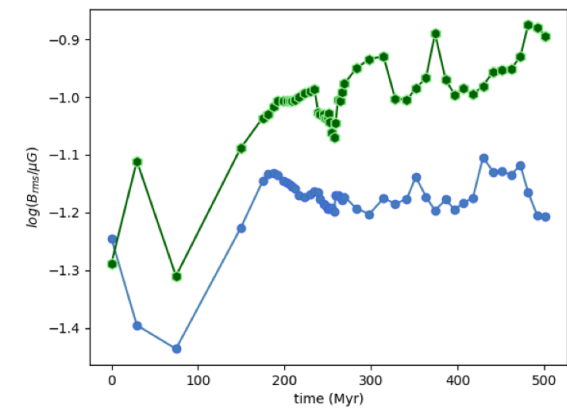
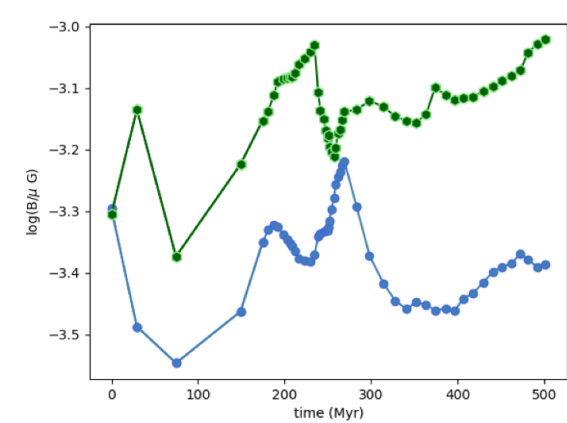
The first estimates for redshifts $z > 1$ yield fields of the order of μG already at these epochs!
(Bernet et al. 2008, Mao et al. 2017, Geach et al. 2023, Chen et al. 2024)



Subtle differences in the model evolution:

Model R is slightly larger in the radial direction

Model R's magnetic field is stronger over a wider radial range



Anti-symmetric RM sky: halo B fields = A0 dynamo

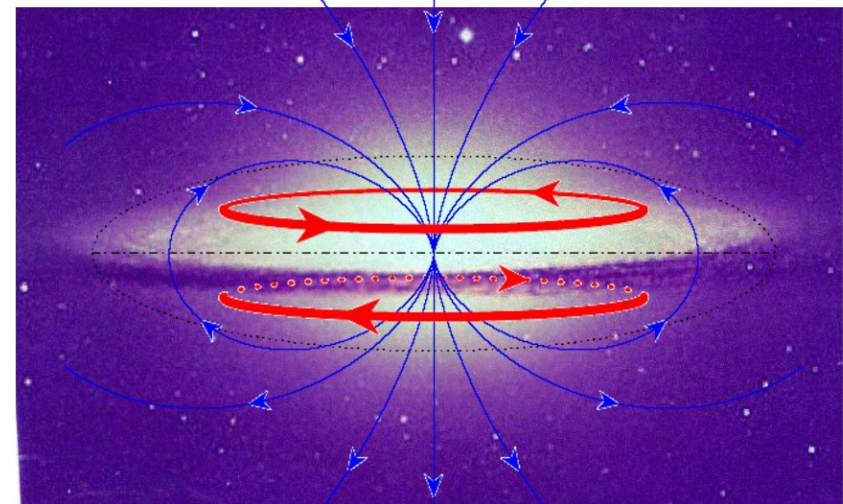
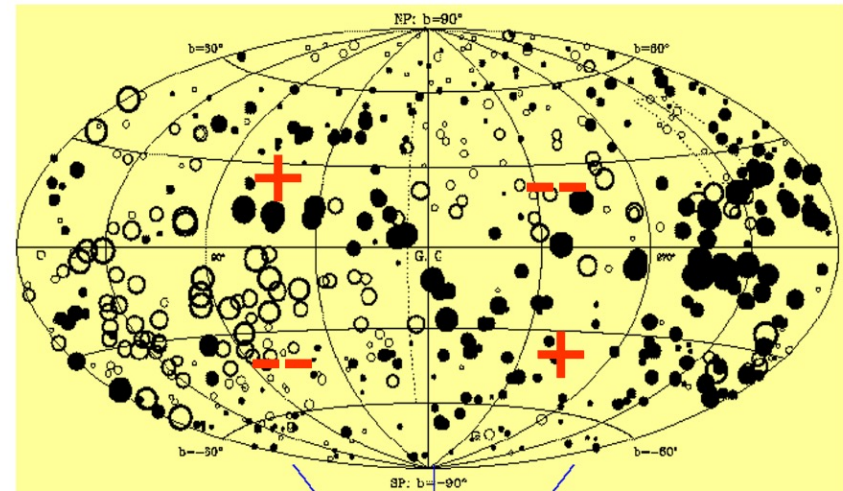
(Han et al. 1997, A&A322, 98)

Evidence for global scale B

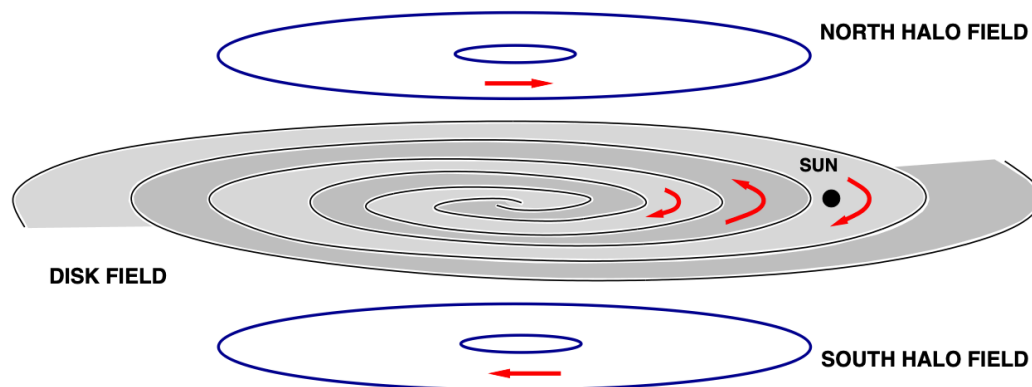
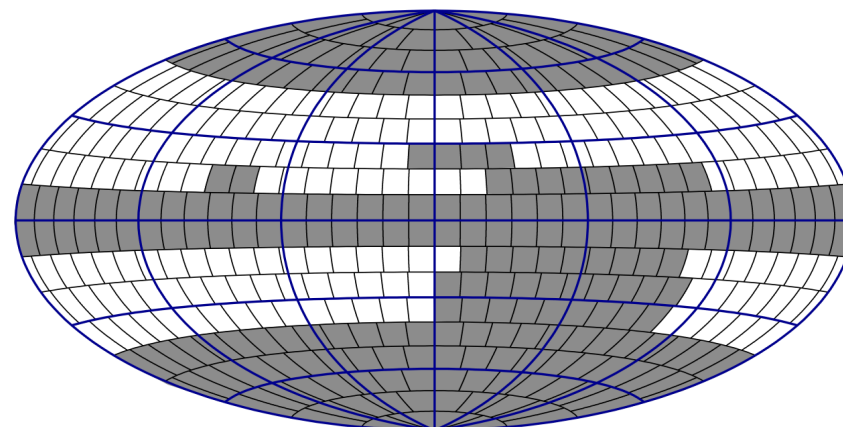
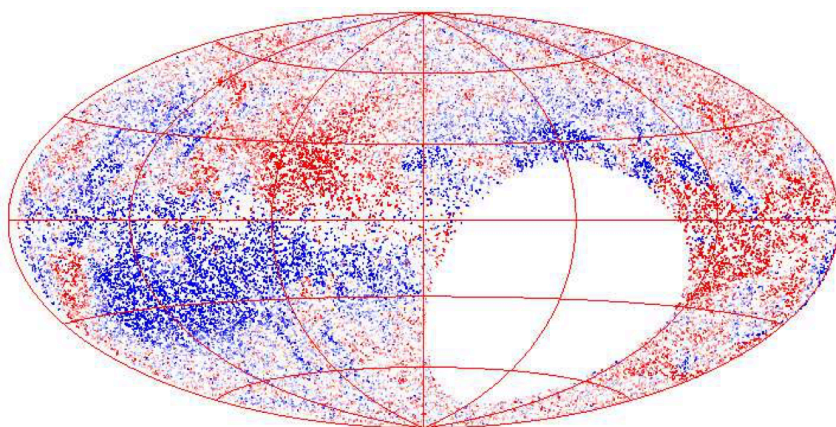
- High anti-symmetry to the Galactic coordinates
- Only in inner Galaxy
- nearby pulsars show it at higher latitudes

Implications

- Consistent with B-field configuration of A0 dynamo
- The first dynamo mode identified on galactic scales



Rotation measure

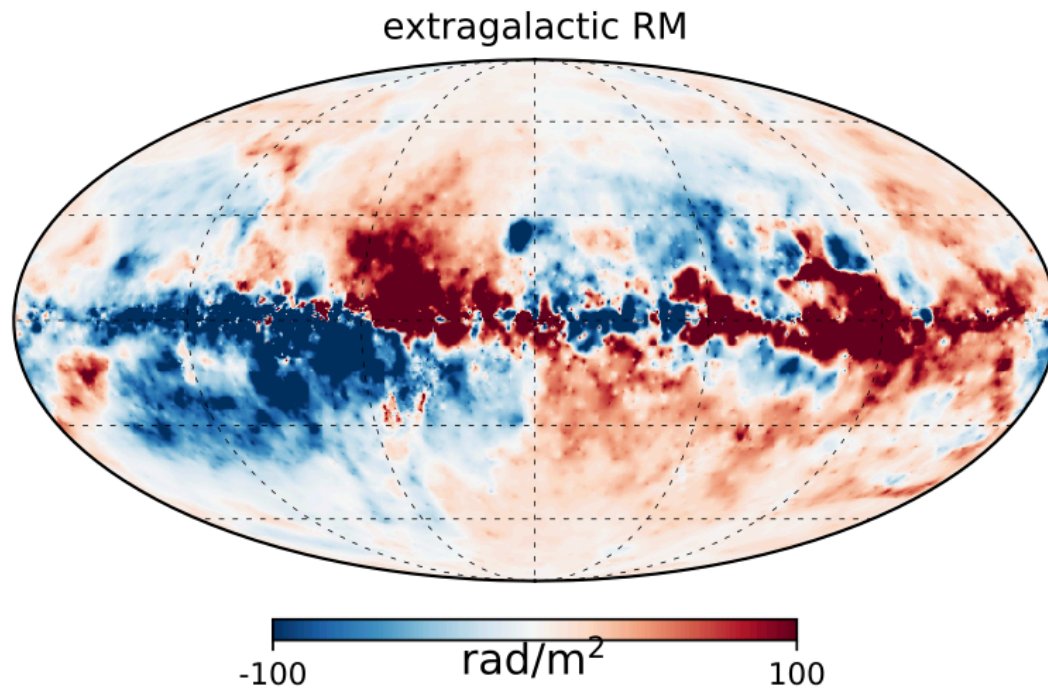


$$\text{RM} \approx 0.812 \int_0^l \left[\frac{n_e(s)}{\text{cm}^{-3}} \right] \left[\frac{B_{\parallel}(s)}{10^{-6} \text{ G}} \right] \left[\frac{ds}{\text{pc}} \right] \text{ rad/m}^2.$$

Pshirkov, Tinyakov, Kronberg
and Newton-McGee

model 2011

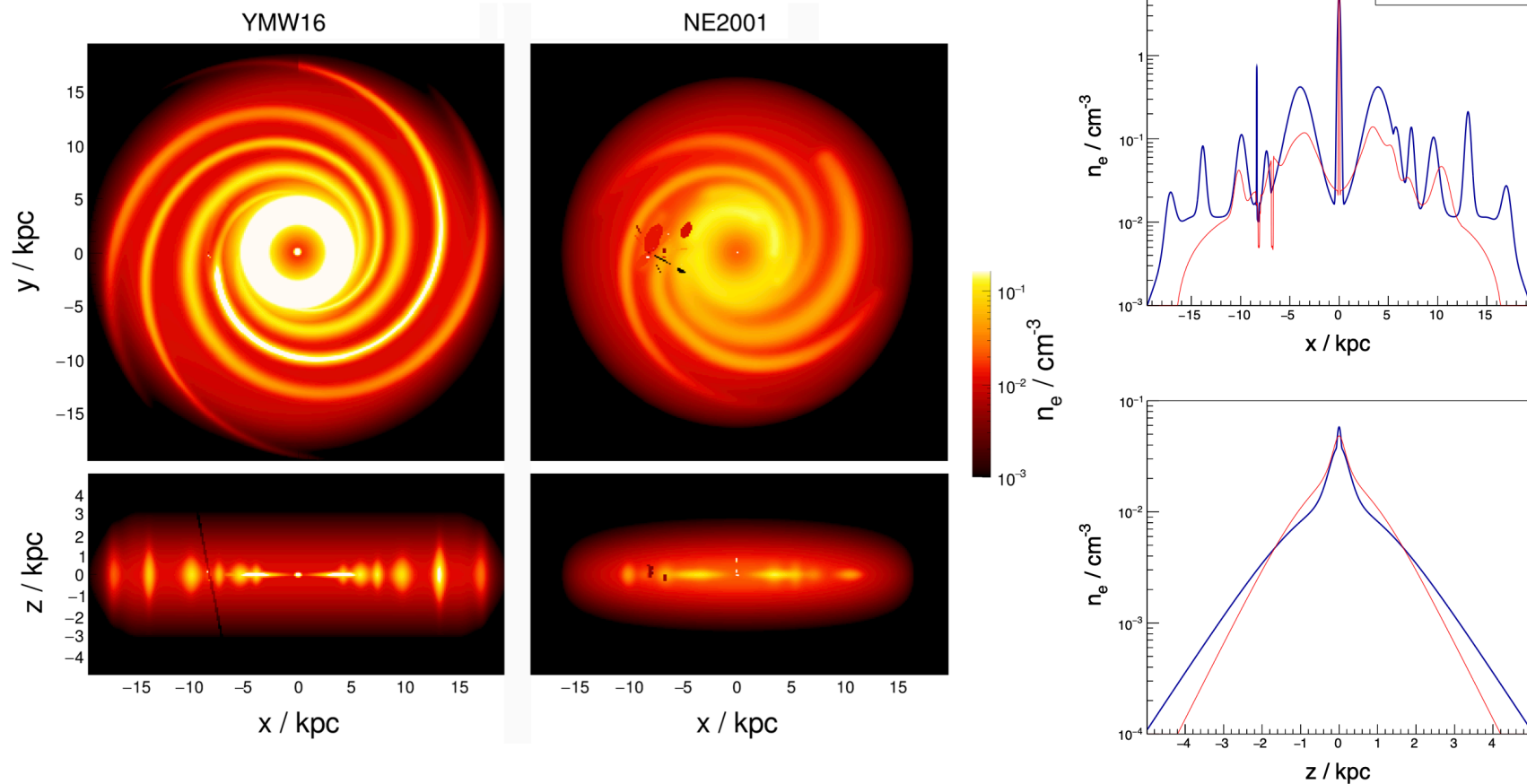
ROTATION MEASURE



60000 extragalactic objects

$$\text{RM} \approx 0.812 \int_0^l \left[\frac{n_e(s)}{\text{cm}^{-3}} \right] \left[\frac{B_{\parallel}(s)}{10^{-6} \text{ G}} \right] \left[\frac{ds}{\text{pc}} \right] \text{ rad/m}^2.$$

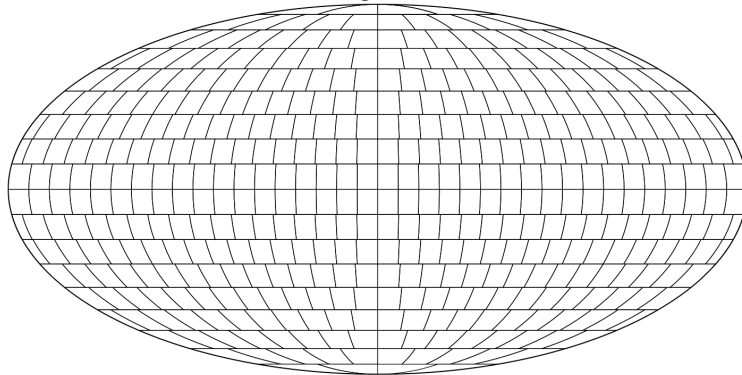
Thermal electrons model



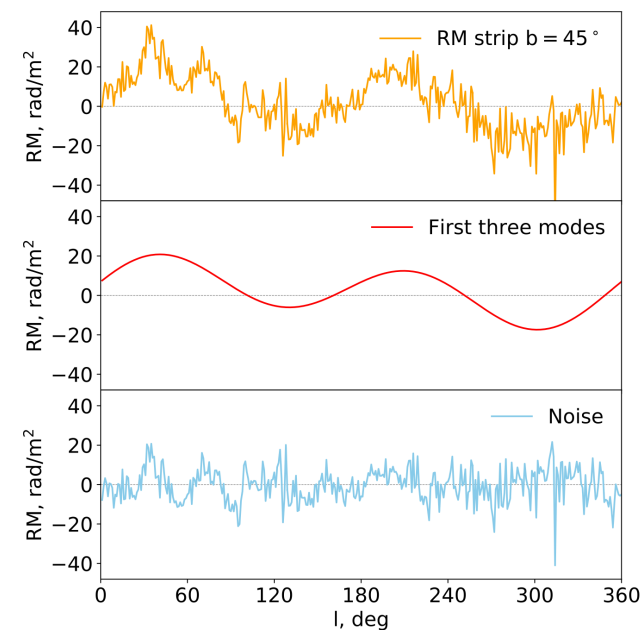
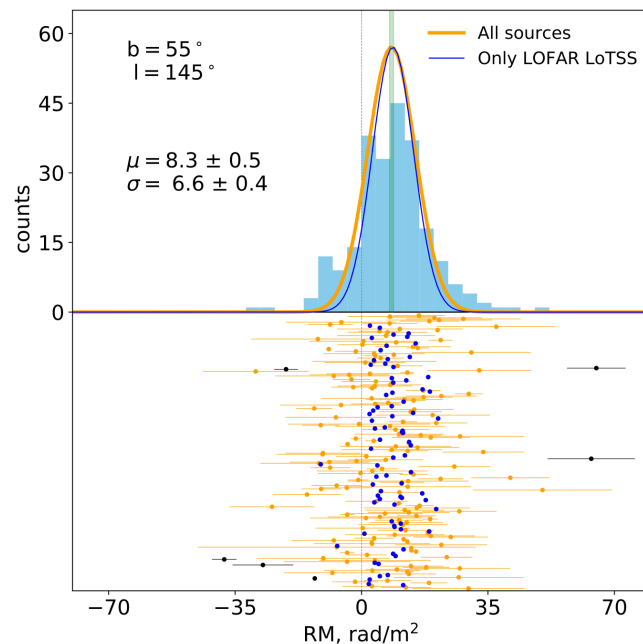
From M.Unger and G.Farrar 2311.12120

Model RM

binning scheme



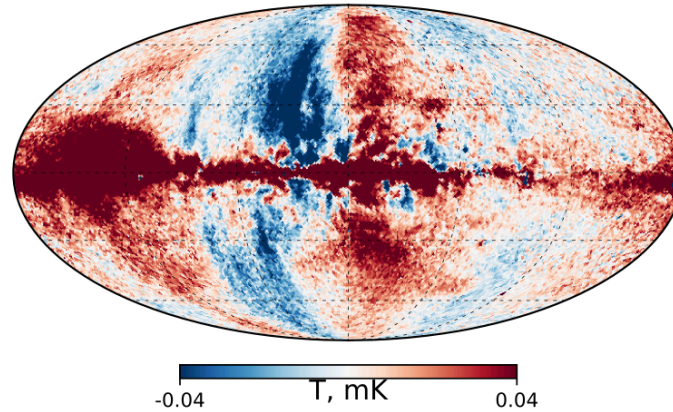
	χ^2	χ^2/ndf	ndf	χ^2_{var}	$\chi^2_{\text{var}}/\text{ndf}$
RM	544	1.92	283	145	0.51
Q	385	1.11	348	238	0.68
U	482	1.38	348	251	0.72
total	1411	1.36	1037	634	0.61



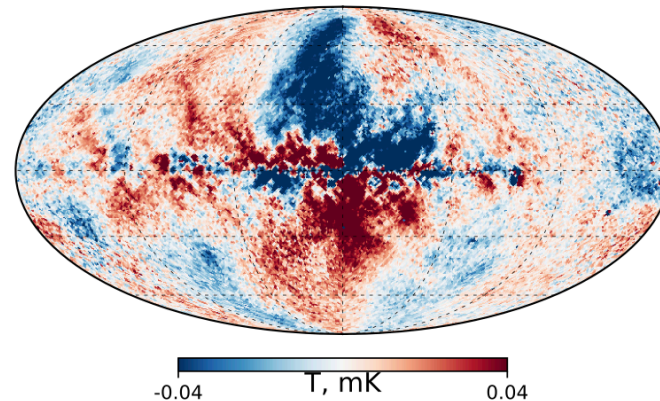
Synchrotron radiation

$$\nu_c \approx 1.6 \left[\frac{B_{\perp}}{10^{-6} \text{ G}} \right] \left[\frac{E}{10 \text{ GeV}} \right]^2 \text{ GHz.}$$

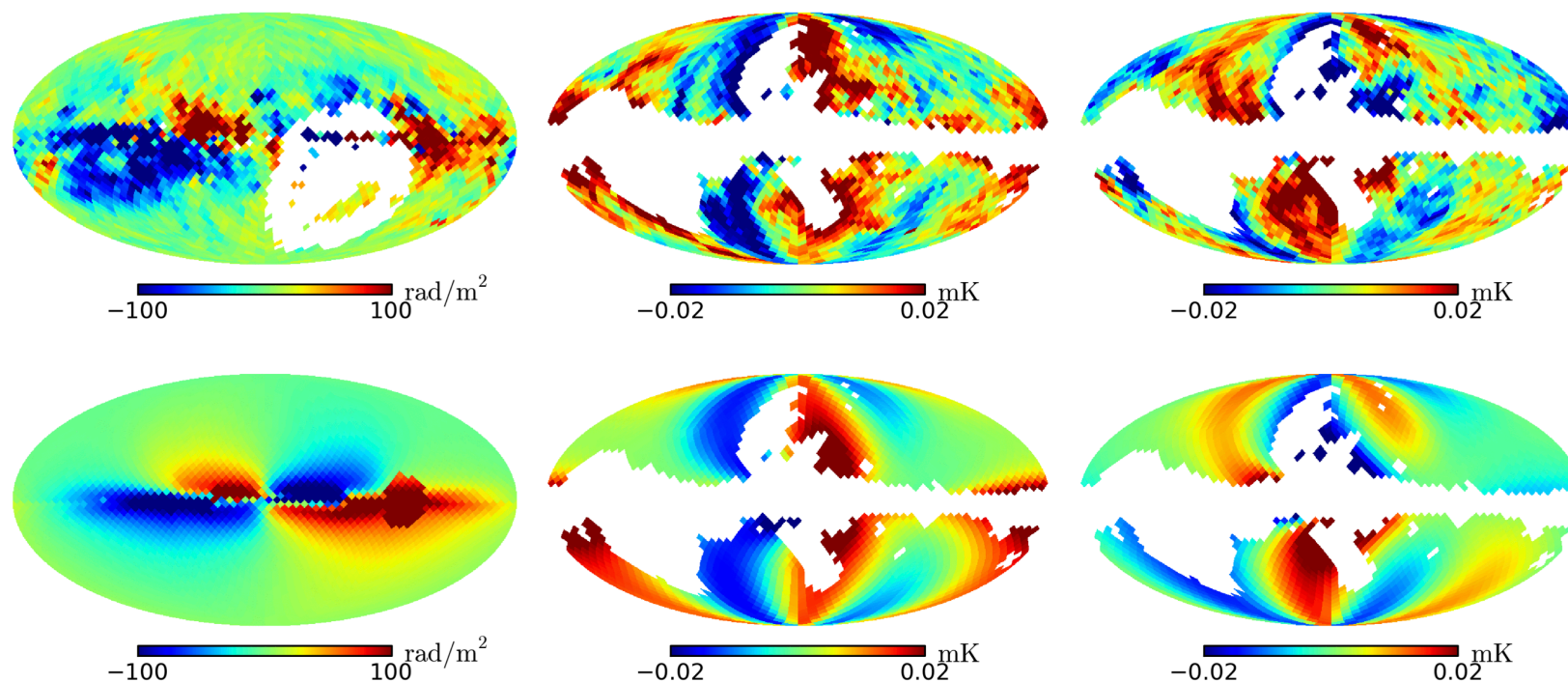
WMAP 23 GHz, Stokes Q



WMAP 23 GHz, Stokes U

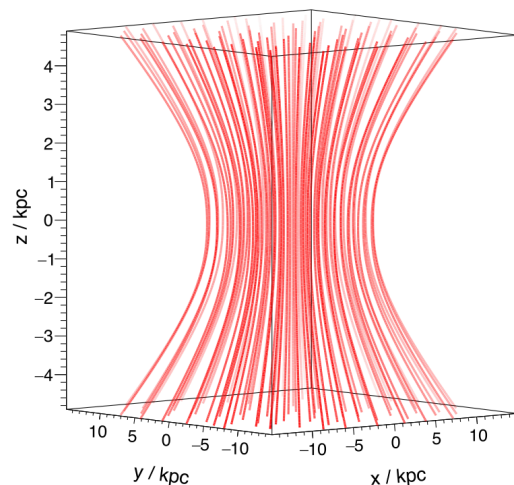


Jansson-Farrar 2012 model

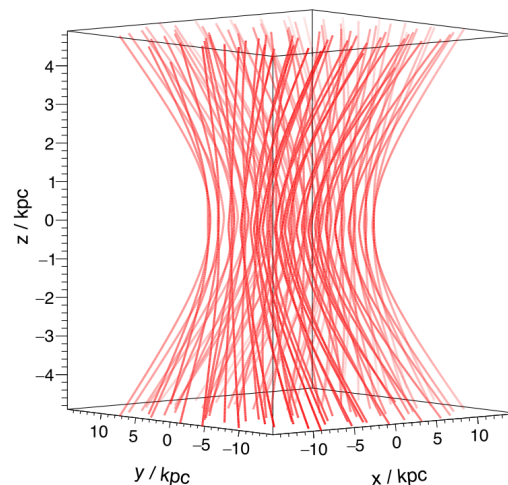


X-shape field, torroidal halo field, disc with spiral arms

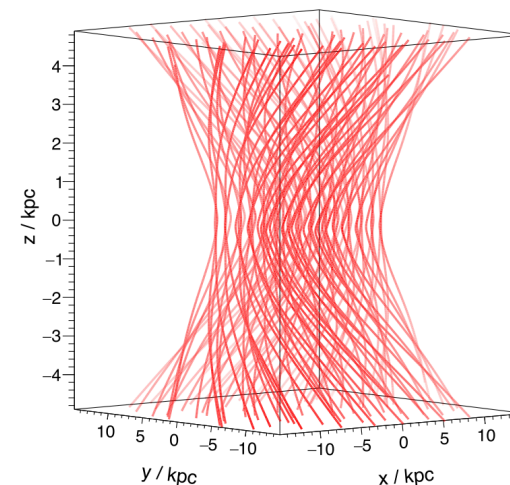
Dynamical halo model



a: $t = 0$ Myr

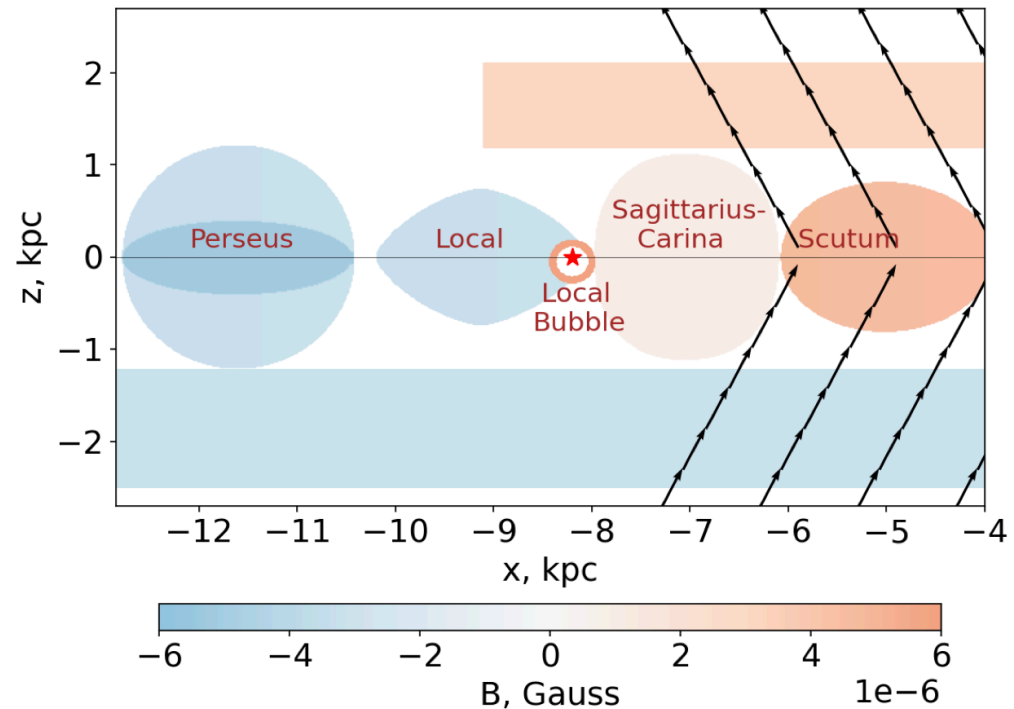
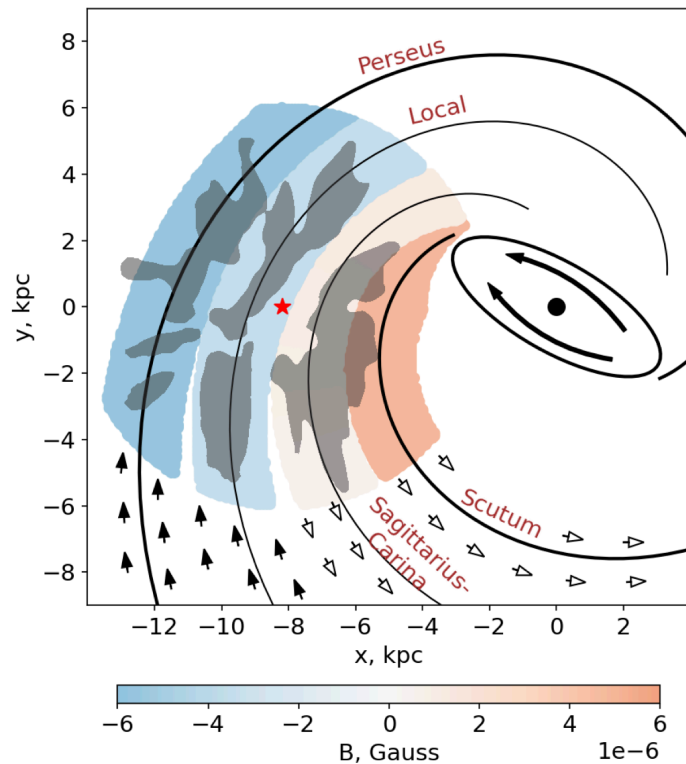


b: $t = 25$ Myr

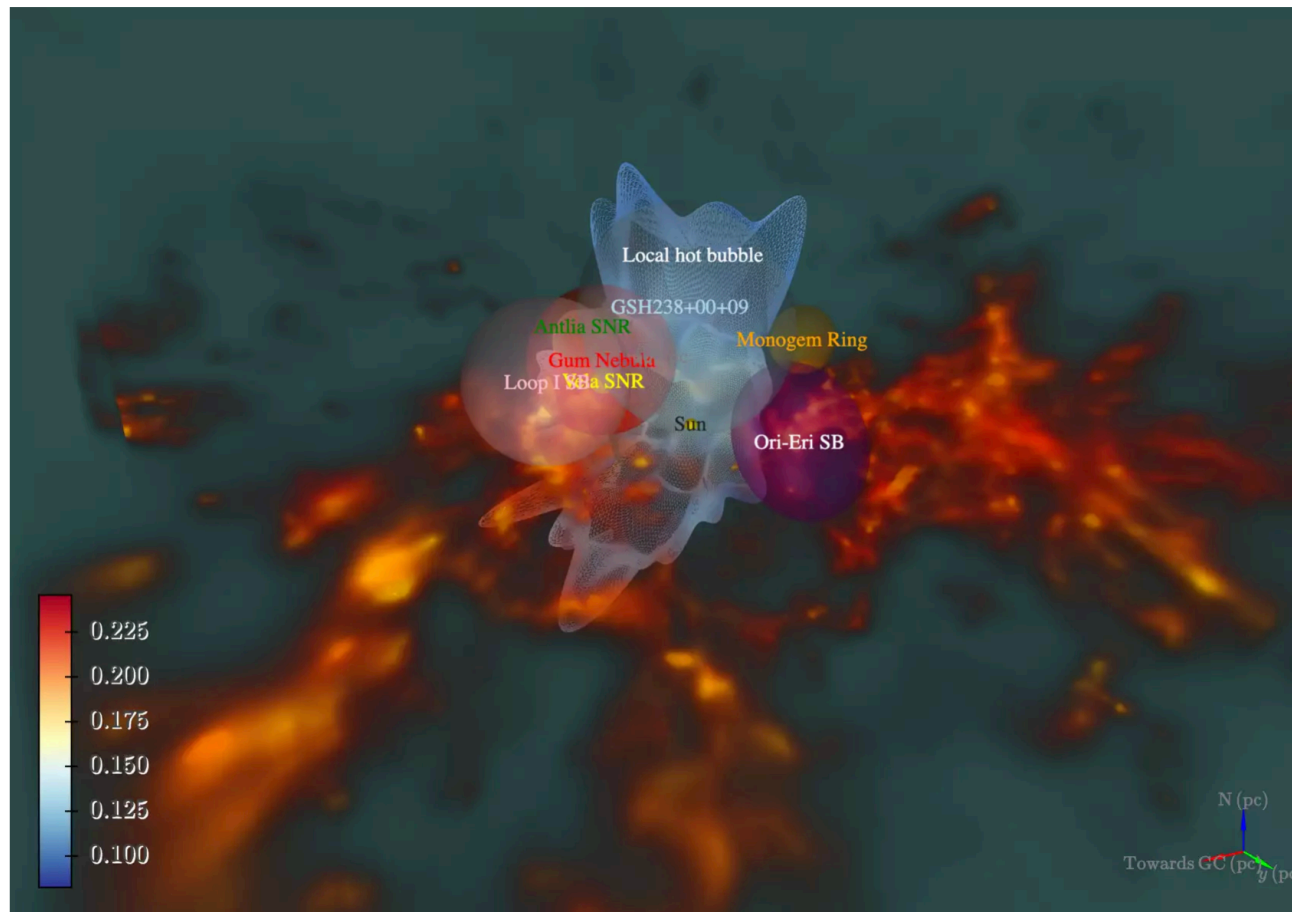


c: $t = 50$ Myr

GMF models: Local Bubble



Local Bubble

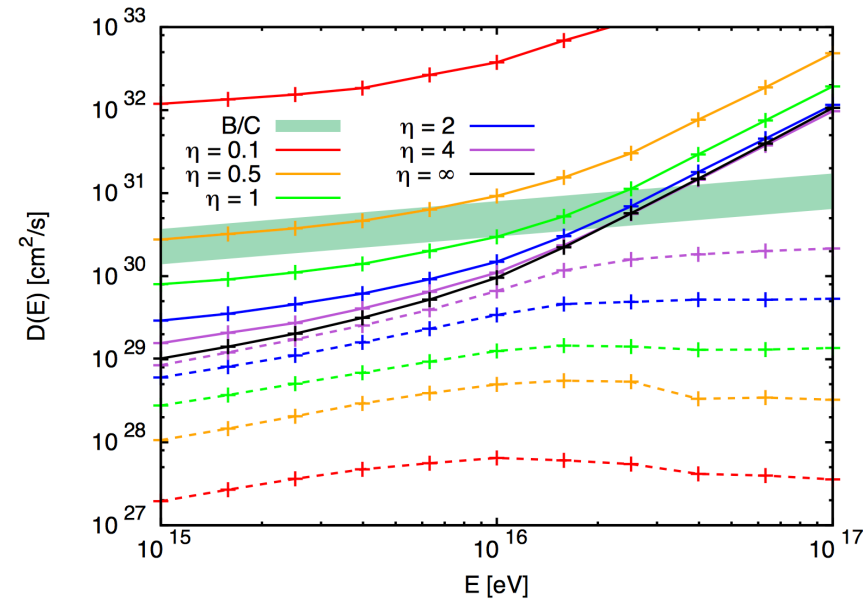
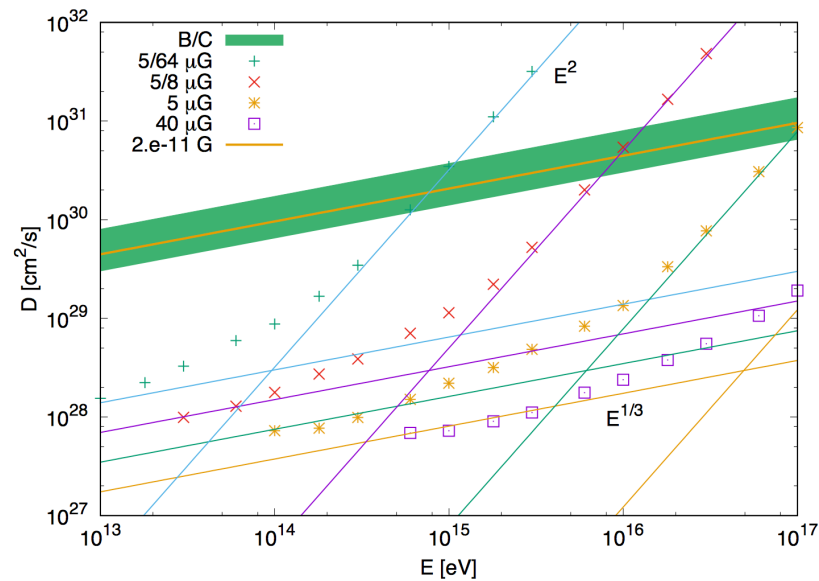


3D model of the solar neighbourhood. The colour bar represents the temperature of the LHB as coloured on the LHB surface. The direction of the Galactic Centre (GC) and Galactic North (N) is shown in the bottom right. The link to the interactive version can be found at the bottom of the page.

[\[less\]](#)

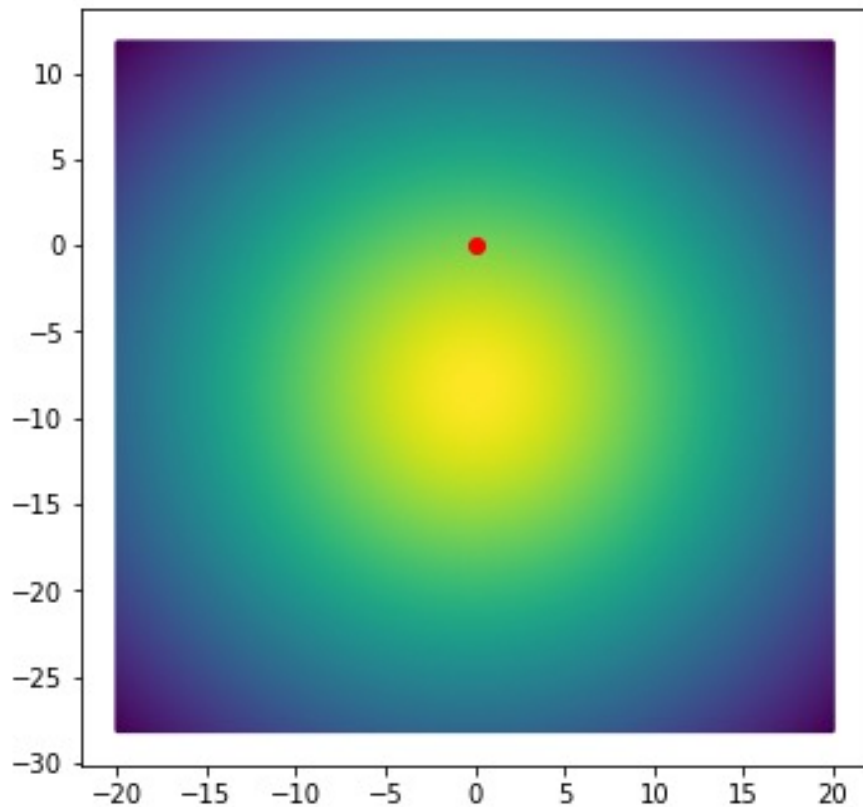
© Michael Yeung / MPE

Escape of CR and magnetic field

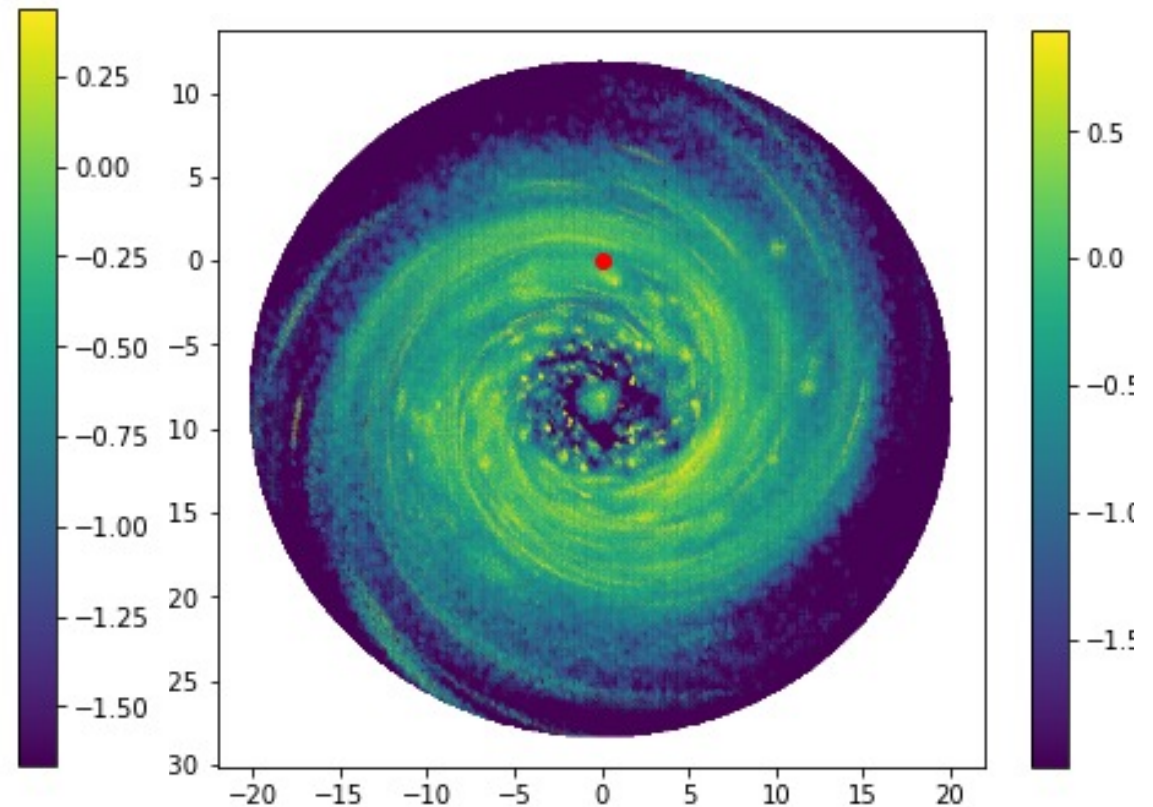


Giacinti et al, 1710.08205

1 PeV CR density in the Gal. plane



P.Lipari & S.Vernetto
(2018)



G.Giacinti & D.S., 2305.10251

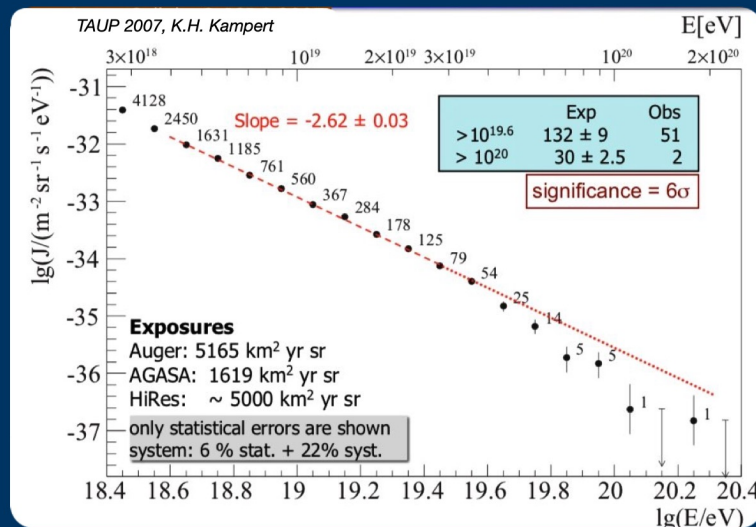
Search for the Sources of Ultra-High Energy Cosmic Rays

Spectrum Auger

Energy spectrum, from $\approx 5000 \text{ km}^2 \text{ sr y}$ to $\approx 100000 \text{ km}^2 \text{ sr y}$

A 20x exposure allows the discovery of a new feature in the energy spectrum...

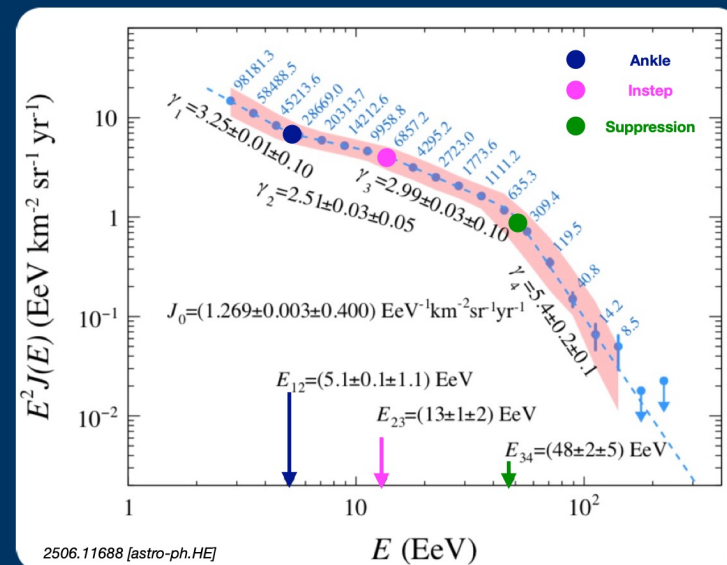
2007



SD-1500: Full efficiency at $3 \times 10^{18} \text{ eV}$
 $\approx 5000 \text{ km}^2 \text{ sr y}$ (AGASAx3)
 ≈ 12000 events ($0-60^\circ$)

Observation of a suppression at $\approx 5 \times 10^{19} \text{ eV}$ (6σ)

2025



SD: Full efficiency at $3 \times 10^{18} \text{ eV}$
 $\approx 105000 \text{ km}^2 \text{ sr y}$ [20x]
 ≈ 310000 events ($0-80^\circ$) [25x]

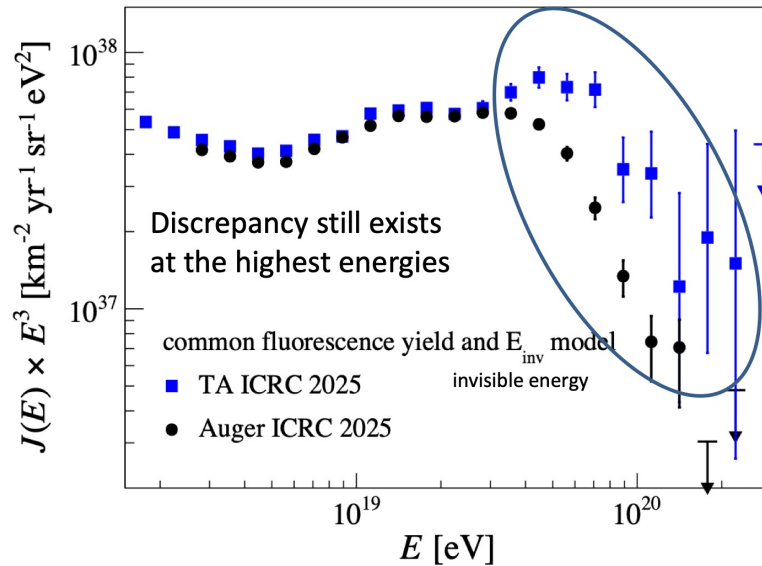
Discovery of a new feature (instep, 5.5σ)

Spectrum Auger/TA

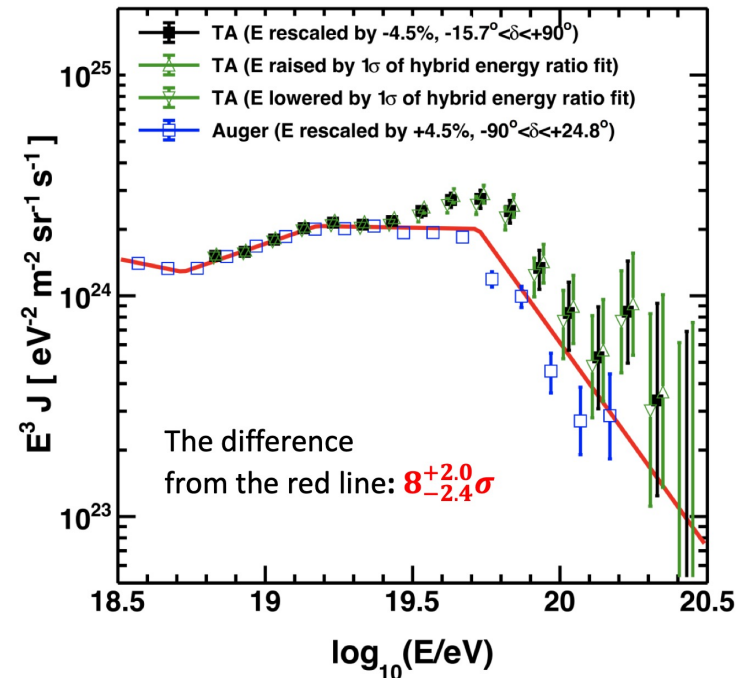
Comparison of TA SD energy spectra

F. Salamida,
ICRC2025

Auger+TA spectrum working group



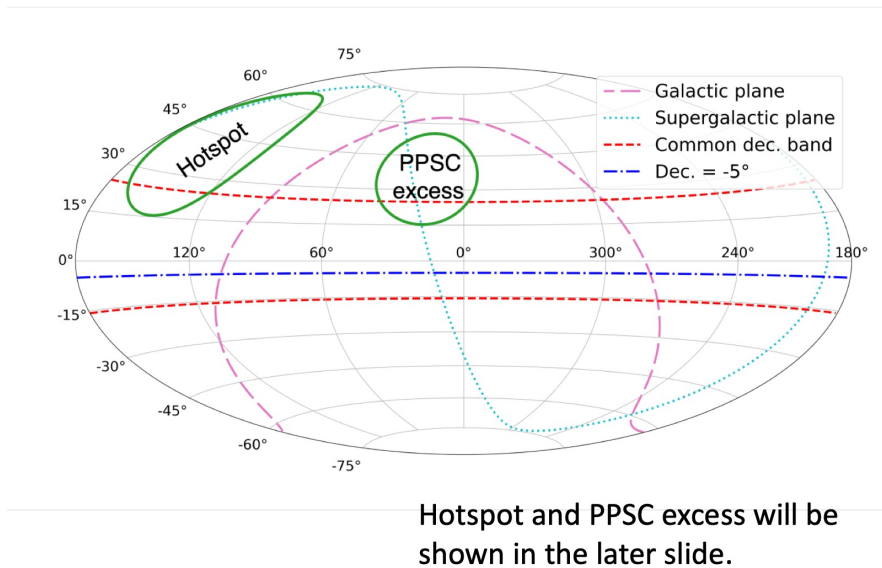
J. Kim,
ICRC2025



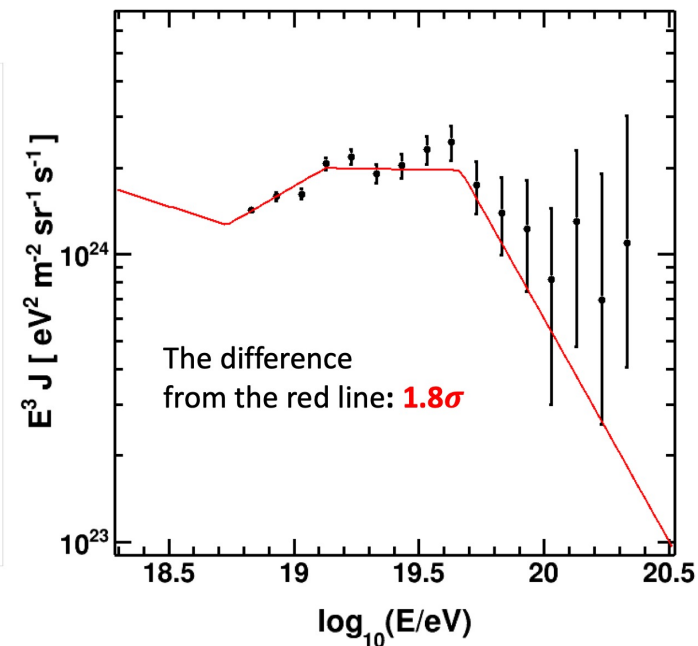
Spectrum Auger/TA

Energy spectrum in $-5^\circ < \delta < 24.8^\circ$ + excess region cuts

J. Kim,
ICRC2025

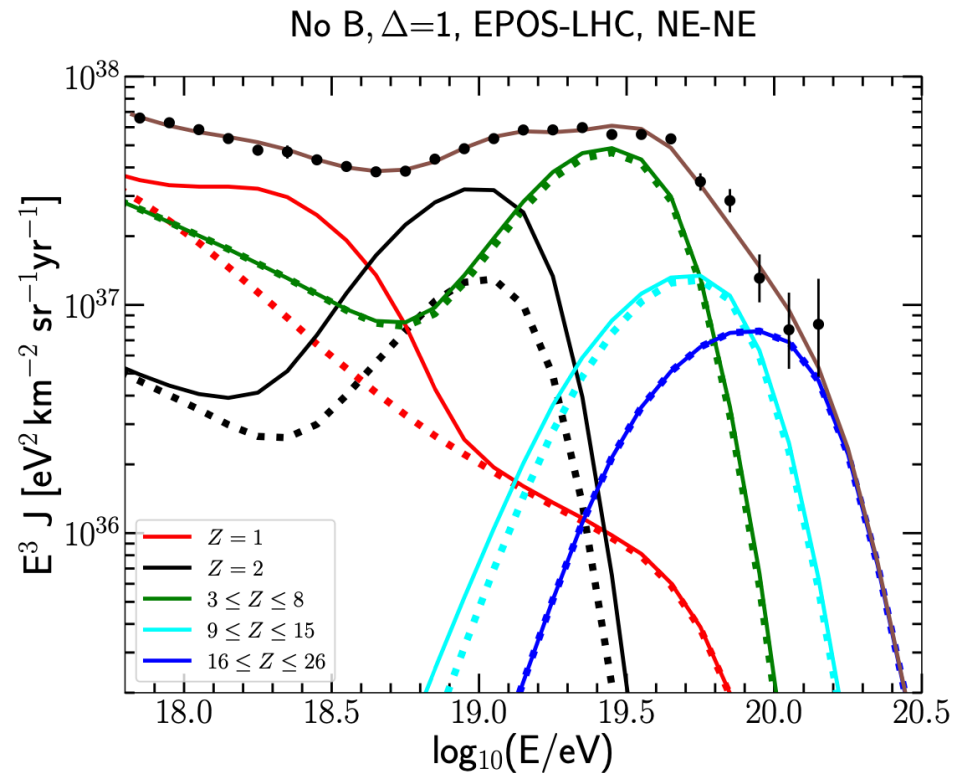


TA SD (2022) $-5^\circ < \delta < 24.8^\circ$ no Hotspot & PPSC

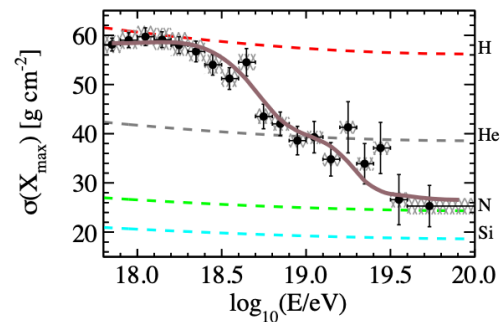
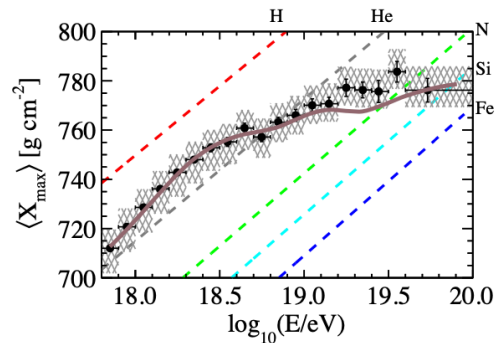


TAUP 2025, Searching for sources of cosmic rays Dmitri Semikoz

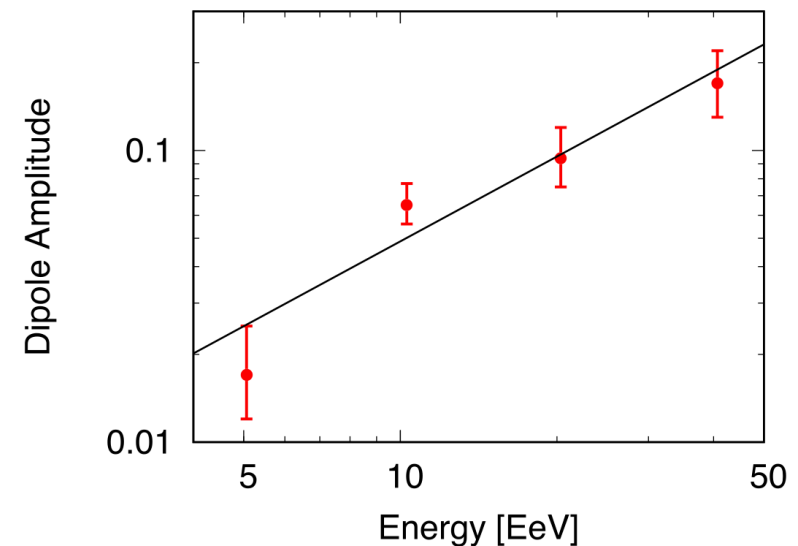
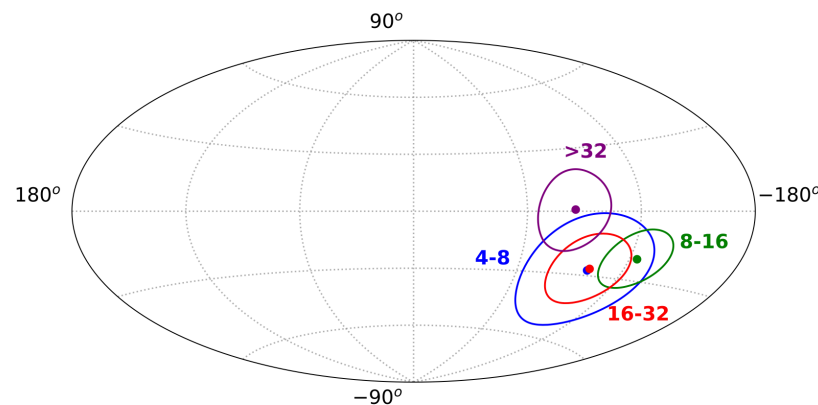
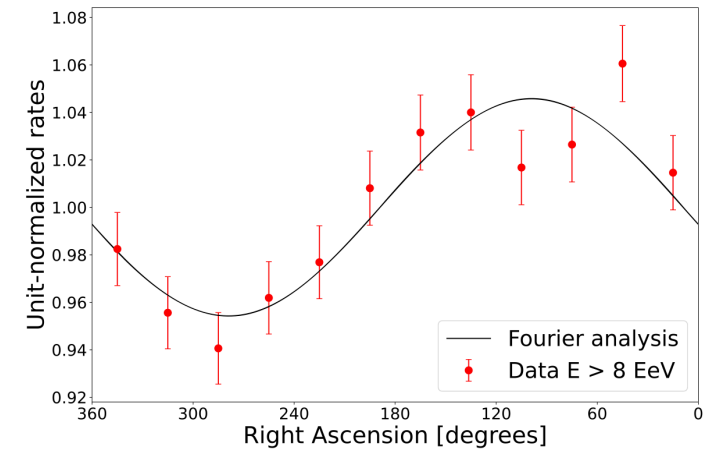
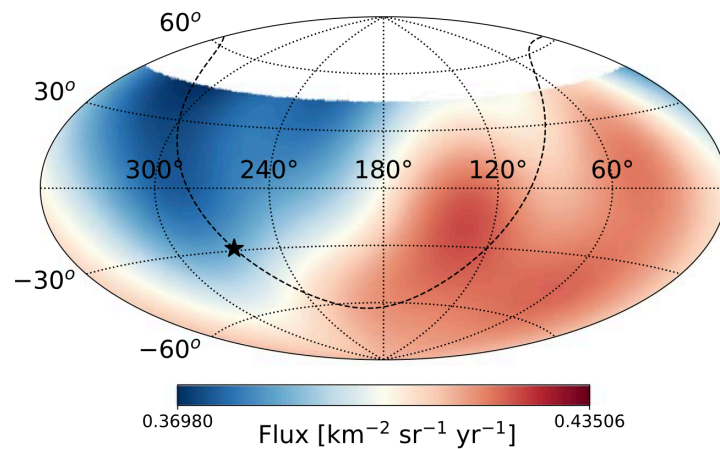
Auger spectrum and composition



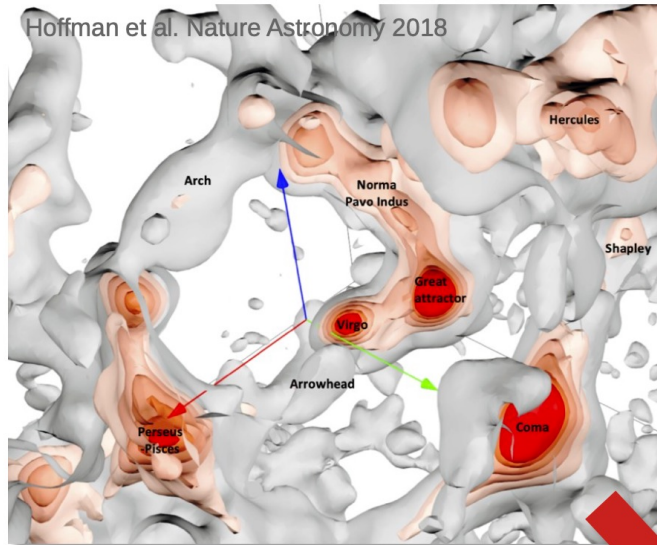
Pierre Auger Collaboration,
2404.03533



Auger dipole 6 sigma



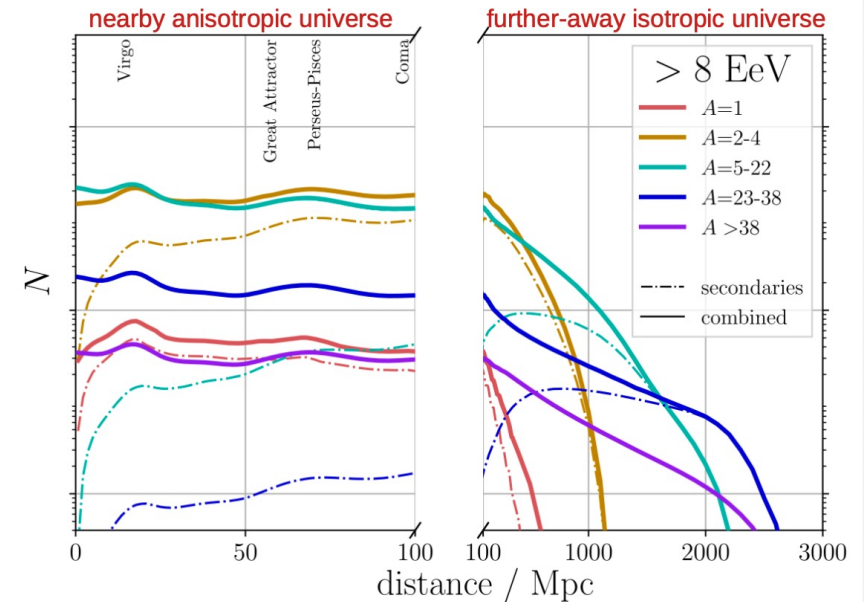
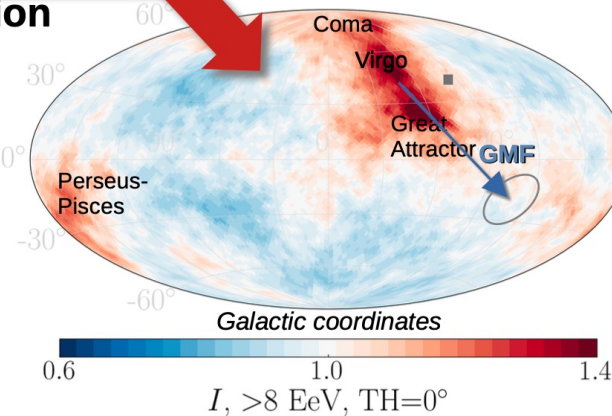
UHECR Flux from the large-scale structure > 8 EeV



use as source distribution

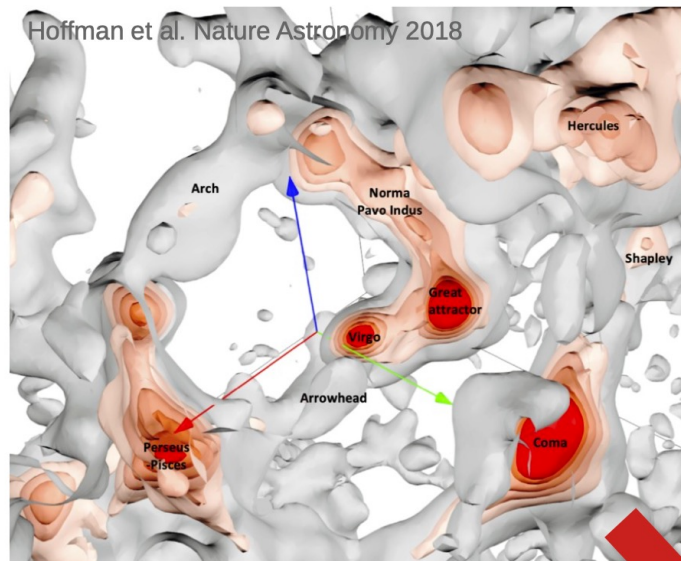
combined fit to
spectrum and
composition data

predicted flux at
edge of Galaxy:



In the LSS + combined fit model,
the dipole at ~8 EeV is generated
by **primary Helium & CNO**
from Virgo, Great Attractor & Coma

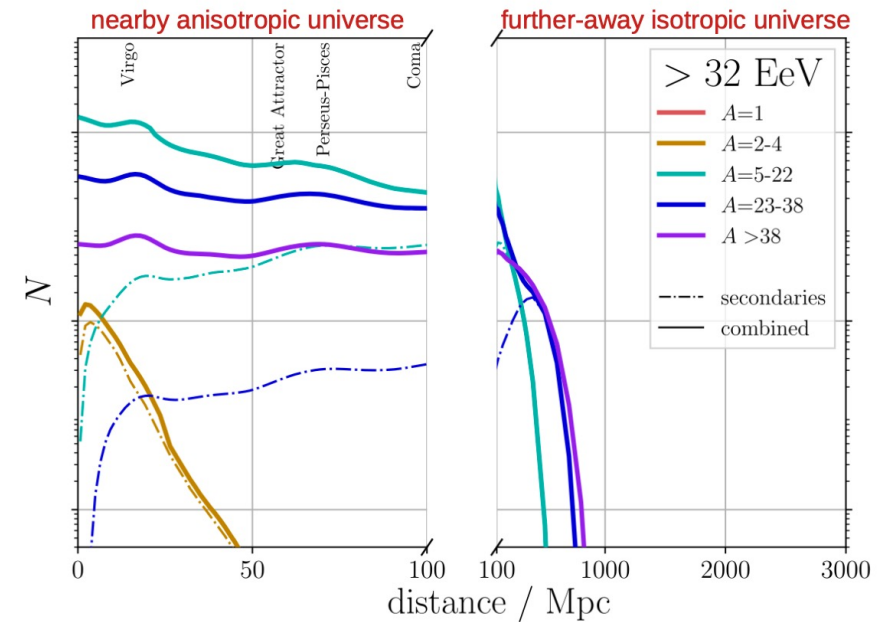
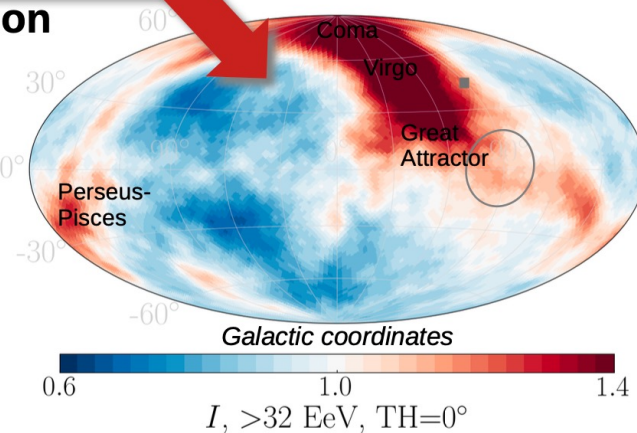
UHECR Flux from the large-scale structure >32 EeV



use as source distribution

combined fit to
spectrum and
composition data

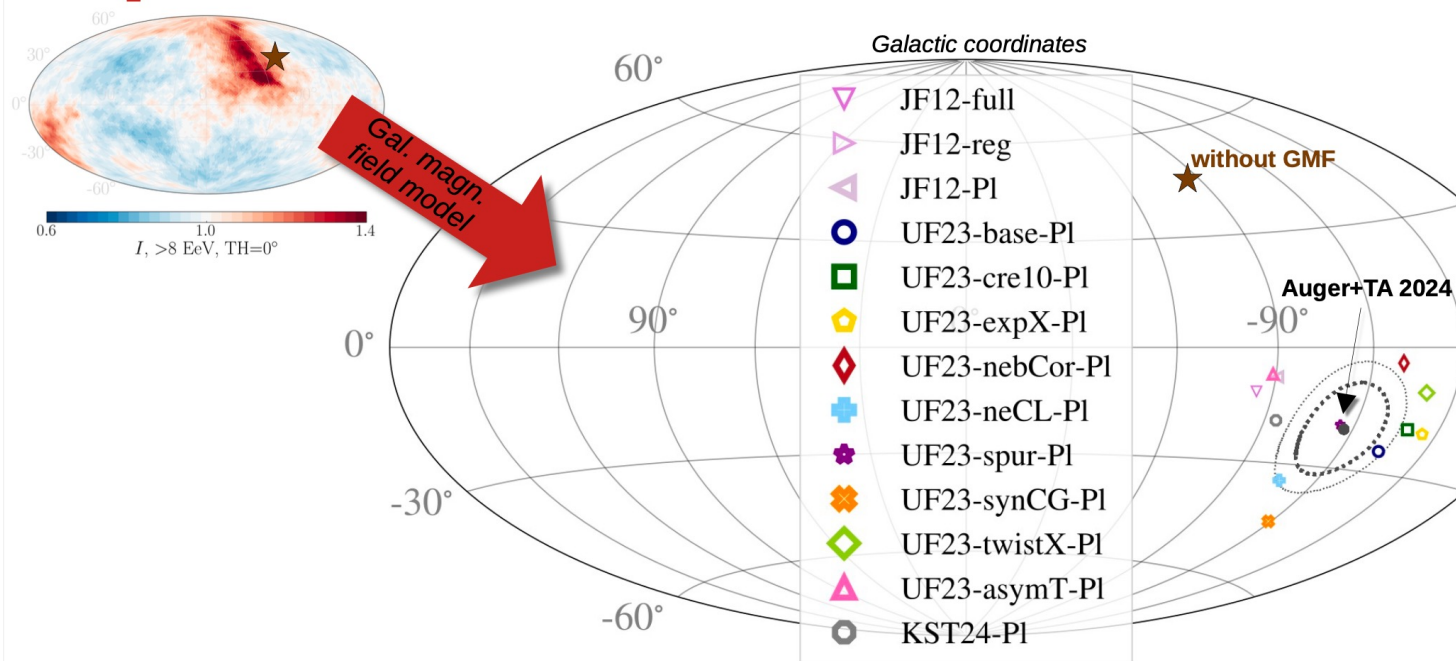
predicted flux at
edge of Galaxy:



flux >32 EeV mostly primary CNO
from within ~ 200 Mpc

→ dipole amplitude rises due to
shrinking propagation length

Dipole direction > 8 EeV



for JF12: difference to predictions based
on 2MRS galaxy catalog $\sim 10^\circ$ ✓
Auger ApJ 976 48 (2024),
Allard et al. A&A A292 (2024)

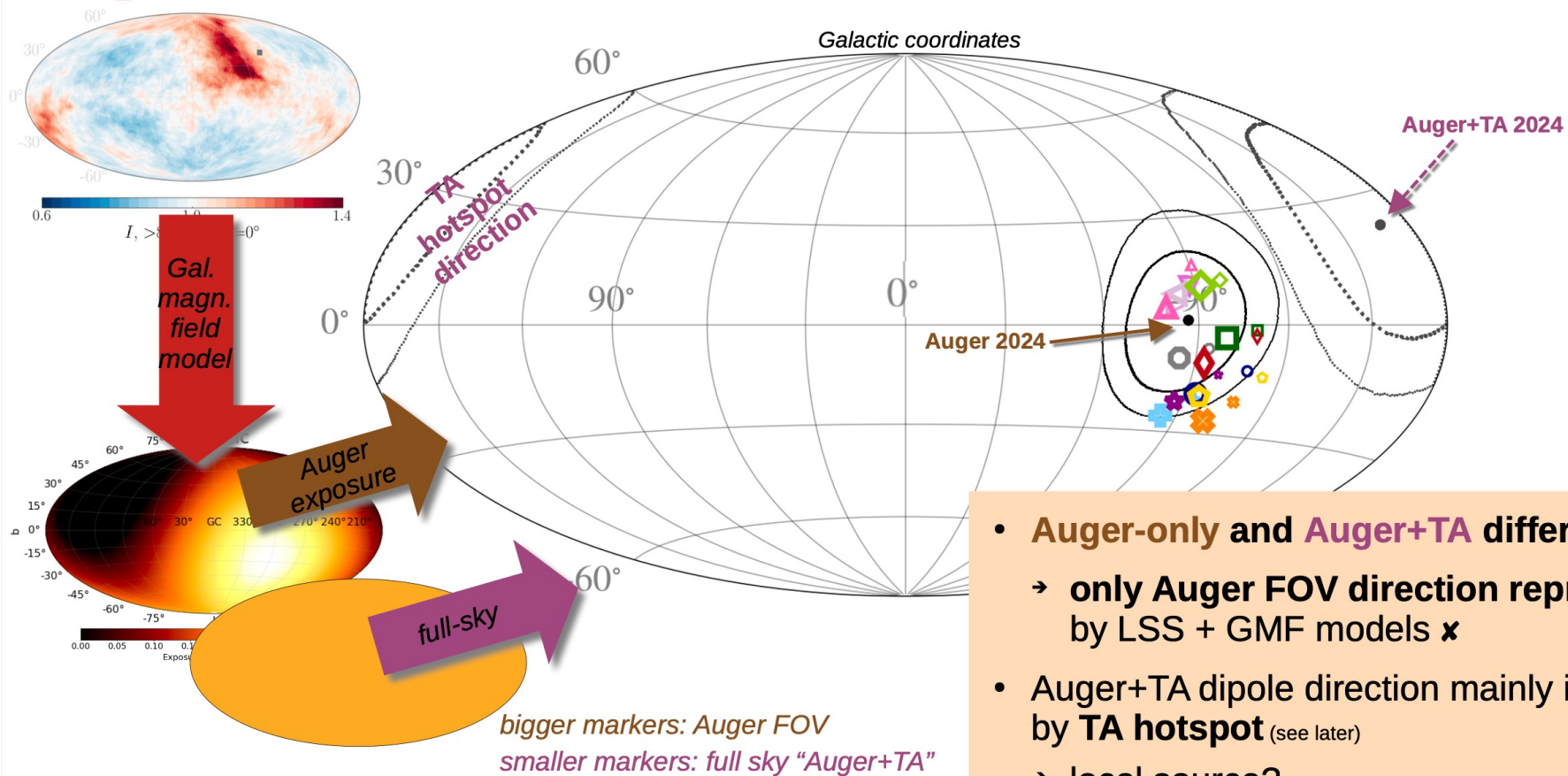
all models predict
dipole direction
close to measured
one ✓

uncertainty
estimate of GMF
model ✓

Note: cannot get
predicted dipole
direction to match
measurements with
proton-only
composition x

Ding, Globus, Farrar ApJL 913 (2021)

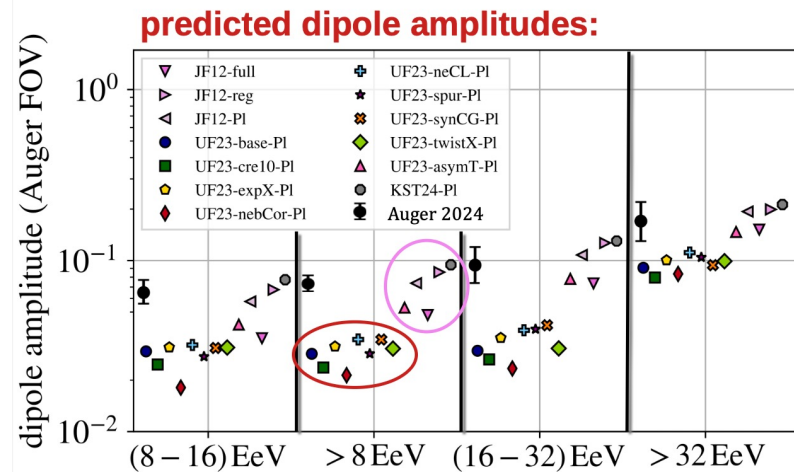
Dipole direction > 32 EeV



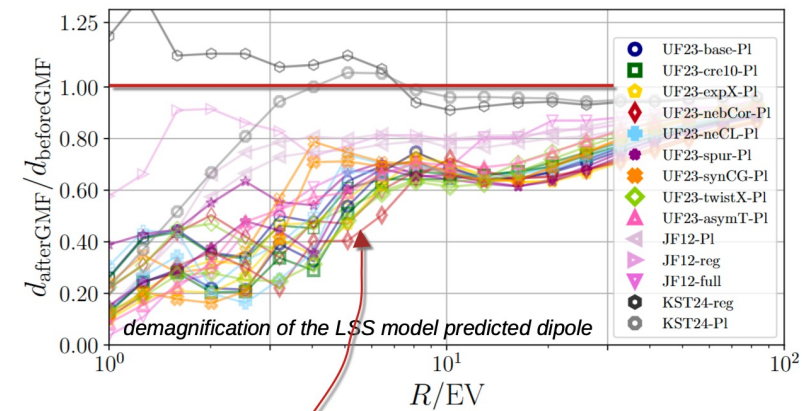
- **Auger-only** and **Auger+TA** differ by 81°
 - only Auger FOV direction reproduced by LSS + GMF models \times
- Auger+TA dipole direction mainly influenced by **TA hotspot** (see later)
 - local source?
 - e.g. M82, see also H. He et al PRD 93 (2016)

Dipole amplitude \leftrightarrow (de-)magnification

continuous model (infinite source density)

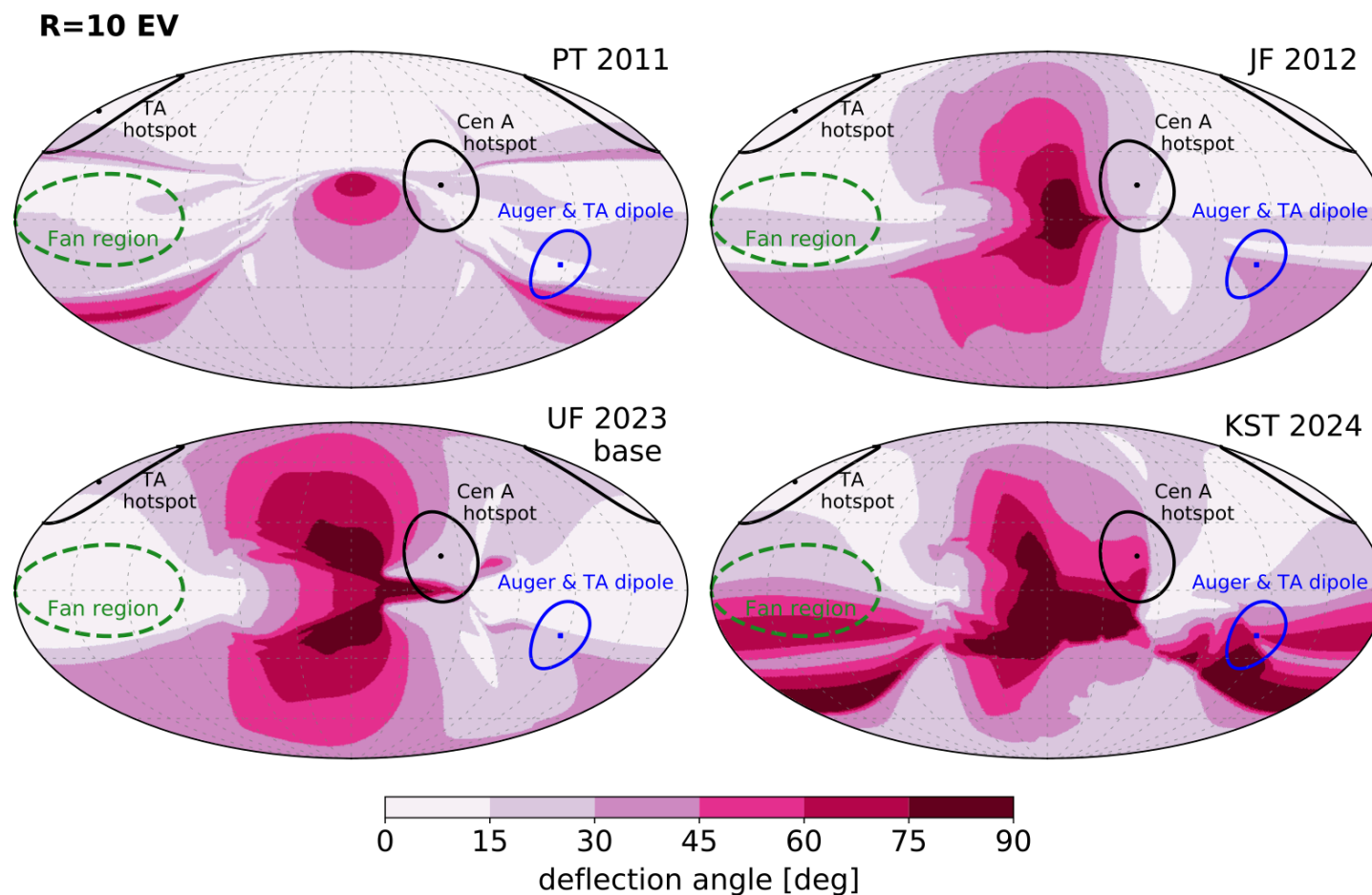


UF23 models predict significantly smaller dipole amplitude than **JF12 / KST24 / UF23-asymT**

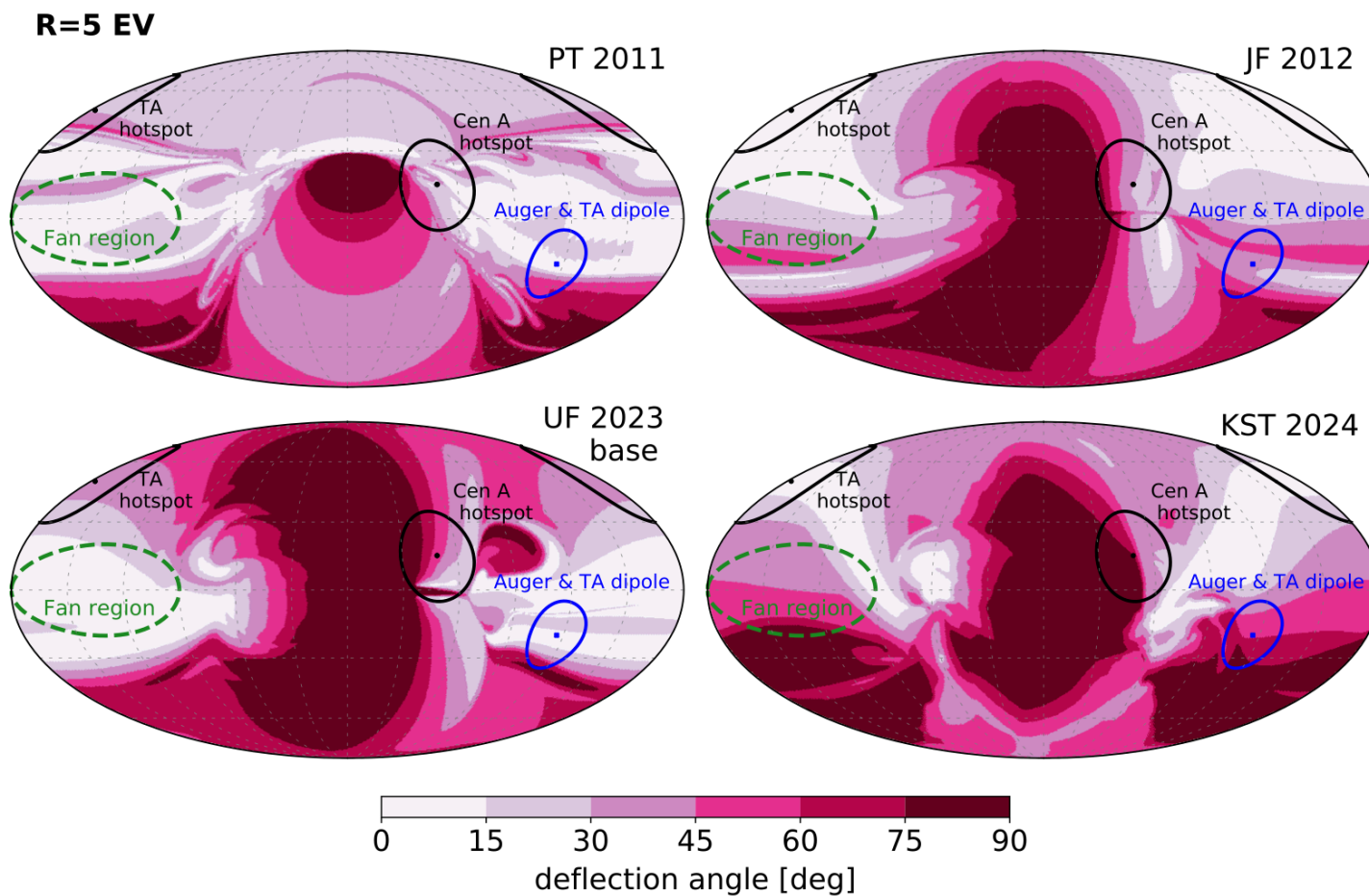


due to (de-)magnification differences!

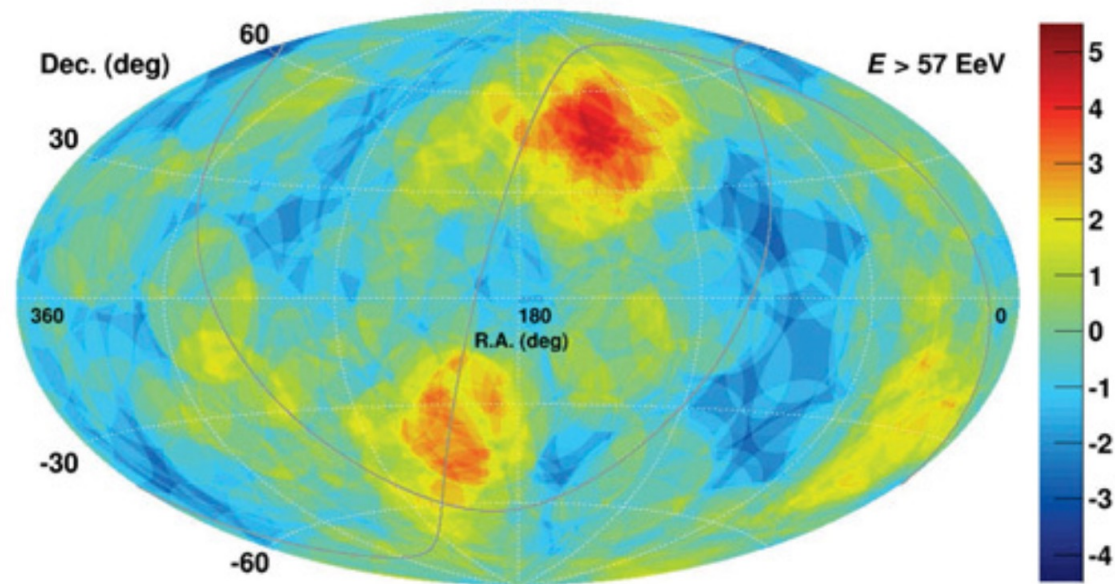
UHECR $R=10$ EV



UHECR $R=5$ EV



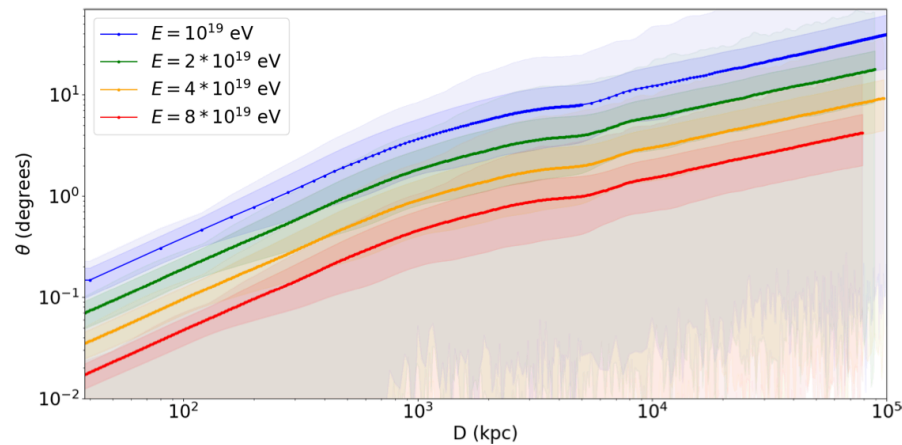
Auger-TA sky map $E > 57 \text{ EeV}$



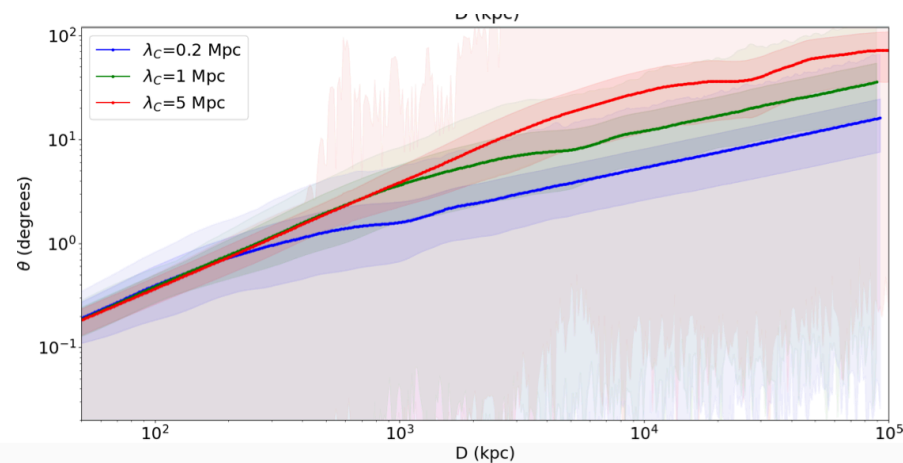
Full sky map combining the Telescope Array and Pierre Auger data events with $E > 5.7 \times 10^{19} \text{ eV}$. The events have oversampling with a 20 @BULLET radius circle. The Telescope Array data set includes 109 events, representing the first 7 years of data collection. The Auger data set includes 157 events, representing 10 years of data. No correction was made for the energy scale difference between the Telescope Array and Pierre Auger data sets.

Auger & TA collaboration

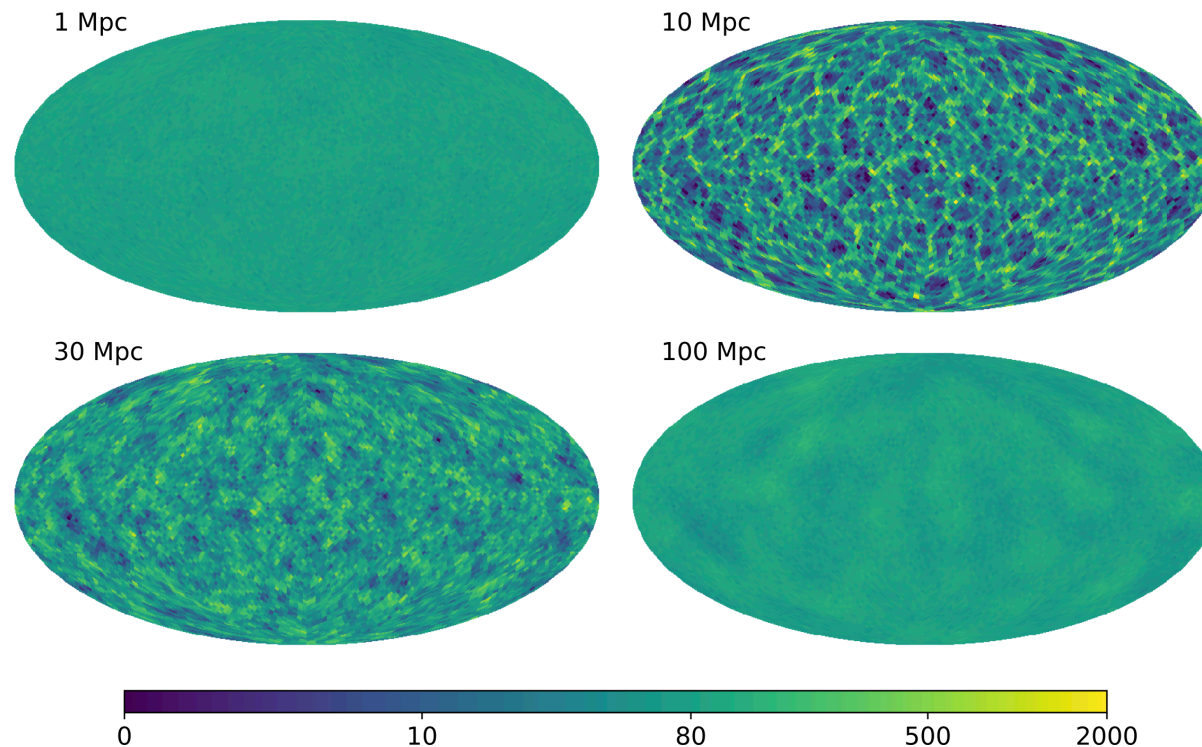
UHECR propagation in IGMF



$$\theta \sim 4^\circ Z \frac{B}{\text{nG}} \frac{10 \text{ EeV}}{E} \sqrt{\frac{D}{\text{Mpc}}} \sqrt{\frac{\lambda_C}{\text{Mpc}}}$$



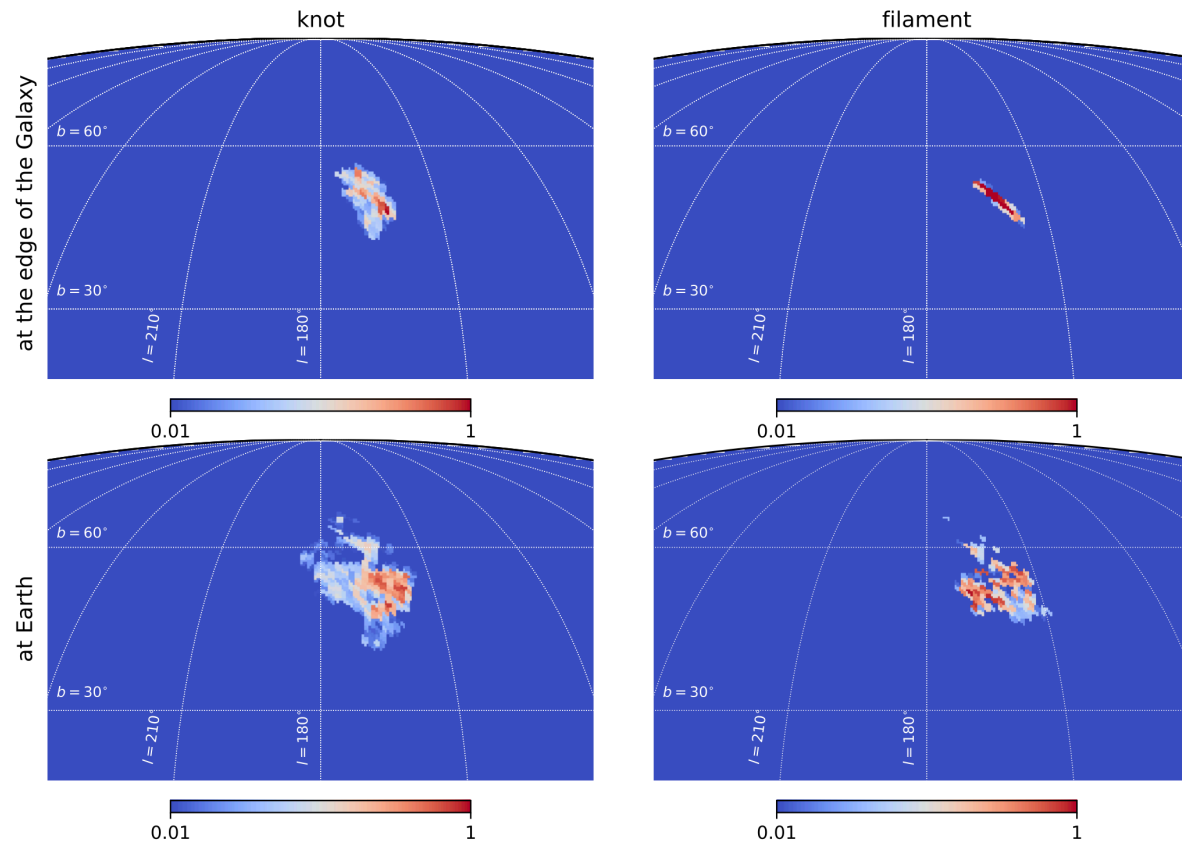
UHECR propagation in IGMF: caustics



$\Lambda=0.3$ Mpc $R=10$ EV

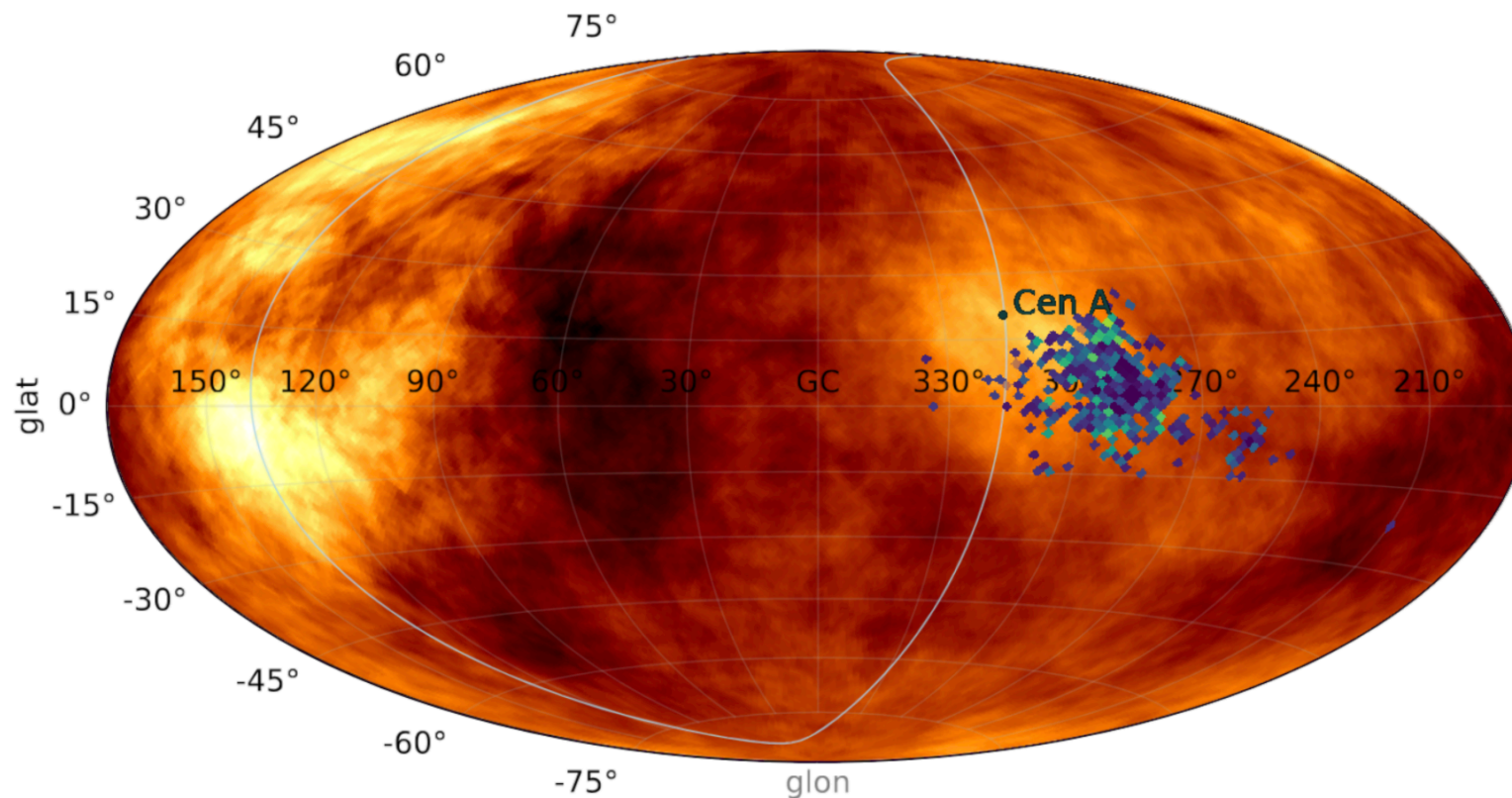
A.Dolgikh, A.Korochkin, G.Rubtsov, D.S. and I.Tkachev, 2212.01494

UHECR source in TA hot spot



A.Dolgikh, A.Korochkin, G.Rubtsov, D.S. and I.Tkachev, 2312.06391

Cen A flux is shifted in JF12 GMF model



K.Dolgi, A.Korochkin, G.Rubtsov, D.S. and I.Tkachev, to appear arXiv:2505...

M83 is of for JF12 GMF model

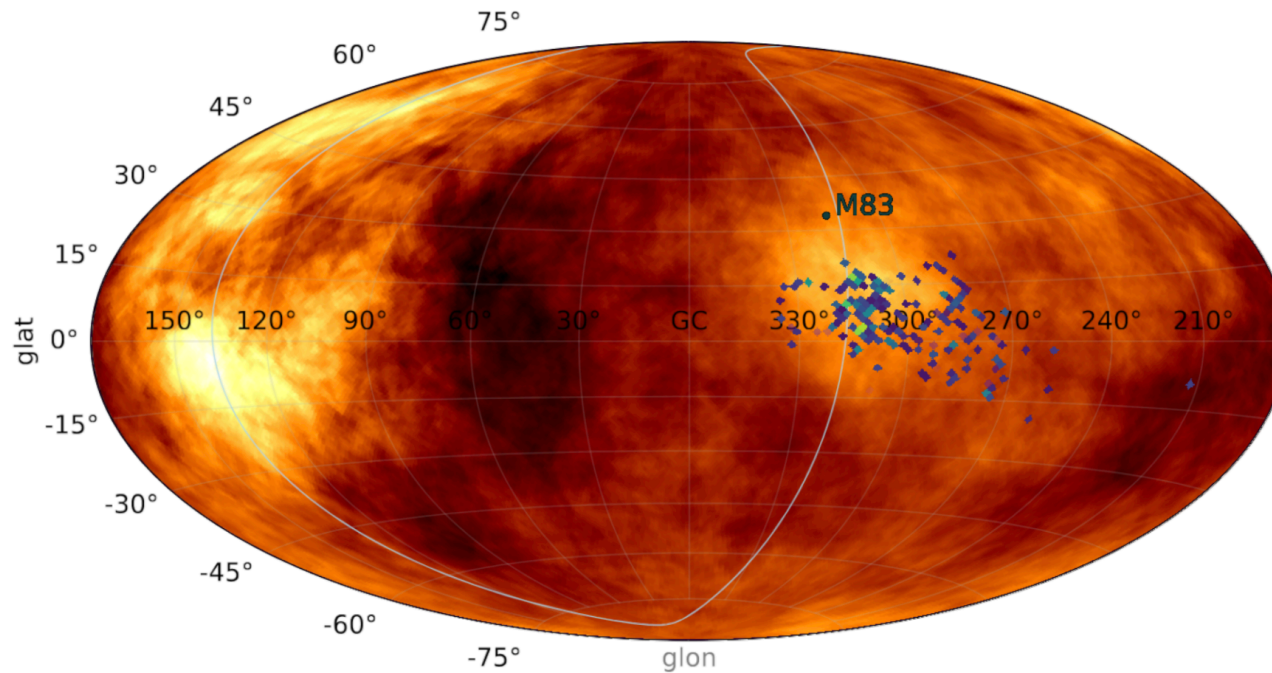
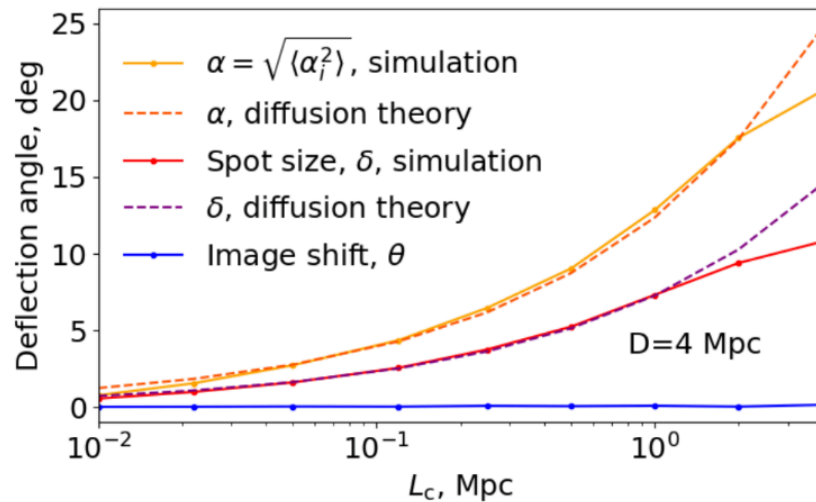
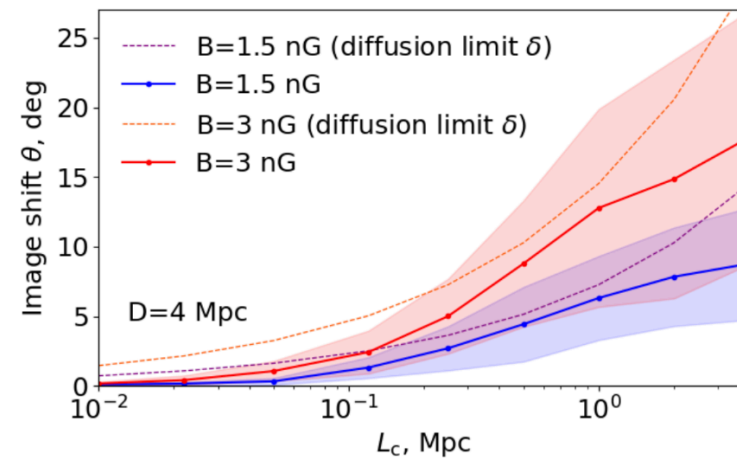
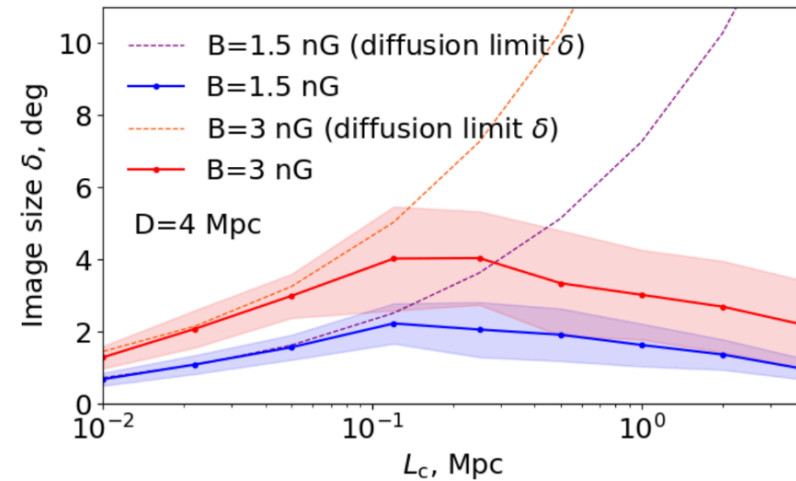


FIG. 3. Arrival directions of the carbon nuclei with $E = 60$ EeV from M 83 for the same magnetic fields and as Fig. 2.

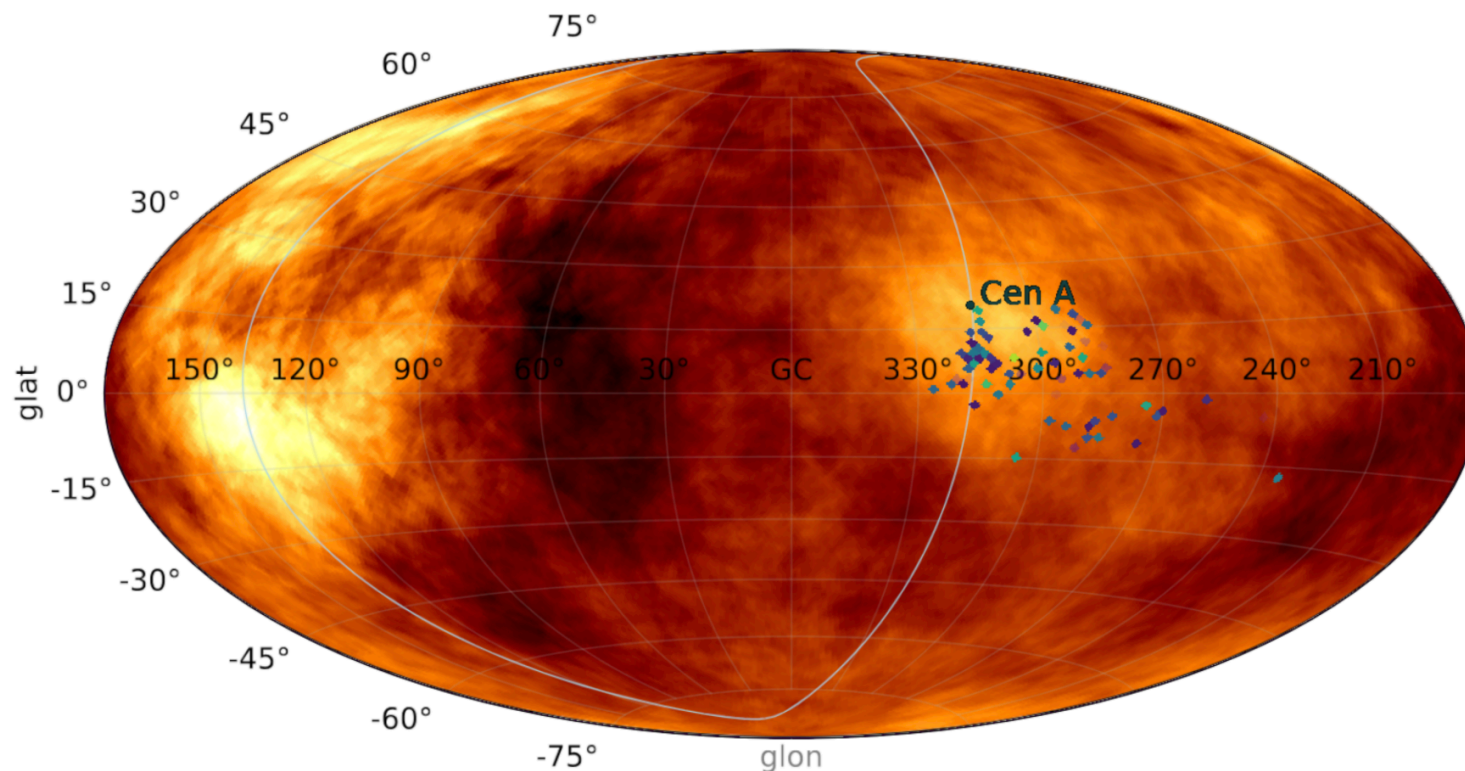
Diffusion in angle



$$\begin{cases} \alpha = 3.74^\circ \cdot Z \left[\frac{B}{1 \text{ nG}} \right] \left[\frac{E}{10^{19} \text{ eV}} \right]^{-1} \left[\frac{D}{10 \text{ Mpc}} \right]^{\frac{1}{2}} \left[\frac{L_{\text{max}}}{500 \text{ kpc}} \right]^{\frac{1}{2}} \\ \delta = \alpha / \sqrt{3} \\ \theta = 0. \end{cases}$$



Cen A back to place due to IGMF



Gamma-rays and neutrinos from Milky Way Galaxy

Gamma-ray detectors

Space-based
EGRET, AGILE,
Fermi



HE: >0.1 GeV
Large FOV
80% duty cycle
 $0.1^\circ \sim 5^\circ$
resolution
 1 m^2 area

IACTs:
H.E.S.S., MAGIC, VERITAS,
CTA



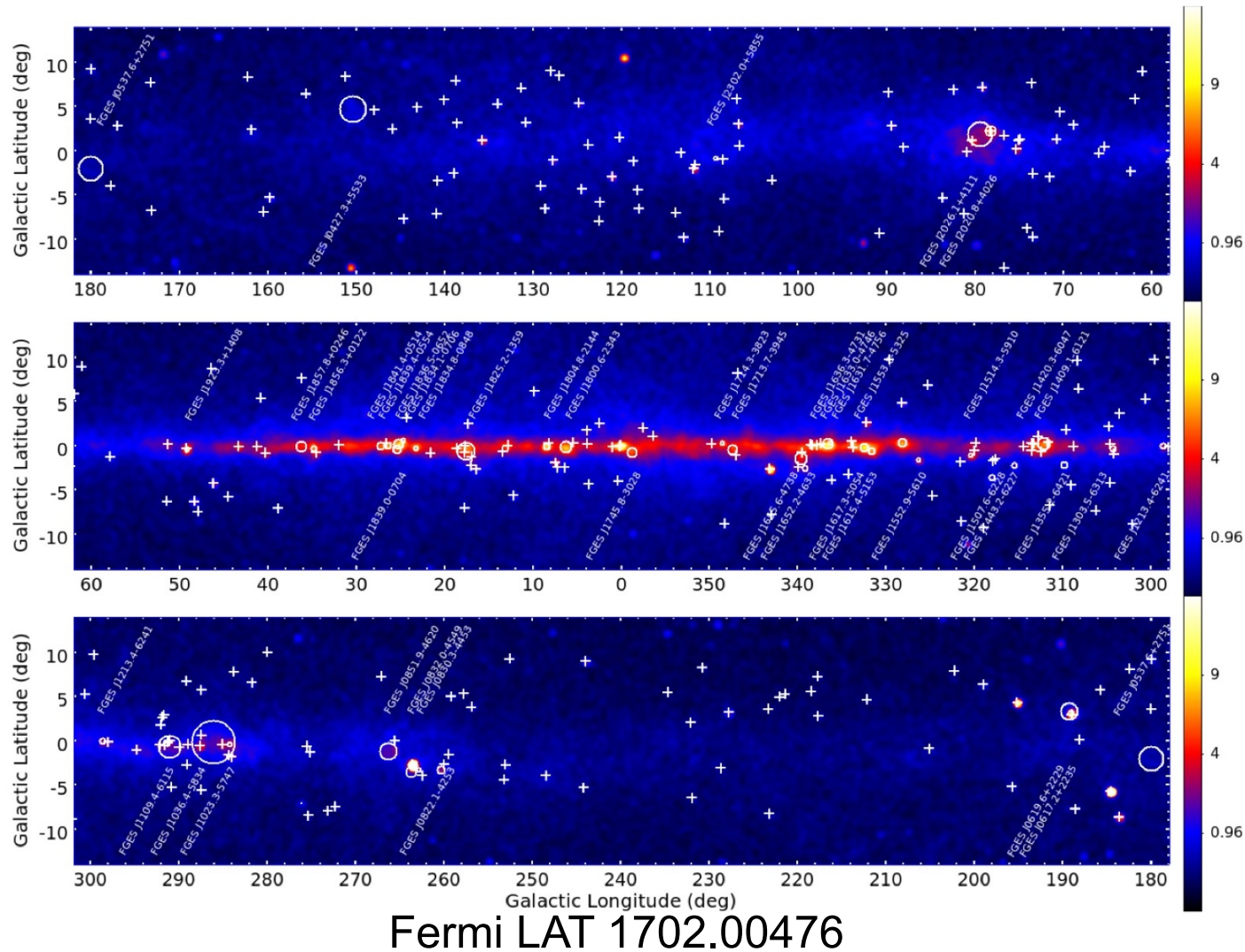
VHE: >0.1 TeV
 $3^\circ \sim 5^\circ$ FOV
15% duty cycle
 $0.06^\circ \sim 0.17^\circ$
resolution
 10^5 m^2 area

EAS arrays:
Milagro, ARGO-YBJ
Tibet Asy, HAWC,
LHAASO, SWGO



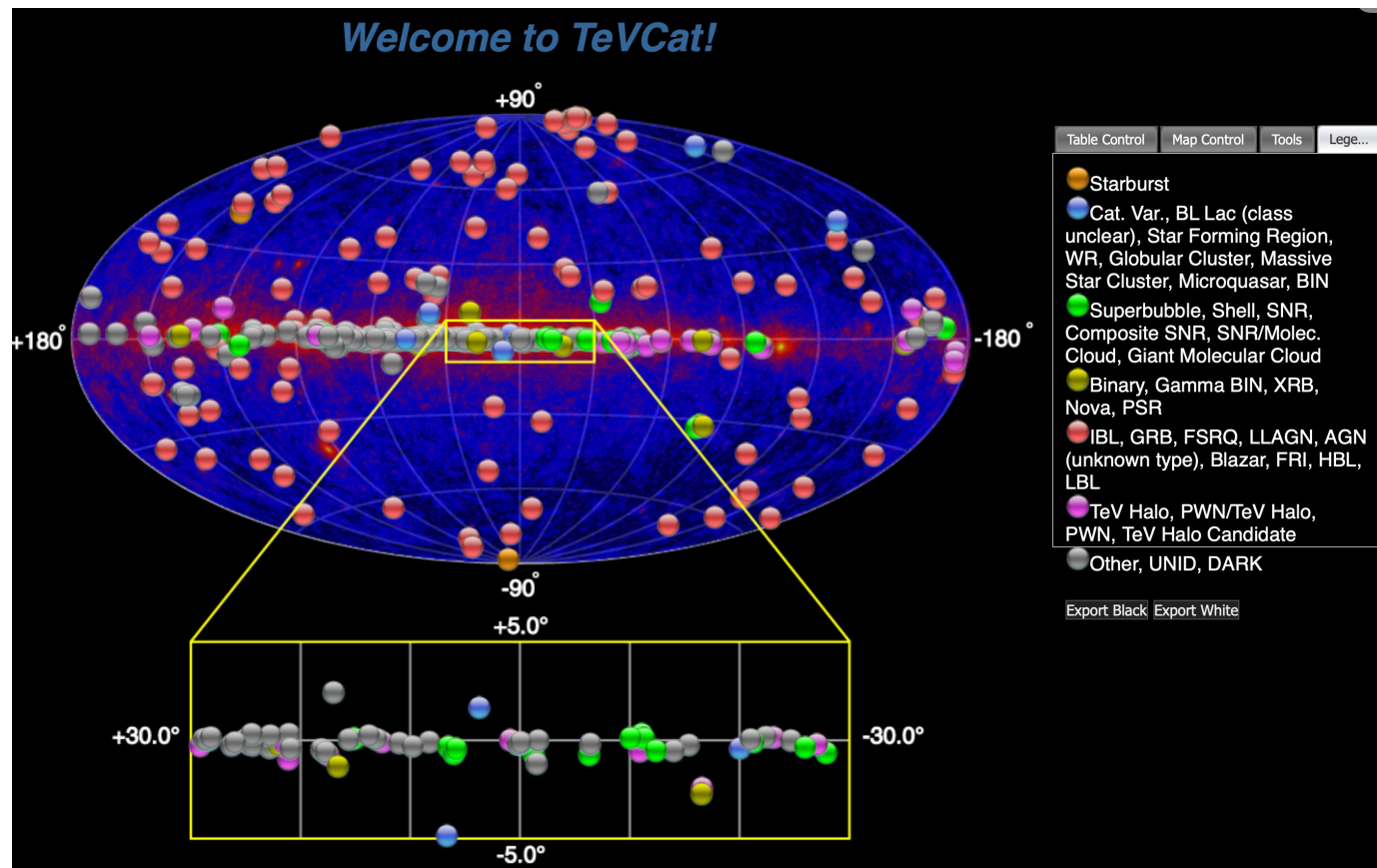
VHE: >0.1 TeV
UHE: >0.1 PeV
Large FOV
100% duty cycle
 $0.1^\circ \sim 1^\circ$ resolution
 10^{3-6} m^2 area

Fermi LAT 600 identified Galactic sources



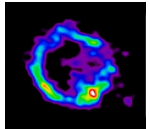
TAUP 2025, Searching for sources of cosmic rays Dmitri Semikoz

Cherenkov telescopes+ HAWC/LHAASO



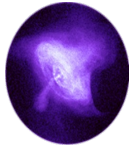
Around 200 sources in the Galactic plane at TeV energies

Galactic sources

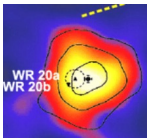


Supernova Remnants

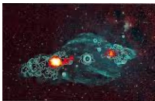
Talk by Songzhan Chen



Pulsar wind nebulas



Star clusters



Microquasars

Pion production

$$N + \gamma_b \Rightarrow N' + \sum \pi^i$$

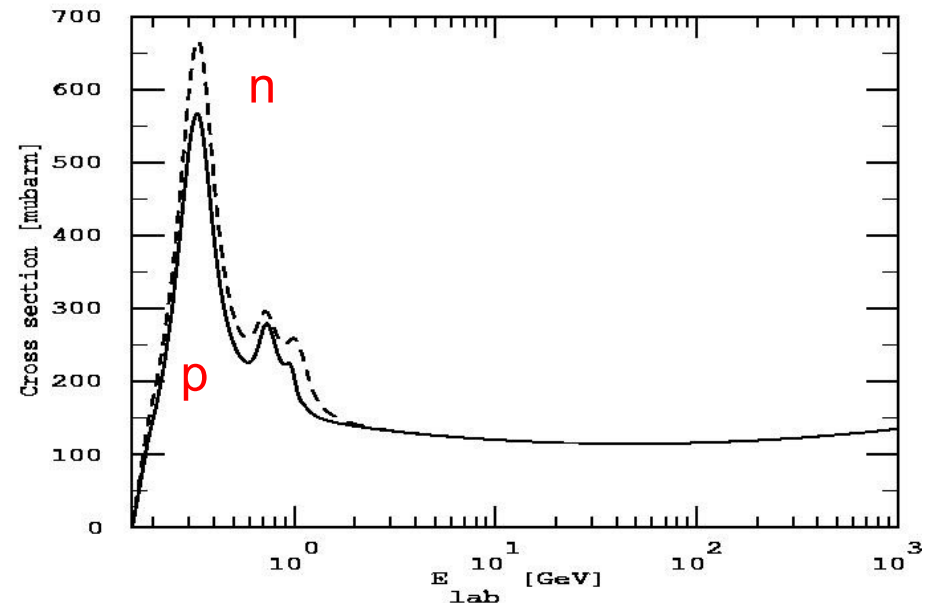
$$N + A_b \Rightarrow N' + \sum \pi^i$$

$$\pi^0 \Rightarrow 2\gamma$$

$$\pi^\pm \Rightarrow \mu^\pm + \nu_\mu$$

$$\mu^\pm \Rightarrow e^\pm + \bar{\nu}_e + \nu_\mu$$

$$n \Rightarrow p + e^- + \bar{\nu}_e$$



Conclusion: CR, photon and neutrino fluxes are connected in well-defined way. If we know one of them we can predict other ones (model dependent) :

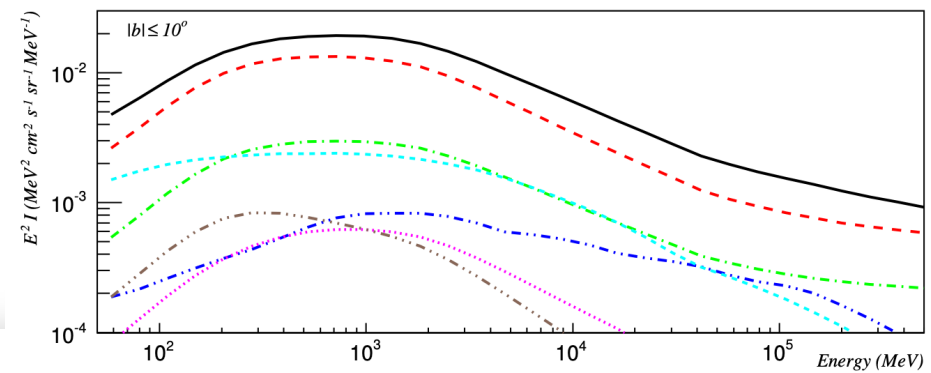
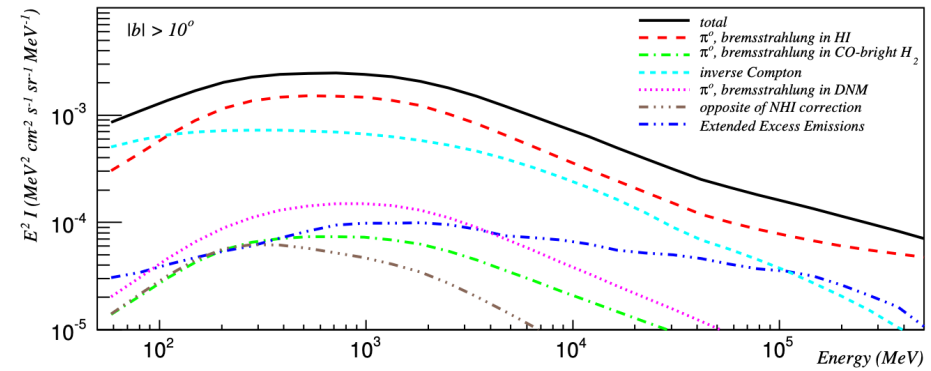
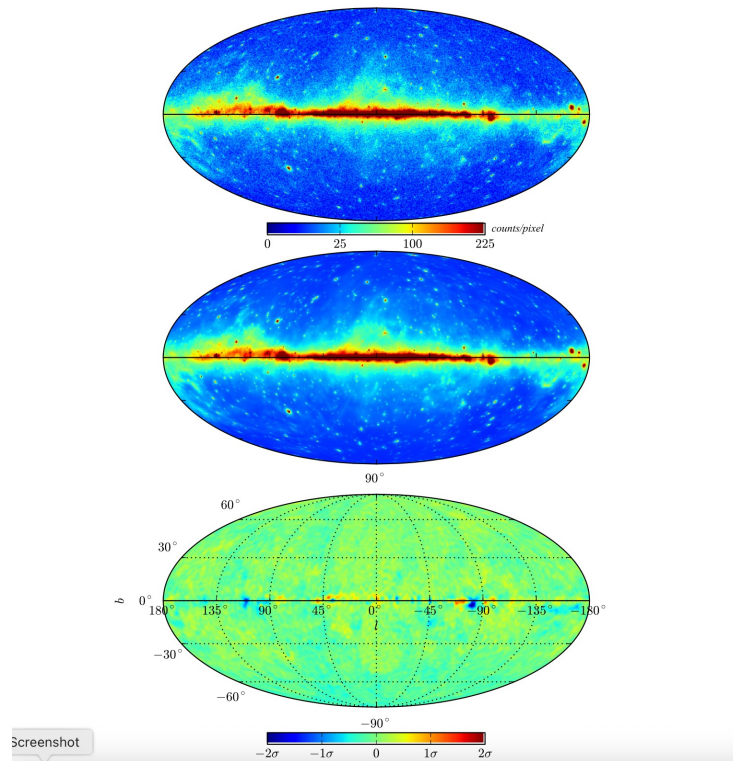
$$E_\gamma^{tot} \sim E_\nu^{tot}$$

Diffuse gamma-ray and neutrino fluxes

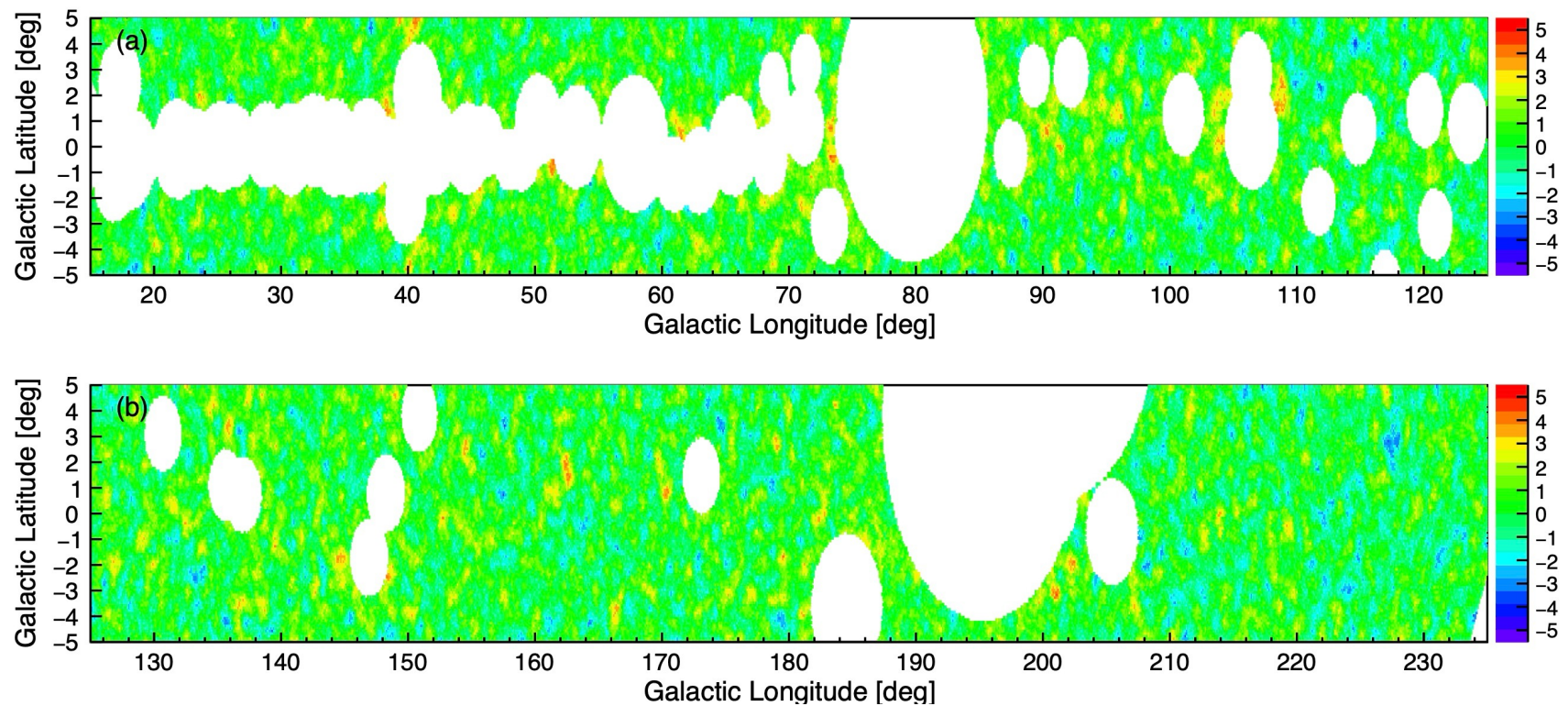
$$\Xi^{A,A'}(E, l, b) = \int_0^\infty ds \, n_{\text{gas}}^{A'}(\mathbf{x}) I_{\text{CR}}^A(E, \mathbf{x})$$

$$I_\nu(E, l, b) = \sum_{A,A'} \int_E^\infty dE' \, \Xi^{A,A'}(E', l, b) \frac{d\sigma^{AA' \rightarrow \nu}(E', E)}{dE}$$

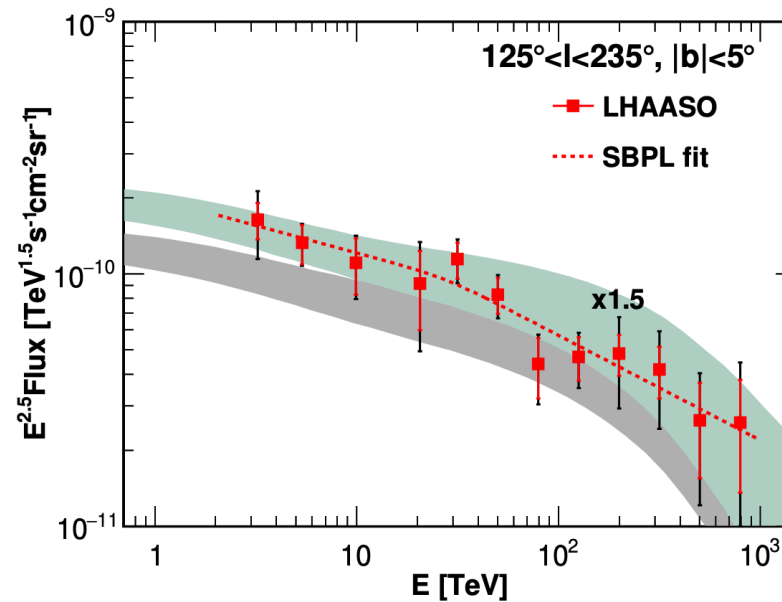
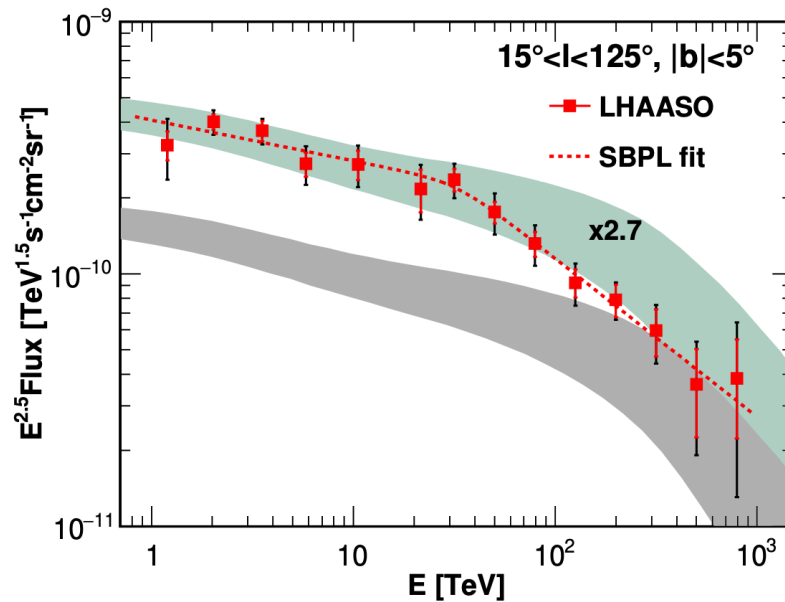
Gamma-ray flux



Mask LHAASO



LHAASO diffuse



$$\Xi^{A,A'}(E, l, b) = \int_0^\infty ds n_{\text{gas}}^{A'}(\mathbf{x}) I_{\text{CR}}^A(E, \mathbf{x})$$

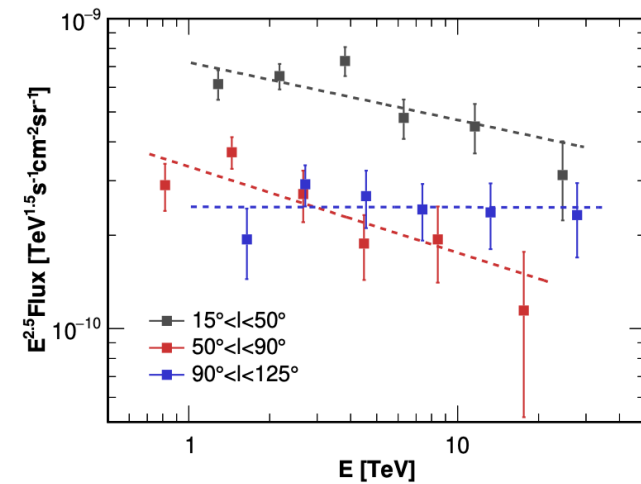
$$I_\nu(E, l, b) = \sum_{A,A'} \int_E^\infty dE' \Xi^{A,A'}(E', l, b) \frac{d\sigma^{AA' \rightarrow \nu}(E', E)}{dE}$$

Variation of diffuse flux over Galaxy

Table 2
Spectrum of the GDE in Various Subregions of the ROI

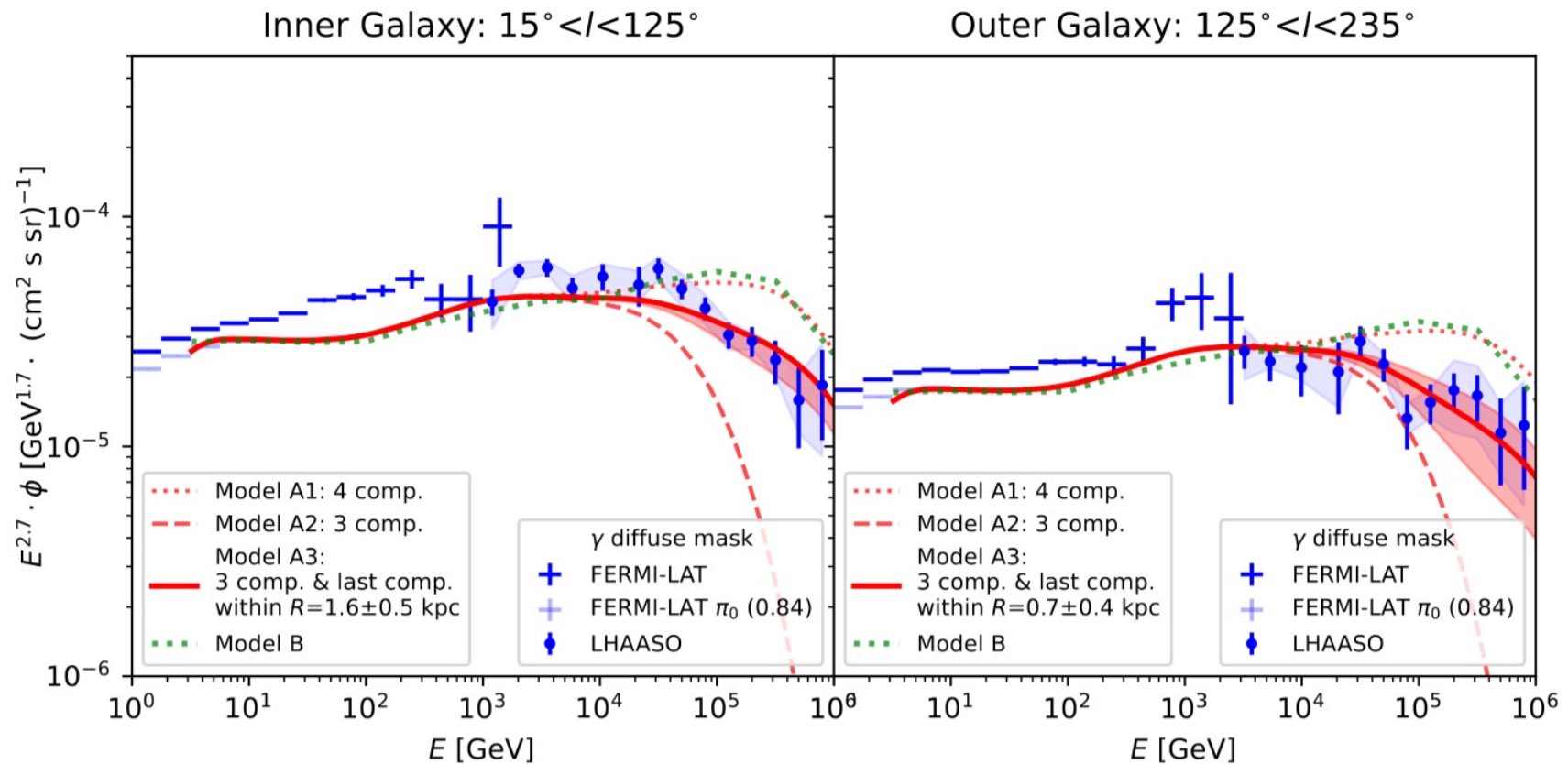
l_{\min} (deg)	l_{\max} (deg)	$ b <$ (deg)	$F_7 \times 10^{-12}$ ($\text{TeV}^{-1} \text{s}^{-1} \text{cm}^{-2} \text{sr}^{-1}$)	Index
43	73	2	$8.89 \pm 0.37_{-0.70}^{+0.48}$	$-2.61 \pm 0.03_{-0.02}^{+0.04}$
43	73	4	$5.45 \pm 0.25_{-0.44}^{+0.38}$	$-2.60 \pm 0.03_{-0.04}^{+0.01}$
43	56	2	9.9 ± 0.6	-2.70 ± 0.04
43	56	4	5.8 ± 0.4	-2.69 ± 0.05
56	64	2	8.9 ± 0.7	-2.58 ± 0.06
56	64	4	5.2 ± 0.5	-2.60 ± 0.07
64	73	2	7.8 ± 0.7	-2.48 ± 0.07
64	73	4	5.5 ± 0.45	-2.51 ± 0.06

HAWC collaboration,
2310.09117



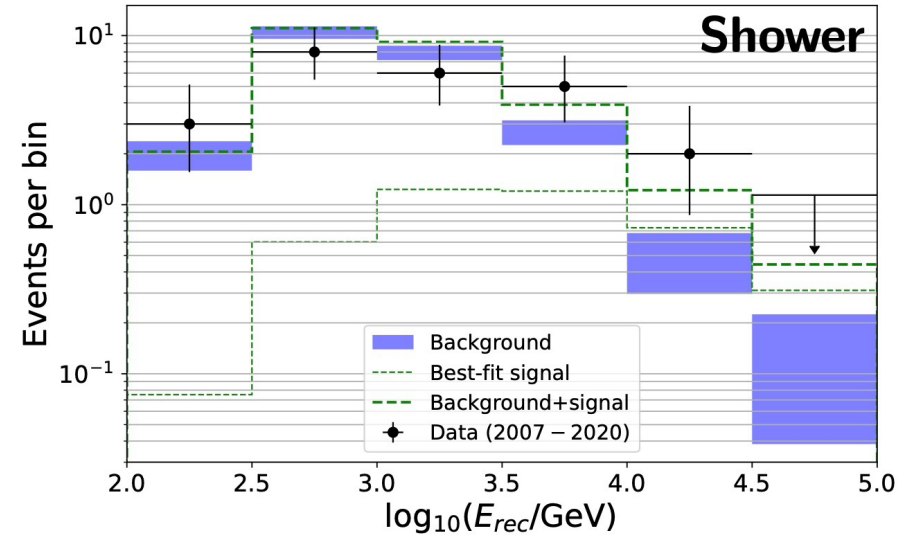
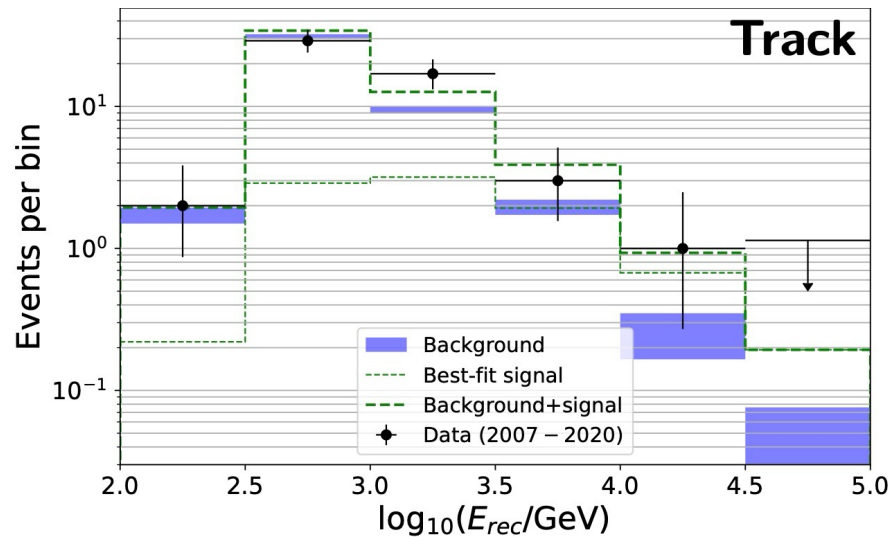
LHAASO collaboration,
arXiv: 2411.01621

Lower knee in Galaxy



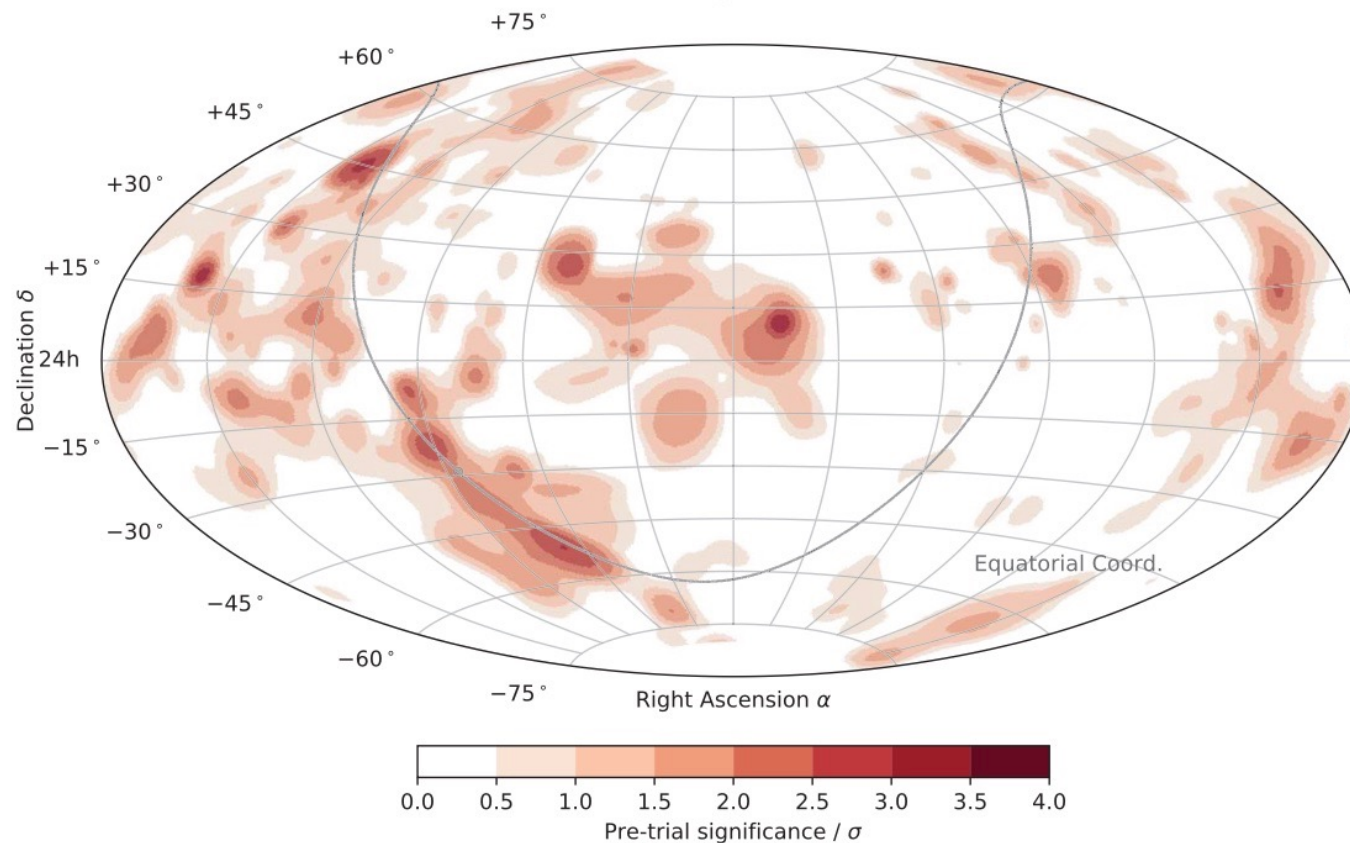
C. Prevotat et al, [2407.11911](#), [2507.10823](#)

Neutrinos from Galactic plane: ANTARES 2022: 2 sigma excess



A.Albert et al, arXiv:2212.11876

IceCube cascades: 4 sigma



IceCube collaboration, Science **380**, 1338 (2023)

Cascades $E > 200$ TeV Baikal and IceCube

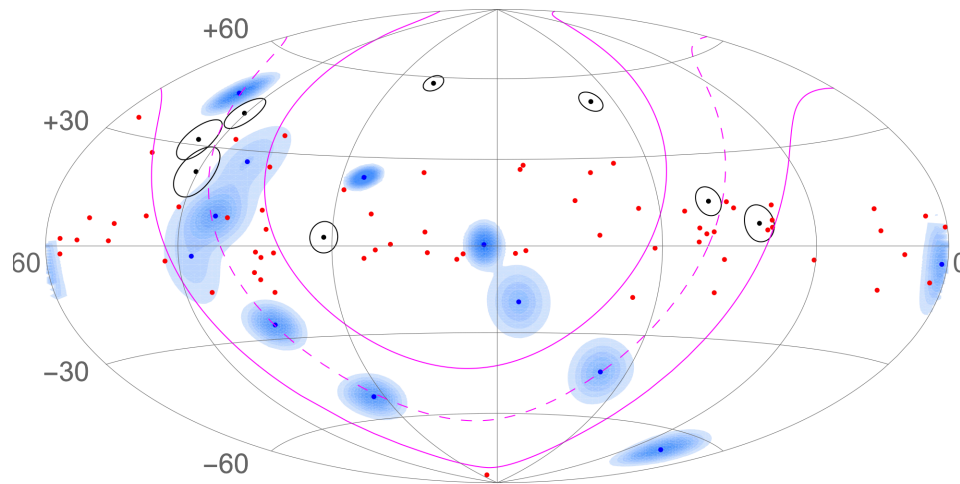


Table 2

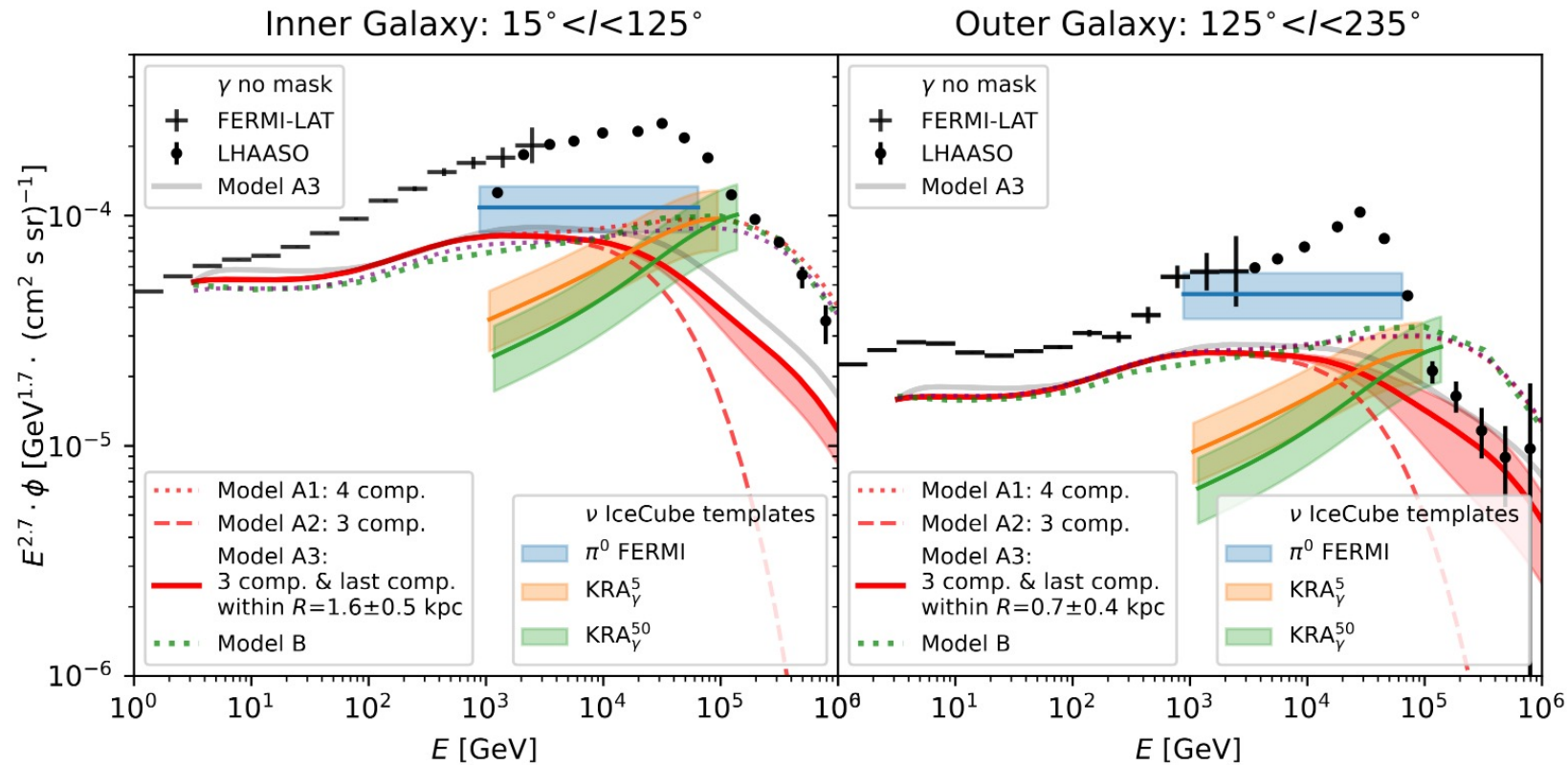
Results (This Work) of the Search for the Galactic Component of the Neutrino Flux above 200 TeV (see the Text for Details)

Sample	$ b _{\text{med}}$ Observed (deg)	$\langle b _{\text{med}} \rangle$ Expected (deg)	p
Baikal-GVD cascades	10.4	31.4	1.4×10^{-2} (2.5σ)
IceCube cascades	12.4	31.9	8.7×10^{-3} (2.6σ)
Combined	12.4	31.5	1.7×10^{-3} (3.1σ)
IceCube tracks	24.7	36.0	1.8×10^{-3} (3.1σ)
All combined	23.4	35.0	3.4×10^{-4} (3.6σ)

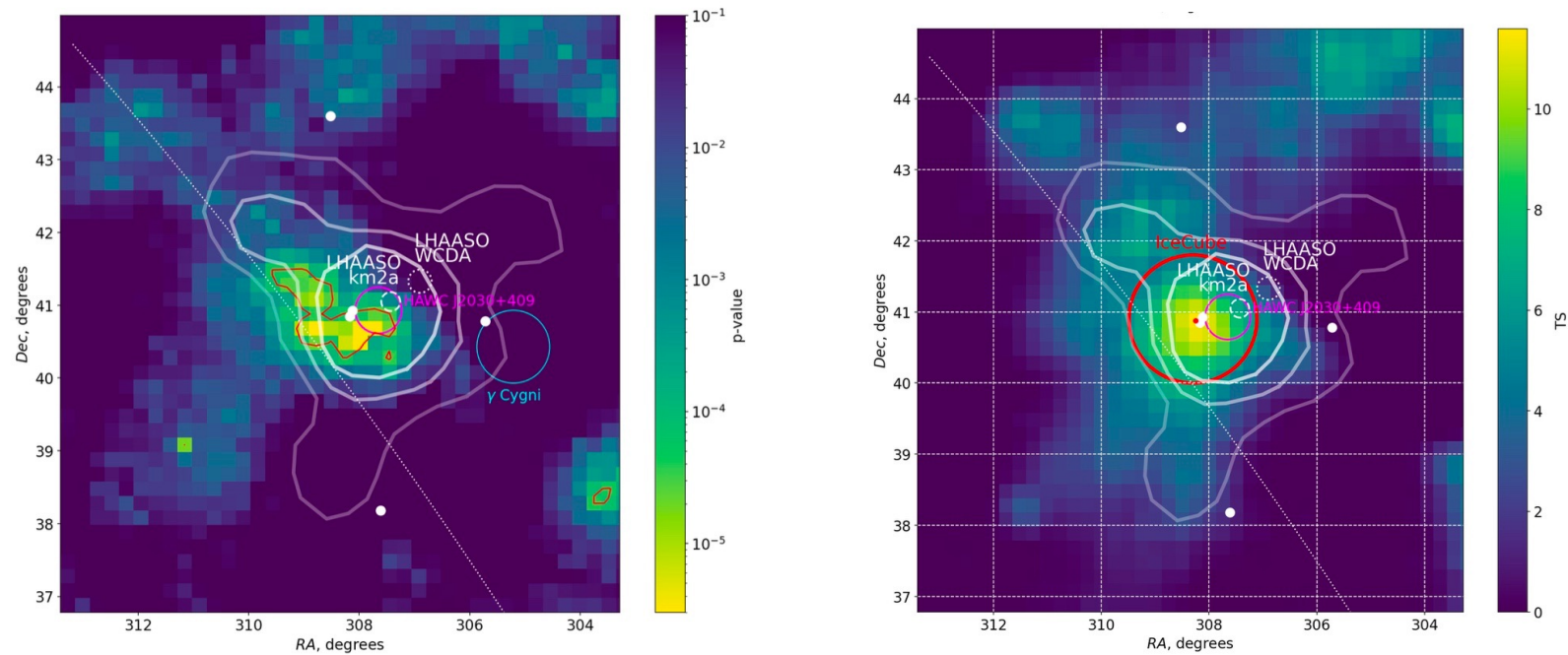
Baikal collaboration,

[2411.05608](https://arxiv.org/abs/2411.05608)

Diffuse neutrino background Galactic plane

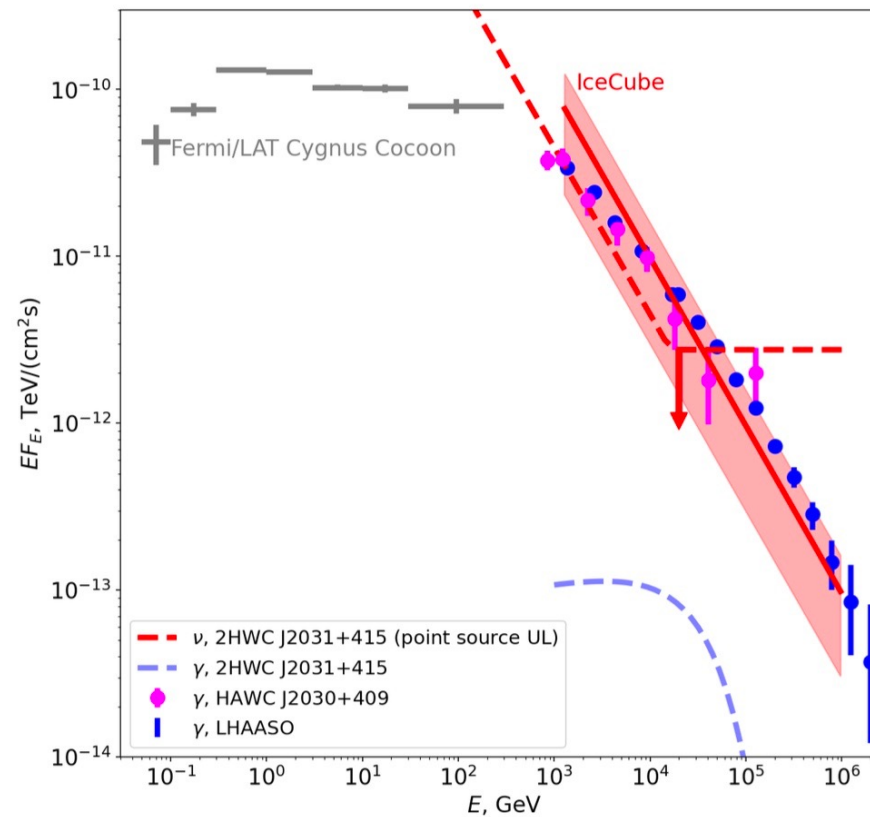


Neutrinos from Cygnus region



A.Neronov et al, arXiv:2311.13711

Neutrinos from Cygnus region



A.Neronov et al, arXiv:2311.13711

Summary

- Cosmic ray flux of individual nuclei measured by satellite experiments from space. AMS02, DAMPE and CALET see several breaks in spectrum, which have to be explained.
- LHAASO for the first time measured proton spectrum at knee from the ground. Composition established at knee with high precision measurements of $\log A$ and total flux.
- As next step we will need good 10 PeV – 1 EeV measurements of mass composition
- Breaks in CR proton spectrum from GeV to PeV energies can be propagation features or due to contributions of the different populations of sources. Break at 300 GeV is due to propagation according to AMS-02
- We start to understand general structure of magnetic field in Milky Way. Local Bubble is important for CR.

Summary

- UHECR dipole can be explained by sources in LSS and GMF.
- UHECR anisotropies at highest energies are from nearby sources, but detailed knowledge of IGMF and GMF does not allow to establish them for the moment
- We can study cosmic ray flux in different places in Galaxy with help of gamma-ray and neutrino observations.
- Diffuse gamma-ray emission from Milky Way was measured by Fermi LAT at energies between 1 GeV and 1 TeV and by LHAASO 1 TeV – 1 PeV. We need SWGO to measure Southern sky
- First signal from neutrinos from the Galaxy in cascades by IceCube. Some hints from ANTARES and Baikal GVD, waiting for KM3NET first results.
- We do not know which part of neutrino signal is from isolated sources. First source in Cygnus region. We need next generation neutrino telescopes to divide signal between sources and diffuse neutrino background from Galaxy: IceCube-gen2, TRIDENT. HUNT